Unintended Environmental Cost of Monetary Tightening: The Federal Reserve and Pollution*

Qichao Wang†

4 July 2025

Abstract

I study the environmental impacts of the US monetary policy shock using air pollution records from satellite images. An unexpected tightening reduces output but increases air pollution. The puzzle is explained by a clean investment channel: An increase in firm financing costs hinders clean investment and subsequently increases pollution. The channel has emerged since the global financial crisis. Consistently, the pollution increase after a tightening coincides with the decreasing renewable energy ratio, and is stronger for cleaner firms and states. Regarding environmental amenities in consumer welfare, the optimal monetary policy should coordinate with fiscal policy to control inflation with a moderate environmental impact.

Keywords: Monetary Policy, Air Pollution, Clean Investment, Clean Energy, Green Finance

JEL codes: E32, E52, G32, Q43, Q53

*I am grateful to Maximilian Boeck, Marc Dordal Carreras, Zhang Chen, David Cook, Ran Duchin, Kaiji Robin Gong, Christopher House, Tairan Huang, Kohei Kawaguchi, Roni Michaely, Matteo Lanzafame, Byoungchan Lee, Yao Amber Li, Deming Luo, Sangyoon Park, Marta Prato, Deyu Rao, Isabelle Roland, Pau Roldan-Blanco, Eric Swanson, Guillermo Verduzco-Bustos, Yong Wang, Juanyi Jenny Xu, Guang Yang, Jiaheng Yu, Donghai Zhang, Haonan Zhou, and other participants at the HKUST CEP Brown-bag Seminar, the HKUST RPg Student Workshop, the HKU Governance and Sustainability PhD Student Workshop, and the Annual Conference of the IAAE 2025 for their helpful comments and suggestions on the project.

†The Department of Economics at The Hong Kong University of Science and Technology. Email: qwangcq@connect.ust.hk.

1 Introduction

While the central bank's main target is stabilizing inflation, its environmental impact can be substantial. Economic activities, dependent on the financing cost, produce environmental impacts, such as air pollution and carbon emissions. As environmental impact is gradually incorporated into economic sustainability measurement, it is increasingly important in policy evaluation. The environmental impact of fiscal policy, including carbon emission policy, has been well studied (Annicchiarico & Di Dio, 2015; Fischer & Springborn, 2011; Heutel, 2012). However, the environmental impact of monetary policy, the other pillar in the macroeconomic policy analysis, remains relatively underexplored (Annicchiarico & Di Dio, 2017; Attílio et al., 2023).

The central bank adjusts monetary policy to moderate economic and financial conditions, subsequently impacting the environment. When the targeted interest rate increases, it passes to firms' cost of capital (Fornaro et al., 2024; Lee et al., 2021), interfering with their investment decisions (Hartzmark & Shue, 2023). Potentially, monetary policy impacts air pollution through its impact on economic activities. During the transition to a greener economy, as the global economy aims, a higher capital cost places barriers to clean investment (Hirth & Steckel, 2016; Steckel & Jakob, 2018; Zhang et al., 2023). The high capital cost eventually slows down the energy transition and the pollution reduction path. In this paper, I study the direction and magnitude of the impact of monetary policy on air pollution. Then, I search for potential channels through which the monetary policy impacts air pollution.

The environment amenity is increasingly important in measuring consumer welfare. As material consumption increases after centuries of globalization, its marginal welfare improvement gradually declines relative to the environment. The decline accelerates due to increased air pollution after the expansion of global industrial production, which worsens air quality. Toxic air pollutants are detrimental to human health (R. A. Liu et al., 2022). If the ultimate target of macroeconomic policies, including the monetary policy

aiming at inflation stabilization, is consumer welfare maximization (Khan et al., 2003), they should place a weight on environmental concerns. The weight should increase with an increasingly global economy. In this paper, I incorporate environmental amenities into consumer welfare. Then, I study the optimal central bank response and compare it with the policy without incorporating the environmental impacts.

I measure air pollution using geospatial data and monitoring station data. While previous studies on air pollution tend to use the latter, they are subject to issues such as availability, measurement standards, and weighting in aggregation (Burney, 2020; Fan et al., 2023). Firstly, monitoring stations are not available in many places, such as the desert area, where city pollution can spill. The stations are also less established in developing countries. Secondly, the measurement standards vary between monitoring stations, as different stations use devices with potentially different accuracy and capturing standards. The issue is critical in cross-regional or cross-country analysis. Thirdly, when aggregating the results from station level to city level or state level, the weight assigned to each station is by discretion. Due to these issues, I adapt the geospatial data of air pollution, which are globally available, under unique measurement, and scalable.

The aggregated clean investment data are available for the US as collected by the Clean Investment Monitor. It is the only national-level dataset on all clean investments and provides the dynamics of clean investment for each subcategory, such as retail and manufacturing. The dataset enables me to identify the channel from financing cost to clean investment, which subsequently impacts air pollution by developing and implementing clean technology.

To connect macroeconomic dynamics with organizational behavior, I also use the Environmental, Social, and Governance (ESG) data of listed firms in the US. These data support the channel starting from monetary tightening. A higher interest rate increases firms' capital costs, whereas cleaner firms with more green investment are more impacted, slowing down the implementation of clean technology and increasing air pollution.

In this study, I firstly test monetary policy's impact on air pollution and economic activity. Air pollution is identified by applying a Principal Component Analysis (PCA) on a list of key air pollutants used to construct the Air Quality Index (AQI). Monetary policy is identified using the MP1 of Jarocinski shocks, which represents conventional monetary policy. I apply the Local Projection (LP) and the Smooth Local Projection (SLP) methods to the change in air pollution depending on the monetary policy shock (MPs). Surprisingly, after the Federal Fund Rate (FFR) increases, output declines, but air pollution increases. Intuitively, air pollution should co-move with output, as it is proportional to industrial activities.

To investigate the seemingly counterintuitive diverting responses by air pollution and output, I check the clean investment response to MPs and the air pollution response to clean investment. I apply the LP method with Instrumental Variable (IV), where the change in air pollution depends on clean investment with MPs as IV. I find that clean investment declines following a tightening, and air pollution increases with the clean investment decline, suggesting that clean investment is channeling the monetary policy's role in air pollution. To test the channel, I also check the changes in stock indices and energy usage after the tightening, and their responses are consistent with the clean investment channel. As a further step, I use firm data and find that the firm capital cost increases following a tightening. More environmentally friendly firms are more sensitive to tightening regarding capital cost change, exit probability, and firm-level pollution. Additionally, I take advantage of the geospatial pollution data to examine air pollution responses to MPs at the state and mesh levels. I find that air pollution increases more in places with a more stringent environment-related credit policy and a higher clean energy dependency ratio. All empirical findings imply that the clean investment channel drives the diverted responses to MPs by air pollution and output.

Based on the empirical findings, I find the optimal monetary policy to maximize consumer welfare after a MPs. I set up an Environmental Dynamic Stochastic General Equilibrium (E-DSGE) model with two types of capital: traditional and environmen-

tal. Traditional capital works like capital in classic DSGE models, boosting production. Environmental capital reduces air pollution per unit of output, as pollution reduction technology improves with clean investment. I also incorporate a fiscal policy with a pollution tax imposed on firms' pollution. Both firms and the government invest in environmental capital. I estimate novel parameters in the model, which do not appear in previous E-DSGE models, by minimizing the absolute values of IRF distance between the model and the baseline SLP. I also use the Bayesian estimate to check the distribution of the parameters of interest. The estimated optimal policy positively responds to air pollution. For a better stabilizing effect, it needs to coordinate with a fiscal policy that levies the pollution tax rate after the pollution increases following a MPs.

1.1 Literature

The study is related to three stands of literature. Firstly, monetary policy impacts the real economy, and optimal monetary policy has been empirically tested to follow a linear rule. Monetary policy impacts the output (Camara et al., 2024; Kolasa & Wesołowski, 2020; Rossi & Zubairy, 2011) and financial markets (Gürkaynak et al., 2022; Lakdawala et al., 2021; Miranda-Agrippino & Rey, 2020). These impacts subsequently pass to investment activities (Christiano et al., 2005; Tenreyro & Thwaites, 2016), which depend on financing costs and aggregated economic activity. Previous empirical findings suggest that the optimal interest rate follows a Taylor rule (Coibion & Gorodnichenko, 2011; Woodford, 2001), where the interest rate is linear to inflation (Khan et al., 2003) or price (Gorodnichenko & Shapiro, 2007). The rule also dictates that the interest rate positively responds to the output gap (Coibion & Gorodnichenko, 2012) so that the output fluctuates less, leading to less fluctuation in consumption. For the central bank, targeting a specified inflation rate and output gap is to maximize consumer welfare through price stability. My paper contributes to the literature by studying the impact of monetary policy on air pollution, a growingly important determinant of consumer welfare. Based on the main empirical findings, I incorporate pollution targeting into the optimal monetary policy rule to improve its optimality in maximizing consumer welfare.

Secondly, the impact of the interest rate on air pollution is closely related to green finance. Monetary policy has a substantial impact on the green financial market (Lupu et al., 2024), including both equity (Gordo et al., 2024) and debt (Tufail et al., 2024). It also impacts clean energy use regarding both production (Chen & Lin, 2024) and consumption (Hashmi et al., 2022), as an increase in FFR reduces clean energy use and subsequently increases pollution. The interest hike potentially passes to firms' cost of capital (Lee et al., 2021), which is important since clean energy investment is capital intensive (Creutzig et al., 2017; Fornaro et al., 2024; Hirth et al., 2015; International Energy Agency, 2021). Environmental modeling suggests that capital cost impacts clean energy deployment (Hirth & Steckel, 2016; Steckel & Jakob, 2018). When clean energy deployment activities decline, air pollution increases, as measured by firm-level carbon dioxide (CO2) and its equivalent (Hartzmark & Shue, 2023). Previous studies have identified the impact of monetary policy on carbon emissions through investment in photovoltaics (PV) in several Asian economies (Zhang et al., 2023). My paper contributes to the literature by focusing on a comprehensive list of air pollutants. They are more detrimental to human health than CO2, which is usually used to measure pollution in the previous literature. The focus on toxic air pollutants increases the relevance of my empirical findings to consumer welfare regarding environmental amenities. I also identify the decomposed channel from monetary policy to firms' cost of capital, subsequently clean investment, and finally air pollution.

Thirdly, the impact of environmental policy, while typically a microeconomic concern, is gradually drawing the attention of macroeconomics. Output tends to co-move with carbon emission (Attílio et al., 2023; Halkos & Paizanos, 2015; Mughal et al., 2021; Ullah et al., 2021). However, its correlation with other air pollutants is less clear, and the mechanism is more complicated (Clay et al., 2021; R. A. Liu et al., 2022; Shukla et al., 2022). Compared to CO2, toxic air pollutants, such as PM2.5, tend to die out soon when exposed to the air, and their spatial spillovers are limited. Therefore, their dynamics can be better measures to adopt clean technology, especially at the regional level. The environmental amenity first appeared in the consumer utility function in

Roback (1982), and was later incorporated into macroeconomic analysis as a pollution-in-utility function from the consumer side (Angelopoulos et al., 2013). The E-DSGE is based on the macroeconomic DSGE framework and introduces concepts in the Integrated Assessment Model (IAM) (Drudi et al., 2021), such as the negative impact of pollution on output. E-DSGE has been used to evaluate different fiscal policy regimes, such as carbon tax, quota, and intensity targets (Chan, 2020; Fischer & Springborn, 2011; Heutel, 2012). It has also been used to study the impact of coordination between fiscal and monetary policies (Annicchiarico & Di Dio, 2015, 2017), where constraints and trade-offs exist. My paper contributes to the literature by differentiating between traditional (brown) and environmental (green) capital in E-DSGE. I also endogenize pollution abatement technology as it is improved by investing in environmental capital. With my model setting, I analyze the welfare of monetary policy by incorporating air pollution, which is increasingly important in determining consumer welfare. I find the optimal coordination between fiscal and monetary policies to maximize consumer welfare.

The rest of the paper is as follows. Section 2 introduces the data used in the study and shows several stylized facts. Section 3 presents the baseline identification and finding. Section 4 identifies the clean investment channel as the mechanism of the baseline finding with empirical evidence at the national, firm, and regional levels. Section 5 proposes the E-DSGE model based on empirical findings and quantitatively identifies the optimal monetary policy. Section 6 extends the empirical findings globally to test the spillover of US monetary policy. Section 7 concludes.

2 Data and Measurements

This section describes the datasets used in the study. Firstly, I introduce the pollution data, including the geospatial data and the way of aggregation. Secondly, I present the exogenous monetary policy shocks (MPs). Thirdly, I explain official national accounts used in the main findings. Lastly, I display supplementary data, such as firm data and financial market indicators used to support the main findings.

2.1 Pollution

The air pollution geospatial data are from CAMS global reanalysis (EAC4) by the ECMWF global reanalysis of atmospheric composition.[1] The dataset has been validated and used in geographic studies (Inness et al., 2019; Z. Liu & Lu, 2024; Tang et al., 2021; Vazquez Santiago et al., 2024). The sample period starts from 2003 with frequency up to every three hours. The spatial resolution is 0.75 degrees (about 75 km at the equator), rendering each mesh (cell) approximately a 75km-by-75km square. The US contains 2,344 meshes. The mesh size is sufficiently accurate for identifying the pollution dynamics at the state level. For each pollutant, I take the population-weighted sum of the recorded amount in each cell that stays within or touches the state boundary. The summarized value is the amount of the pollutant in the state.[2].

Previously, economic studies tend to use monitoring station data to track the air pollution dynamics. For the US, the most widely used dataset is from the Environmental Protection Agency (USEPA, or EPA).[3] Table A.3 shows an example of selected PM2.5 data. However, their data are subject to three critical issues: Firstly, the dataset is not available everywhere. Secondly, the measurement standards differ by station, as rows 5 and 6 of the table record values substantially differ by measurement method at the same station. The values also substantially differ at the same station even when the method is identical, as shown by rows 1 and 2 or 3 and 4. Thirdly, when aggregating to the state level, the weight of each station is subject to discretion,[4] and the recorded values at different stations (such as the station of the first two rows and the second two rows) can substantially differ. Comparing with monitoring station data, the geospatial dataset is globally available, applies the same accounting standard across regions, and automatically guarantees an unbiased aggregation. Therefore, I adopt geospatial data

[1]The dataset is publicly available on the website of Atmosphere Monitoring Service at copernicus.eu.

[2]For more details about the method I use to aggregate the meshes to the country or state levels, see Appendix A.2

[3]For China, a web-scraping-based dataset is publicly available at quotsoft-dot-net.

[4]A generally used weighting method to weight each station in an aggregated region is to firstly find the geographic center of the region, then assign each station a weight inversely proportional to the distance between the geographic center and the station.

to measure aggregated pollution dynamics at national and state levels. I also use the monitoring station data as a robustness check.

Based on constructing an air quality index (AQI) by air monitoring stations such as the USEPA, I apply the PCA to a list of indicators. The six components I use include PM10, PM2.5, total carbon monoxide (CO), total nitrogen dioxide (NO2), total ozone (O3), and total sulfur dioxide (SO2), consistent with the components of AQI. I apply the PCA on the monthly time series of each component, then extract the first principal component (PC1) as the pollution indicator.[5] PC1 explains more than 90 percent of the total variations of the six components and is, therefore, a reasonable proxy of air quality. The coefficients of all pollutants in PC1 are overwhelmingly positive, except O3, which is negatively correlated with NO2 (Almond et al., 2021). For each pollutant, I apply seasonal adjustment on the aggregated time series using ARIMA-13-SEATS before the PCA.[6]

The dynamics of US pollution (PC1) is in Figure 1. As shown by the HP-filtered trend, pollution has experienced continuous decline since the early 2000s and continues to decline after the Global Financial Crisis (GFC). The Quantitative Easing (QE) period after the GFC and before late 2014 corresponds to a remarkable decline in pollution. The declining trend temporarily paused in 2017, when the US withdrew from the Paris Agreement.

[5]For the detailed description of the method and the PCA statistics, see Appendix A.2.

[6]The application is available using the R function `seasonal::seas`. For time series with frequencies higher than monthly, the R function `dsa::dsa` is useful.

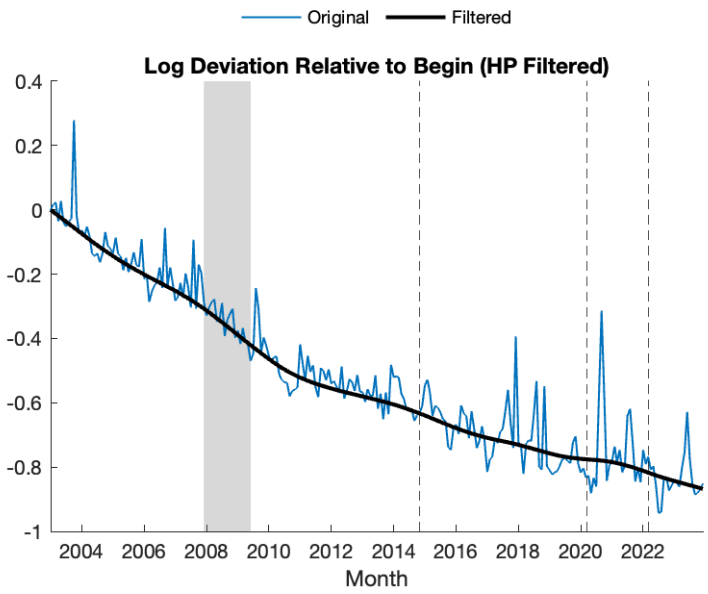

Figure 1: US Pollution Dynamics

Notes: The "Original" series is the seasonally adjusted time series. For the "Filtered" series, the lambda parameter of the HP filter is 14,400. The gray rectangle represents the period from December 2007 to June 2009, corresponding to the Global Financial Crisis (GFC). The dash lines represent the dates 2014/10/29, 2020/03/15, and 2022/03/09, corresponding to Fed policy regime changes.

2.2 Monetary Policy Shock

The baseline monetary policy shock (MPs) used in the study is extracted from 30-minute high-frequency changes in federal fund rates around the Federal Open Market Committee (FOMC) meetings, which captures the unexpected part of interest rate changes.[7] FOMC meetings are usually held on average 8 times each year. We focus on the meetings from 2003 to 2023, as the pollution data start from 2003. 181 FOMC meetings were held during the selected period, and the extracted baseline MPs (MP1) is shown in Figure 2.

[7]The data are from the personal website of Marek Jarocinski.

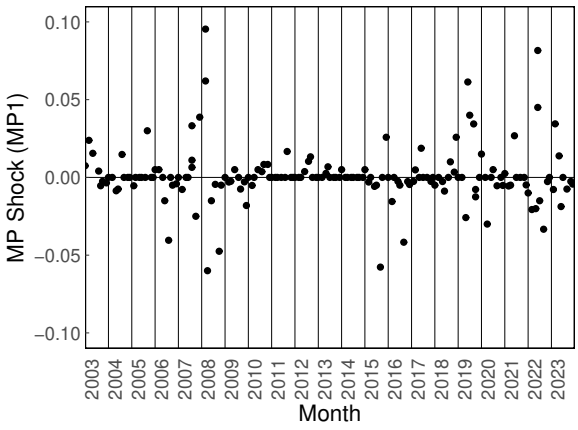

Figure 2: Proxies of Monetary Policy Shock: Baseline

Notes: For each MPs event, the corresponding date is the day when the FOMC is held.

2.3 Other Data

To support my main findings, I also use national account records from the US and other countries, firm data, financial market data, power plant data, carbon emission data, weather data, population density data, and nighttime light (NTL) data. For more details, see Appendix A.3.

The summary statistics of the monthly panel data I use are in Table A.1,[8] and the summary statistics of the quarterly panel data I use are in Table A.2.

3 Responses to Shock

I adopt the local projection (LP, Jordà, 2005) method to study the effects of monetary policy on pollution. The method enables the event-study approach to identify the impact of monetary shock in the presence of confounding factors (Jarociński, 2024; Swanson, 2021). Specifically, I apply the following regression equation.

$$y_{t+h} - y_{t-1} = \sum_{q=1}^{Q} \phi_q^{(h)} \Delta y_{t-q} + \sum_{m=0}^{M} \beta_m^{(h)} x_{t-m} + \sum_{r=1}^{R} \gamma_r^{(h)} W_{t-r} + u_{t+h|t} \tag{1}$$

[8]For GDP, I convert the quarterly series to monthly through the MATLAB function `interp1`, which applies linear interpolation on missing data points.

where y_t is pollution, GDP, or CPI in month t, Δy_t is the change of y in month t relative to month $t-1$, x is the high-frequency FFR shock around the FOMC announcement.[9] I use AIC criteria to choose the lags of pollution and the shocks. In the extended specifications, I add the control W (including changes in other dependent variables in the LP setting).

To deal with the turbulence frequently encountered when entering alternative data in LP, I implement the smooth local projection (SLP, Barnichon and Brownlees, 2019) as the baseline identification.

Applying the equation for $h = 0, \cdots, H$, the IRF is obtained from $\{\beta_0^{(0)}, \cdots, \beta_0^{(H)}\}$. I look up to $H = 30$ months, or 2.5 years. The IRF of the baseline SLP regressions is shown in Figure 3. After a one-unit conventional MPs, output drops by 0.19 log points at its peak 10 months after the shock. Pollution increases by 0.62 log point at its peak 25 months after the shock.[10]

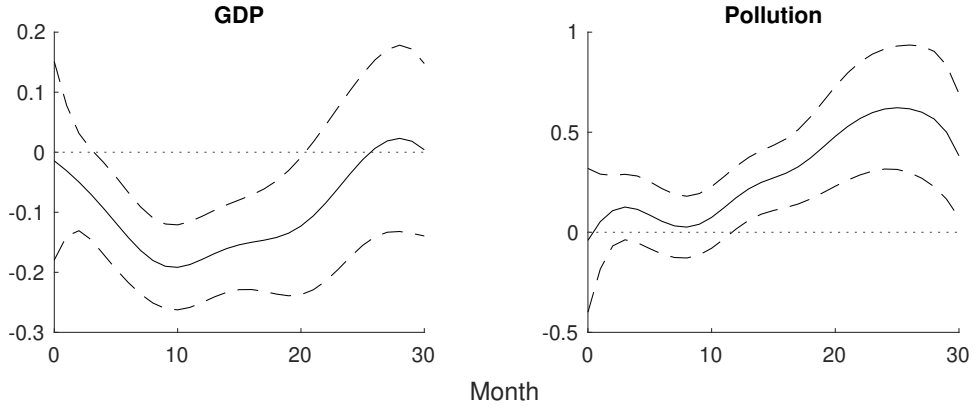

Figure 3: Pollution Response to MPs, Baseline (GDP and Pollution)

Notes: MPs is aggregated to the monthly frequencies consistent with the dependent variable. The number of lags of the dependent variable (Q) and the shock (M) are selected by the AIC criteria for up to 4 periods. The dashed ribbons are the 90 percent confidence intervals generated based on the Newey-West standard errors.

The result is surprising: After the monetary tightening, output declines but pollution

[9] I only study the effects of conventional monetary policy in the baseline. The comparison with unconventional monetary policy will be discussed later.

[10] The MP1 shock used here has a period-wise standard deviation of 0.072, or monthly standard deviation of about 0.05.

increases. Intuitively, air pollution should co-move with output, as it positively correlates with economic activities (Clay et al., 2021). The mechanism behind the diverging paths of output and pollution after tightening remains to be solved.

3.1 Robustness

From the deviating paths of output and pollution, the first check to look at is the change in pollution per unit of output by the MPs. If clean investment decreases following a tightening, pollution per unit of output should increase, as shown in Figure 4. The effect turns significantly positive 12 months after the MPs before gradually growing, implying a lagged response of pollution to monetary policy and investment activities.

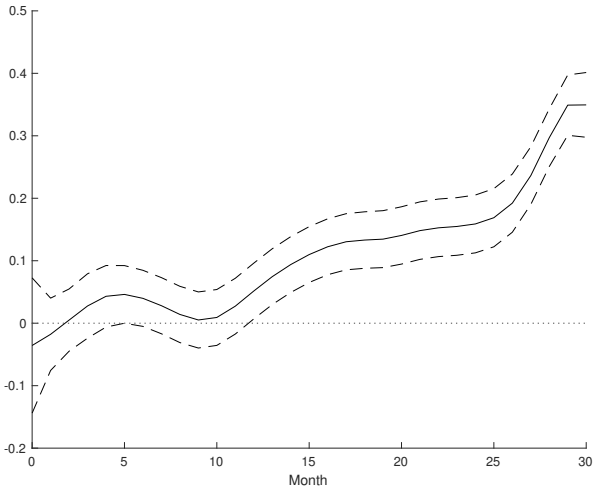

Figure 4: Pollution per Unit of GDP Response to MPs

Notes: MPs is aggregated to the monthly frequencies consistent with the dependent variable. The number of lags of the dependent variable (Q) and the shock (M) are selected by the AIC criteria for up to 4 periods. The dashed ribbons are the 90 percent confidence intervals generated based on the Newey-West standard errors.

To address the potential issues caused by the arbitrary PCA, I look at the responses to the tightening by different pollutants. The IRF to MPs for each pollutant predominantly explained by the first component from the the PCA is in Figure 5. All the pollutants increase after tightening.

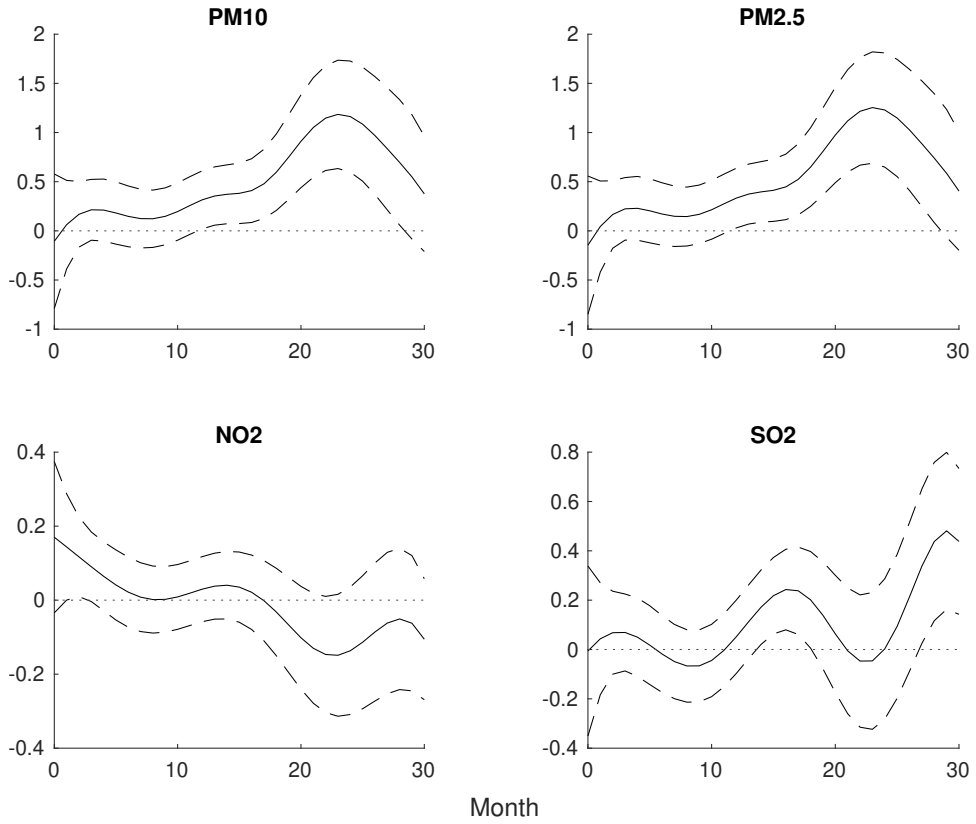

Figure 5: Pollution Response to MPs, by Pollutant

Notes: MPs is aggregated to the monthly frequencies consistent with the dependent variable. The number of lags of the dependent variable (Q) and the shock (M) are selected by the AIC criteria for up to 4 periods. The dashed ribbons are the 90 percent confidence intervals generated based on the Newey-West standard errors.

I also investigate the time-varying pollution responses to MPs. I divide the sample into three periods: before GFC, post-GFC and before the withdrawal from the Paris Agreement, and since the withdrawal. The IRF results for each period are in Figure 6. The positive response, especially the long-term positive response, is driven by the last period. The period before the GFC shows an overall negative response, as pollution co-moves with output and does not depend on clean investment. The different responses across the three periods are consistent with the recent surge in clean investment, when clean investment in the US has become the new general trend.

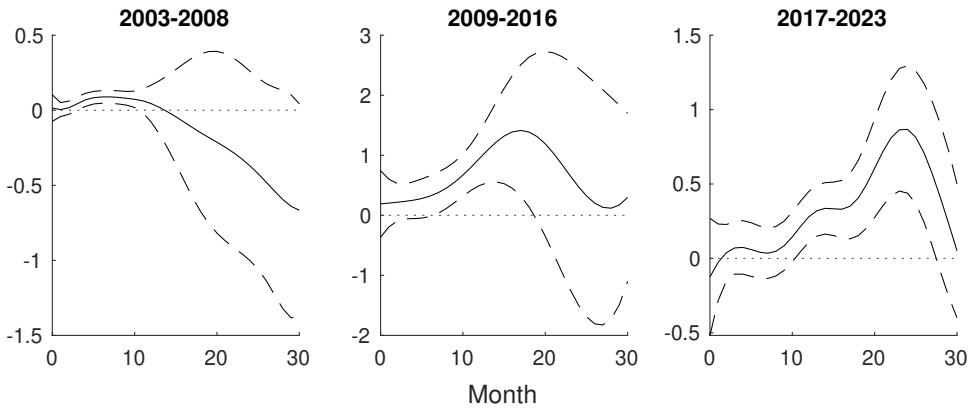

Figure 6: Pollution Response to MPs, by Period

Notes: MPs is aggregated to the monthly frequencies consistent with the dependent variable. The number of lags of the dependent variable (Q) and the shock (M) are selected by the AIC criteria for up to 4 periods. The dashed ribbons are the 90 percent confidence intervals generated based on the Newey-West standard errors.

The baseline result is robust to other checks. (1) The responses remain qualitatively the same with the minimum delay assumption, as shown in Figure B.1. (2) Extending the IRF horizon to longer periods (60 months, or 5 years), the positive pollution response stays, as shown in Figure B.2. (3) By assuming that there are no lagged responses in MPs and only one lagged period of pollution, the results remain, as shown in Figure B.3. (4) Using the LP-IV identification with endogenous FFR and MPs as IV, the result qualitatively remains, as shown in Figure B.4. (5) By replacing GDP with industrial production (IP), which is available monthly, as the proxy of output, the result still holds, as shown in Figure B.5. (6) The pollution responses to the MPs are positive to the sign of the MPs when the shock is either positive or negative, as shown in Figure B.6. (7) Pollution is potentially determined by the weather conditions regardless of economic activities. To exclude this potential channel, I control for the average monthly temperature, and the result remains qualitatively unchanged after adding the control, as shown in Figure B.7. (8) I test for the potential pretrend of the pollution before the shock, and I do not find any significant pretrend, as shown in Figure B.8. (9) The responses potentially differ across periods, as the mechanism of monetary transmission changes in a low-interest

environment. However, I find positive pollution responses to be universal in both QE and non-QE periods, as shown in Figure B.9, and in both ZLB binding and non-binding periods, as shown in Figure B.10. (10) When I change the Jarocinski MP1 response to other conventional MPs, the positive response remains, as shown in the upper half of Figure B.11. However, the positive response does not apply to unconventional MPs, as shown in the lower half, suggesting that the environmental impact of MPs is transmitted only through conventional monetary policy. (11) By applying the PCA analysis to the aggregated pollution of all countries instead of the US itself, the result does not qualitatively change, as shown in Figure B.12. (12) Using weekly pollution series, pollution response to MPs remains positive, as shown in Figure B.13. (13) Using quarterly pollution series aggregated from the monthly series, pollution response to MPs remains positive, as shown in Figure B.14. (14) Using the pollution series from the EPA monitor station data with the same PCA method as in the baseline, the long-term positive pollution response remains significant and substantial, as shown in Figure B.15. (15) Adding the second principal component (PC2) in the PCA to the baseline LP, the baseline results do not qualitatively change, as shown in Figure B.16. (16) The positive pollution response to MPs holds not only for the US but also for the EU (Figure B.17) and Japan (Figure B.18). In both cases, the pollution only positively responds to domestic MPs instead of the US shock, suggesting the channel to be predominantly domestic.

4 Clean Investment Channel

In this section, I illustrate that the baseline finding is consistent with a clean investment channel. Firstly, investment declines after tightening, especially clean investments that impact air pollution. Secondly, the use of renewable energy declines in the long run, suggesting less adoption of clean technology during the transition phase. Thirdly, firm-level evidence suggests that cleaner firms are more sensitive, more likely to exit, and have more pollution increase after tightening. Finally, regional analysis implies that places with lower green premiums and higher clean energy dependency have more pollution

increase after a tightening. All these findings support the channel, and the connection of the steps is illustrated in the flowchart in Figure 7.

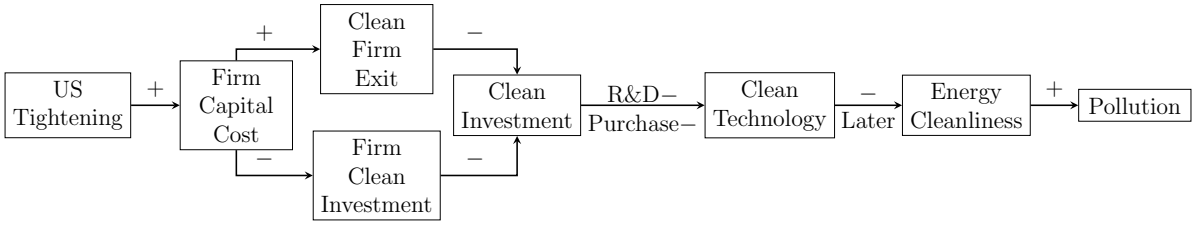

Figure 7: Flowchart of the Mechanism

4.1 Clean vs Non-clean Investment

Monetary policy impacts the economy through the interest rate, which directly affects investment activities, including clean investment. Since the end of the GFC, the Fed has started three rounds of Quantitative Easing (QE) to stimulate the economy, exposing the economy to a low-interest rate environment. Such an environment boosts investment, particularly capital-intensive clean investment. As shown in Figure 8, FFR stayed close to zero after the GFC until the end of 2014, when US exited the QE. Firms' cost of capital declined concurrently, implying the transmission from low FFR to low firm capital cost. The low FFR and capital cost are accompanied by an increase in clean energy share, defined as the percentage of clean energy capacity among newly commissioned power plants.[11] Intuitively, the low-interest environment nurtures clean investment, boosting the use of clean energy.

[11] Clean energy includes biomass, geothermal, hydropower, nuclear, solar and wind. Non-clean energy includes coal, oil and gas.

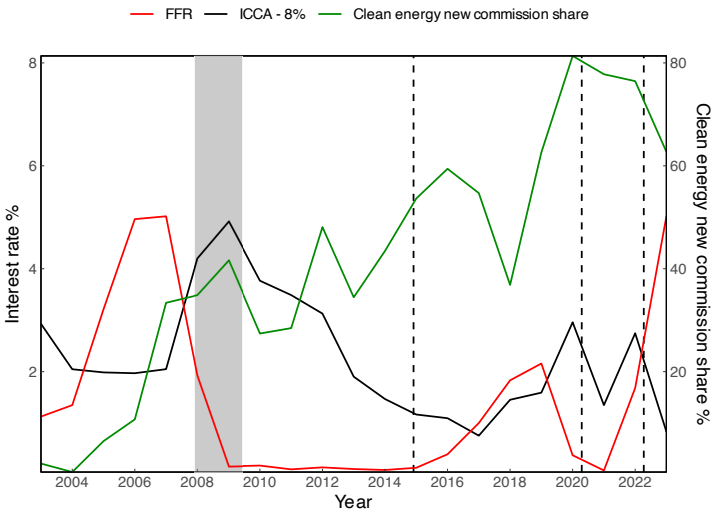

Figure 8: FFR, Cost of Capital, and Clean Energy New Commission Share

Notes: For each year, the ICCA is calculated as the average of all firms in all months. The gray rectangle represents the period from December 2007 to June 2009, corresponding to the Global Financial Crisis (GFC). The dash lines represent the dates 2014/10/29, 2020/03/15, and 2022/03/09, corresponding to Fed policy regime changes.

The importance of clean energy started to increase after the GFC. While most newly opened power plants used non-clean technology before the GFC, the share of clean technology turned substantial afterward, as shown by the cumulative capacity of newly opened power plants since 1993 in Figure 9. By 2023, clean technology-based power plants account for more than a third of the cumulative new capacity, in contrast to less than 5 percent in 2007. The total clean investment also experienced a steady increase throughout the year, as shown by Figure 10. Air pollution declines during the period, as in Figure 1. Therefore, the increase in clean energy new commission share is likely driven by the low interest rate environment and improves air quality.

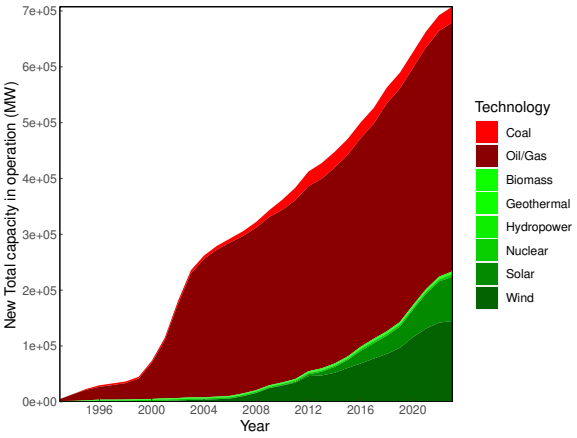

Figure 9: New Power Plant Capacity Commissioned by Year, US

Notes: The capacity of commission is the cumulative value since 1993, the beginning of the sample period.

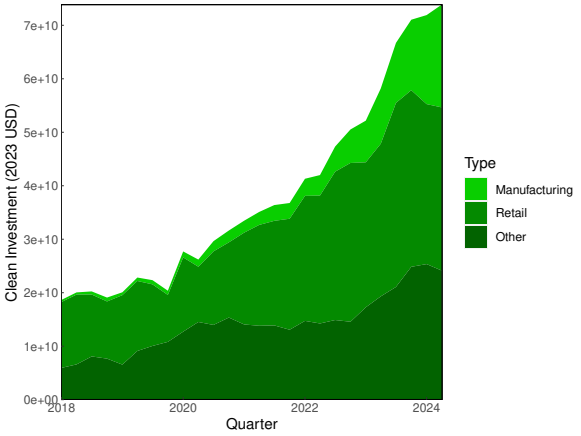

Figure 10: Clean Investment by Quarter, US

Notes: Technologies included in each segment (type) follow the overall investment trends for the US economy as reported by the Bureau of Economic Analysis (BEA).

To associate the observed increase in air quality with monetary policy, I firstly look at the impact of interest rates on clean investment. I use quarterly aggregated investment data and aggregate monthly MPs to quarters. As shown in Figure 11, among investments, the sensitivity of clean investment is particularly high to tightening, consistent with the capital-intensive property of clean investment. Manufacturing clean investment, which represents clean technology development, and retail clean investment, which represents clean technology adoption by households and businesses, are particularly slashed by a tightening. I define investment cleanliness as the ratio of all clean investment over all investment, and it decreases following as tightening. The results show that clean investment is highly sensitive to MPs, and the response is quick.

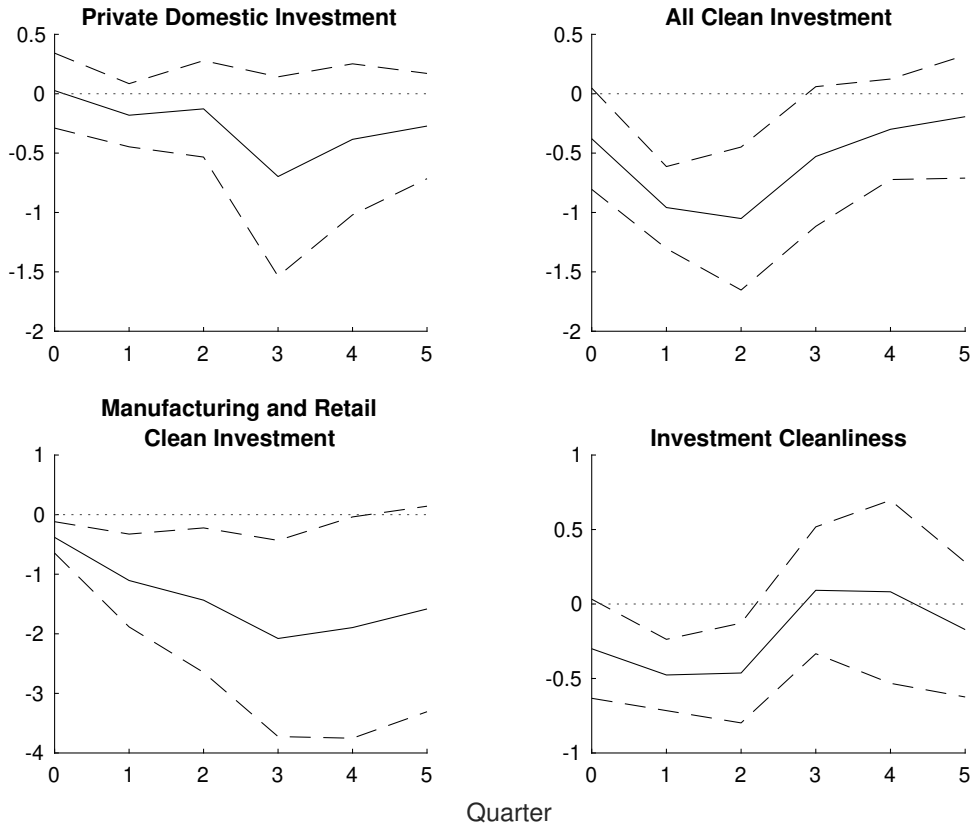

Figure 11: Clean Investment Response to MPs

Notes: MPs is aggregated to the quarterly frequencies consistent with the dependent variable. The number of lags of the dependent variable (Q) and the shock (M) are selected by the AIC criteria for up to 4 periods. The dashed ribbons are the 90 percent confidence intervals generated based on the Newey-West standard errors.

Next, I look at the response of air pollution to clean investment. Since the interest rate is unlikely to affect air quality through ways other than clean investment, and it drives clean investment, as shown above, I use the exogenous MPs as an IV of clean investment in the LP of pollution on clean investment. The IRF in Figure 12 shows that pollution decreases after clean investment increases. Pollution per unit of GDP also decreases, as shown in Figure C.1. Therefore, tightening discourages clean investment, which eventually worsens air quality.

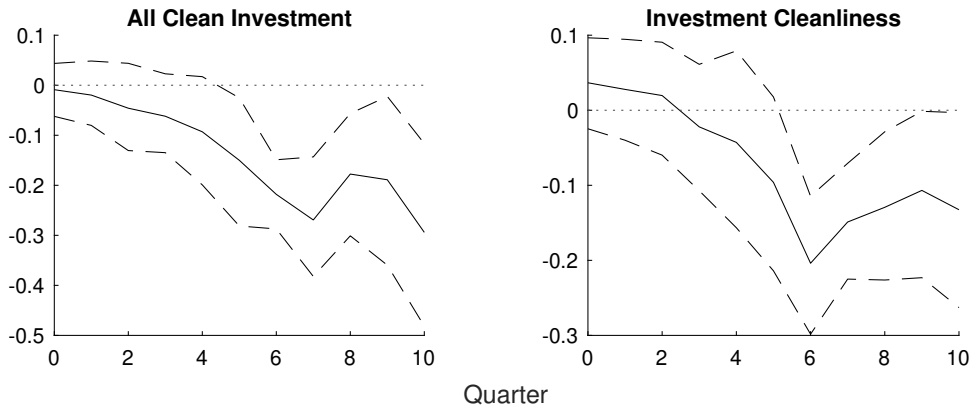

Figure 12: Pollution Response to Clean Investment (IV: MPs)

Notes: MPs is aggregated to the quarterly frequencies consistent with the dependent variable. In the first stage, the number of lags of the endogenous variable is selected by the AIC criteria for up to 4 periods. In the second stage, the number of lags of the dependent variable (Q) and the endogenous variable (M) are selected by the AIC criteria for up to 4 periods. The dashed ribbons are the 90 percent confidence intervals generated by bootstrapping with 1,000 draws.

The magnitude and time horizon of air pollution response to MPs using the two-stage LP-IV identification (through endogenous clean investment) roughly match the baseline. In the baseline, pollution increases by 0.62 log point after a one-unit MPs, and the peak comes 25 months (8 quarters) after the shock. From the perspective of all clean investments, investment decreases by 1 log point one quarter after a one-unit MPs, and pollution increases by about 0.3 log points seven quarters after the investment decline. From the manufacturing and retail clean investment perspective (Figure C.2), investment declines by 2 log points three quarters after a one-unit MPs, and pollution increases by 0.4 log points seven quarters after the investment decline.[12]

The stock market also reflects the decline in clean investment by tightening. I use daily closed prices of stock market indices and the MPs in corresponding FOMC dates. As shown in Figure 13, stock market indices fall after tightening, especially indices with clean

[12]The baseline uses monthly frequency, and the peak response is 0.62 log point, higher than the 0.3 or 0.4 log points implied by LP-IV. However, the monthly peak should be higher than the quarterly peak, and averaging the responses to quarterly frequency lowers the peak impact. By aggregating the time series to quarterly with the same specification as the baseline, the peak response turns to about 0.52 log points 8 quarters after the MPs, which matches closer to the magnitude implied by LP-IV.

investment concepts. For both NASDAQ and S&P 500, the magnitude of the decline is stronger for the subindices that represent clean investment, including NASDAQ Renewable Energy Equipment (RE), NASDAQ Clean Edge Green Energy (CELS), S&P 500 Clean Power, and S&P 500 Cleantech.[13] With a forward-looking property, the response to MPs by clean investment-related equity is stronger than aggregated clean investment in magnitude, and its results support the clean investment channel.

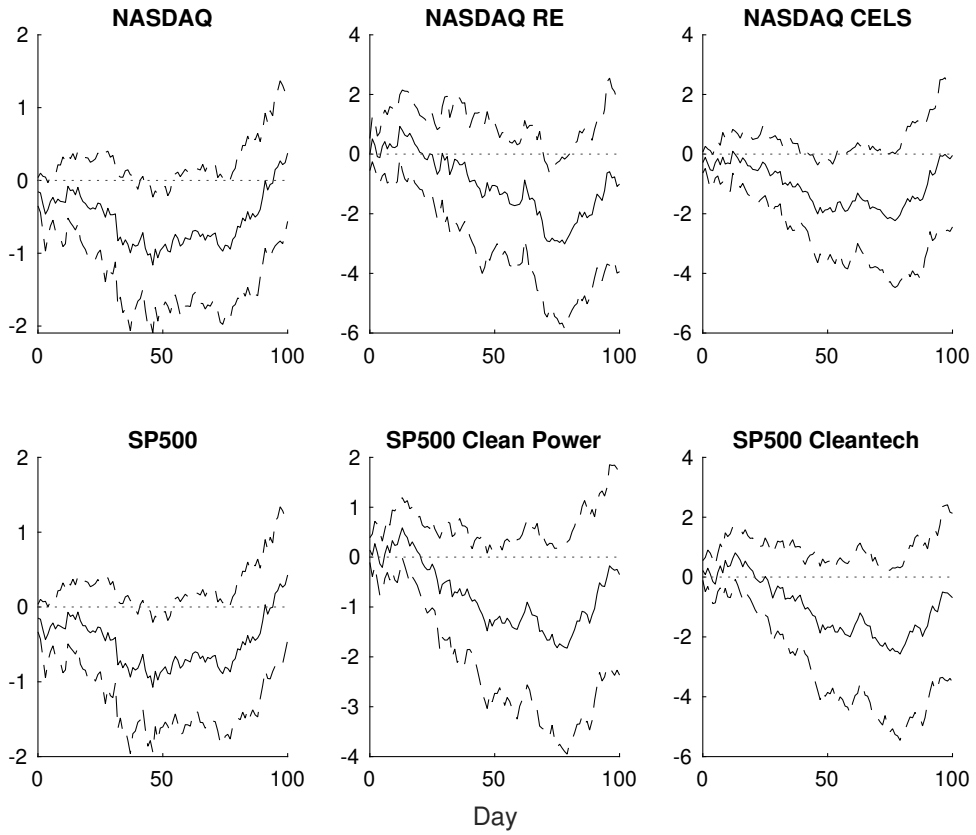

Figure 13: Equity Market Response to MPs

Notes: The number of lags of the dependent variable (Q) and the shock (M) are selected by the AIC criteria for up to 4 periods. The dashed ribbons are the 90 percent confidence intervals generated based on the Newey-West standard errors.

[13]NASDAQ RE and NASDAQ CELS indices have been available since early 2015. S&P 500 Kensho Clean Power and S&P Kensho Cleantech indices have been available since late 2016. Therefore, I subsample these indices to the period since 2016Q4 for data availability and comparability. I also exclude the period after 2022Q1 to avoid the stock market turbulence since then.

4.2 Clean Energy Share

If clean investment declines following a tightening, and it impacts air pollution through clean energy use, the tightening will impact the energy use structure. The traditional and clean energy usage responses to MPs, as shown in Figure 14, support the channel. Fossil fuel production increases, while renewable energy (RE) production declines following a tightening. The decline in renewable energy use aligns with previous literature (Chen & Lin, 2024; Hashmi et al., 2022). The short-term dynamics are potentially due to the decline in fossil fuel prices after tightening, as shown in Figure C.3. My new finding is that the decline in renewable energy use does not recover, implying a long-term structural change in energy use. Potentially, a tightening slows down the ongoing transition towards clean energy by raising the cost of clean investment. The energy cleanness worsens as a result of the lower clean investment.

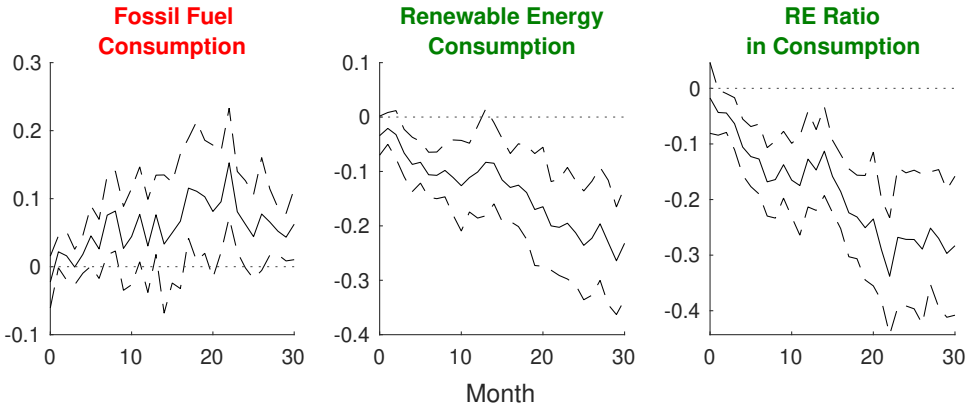

Figure 14: Clean Energy Use Response to MPs

Notes: MPs is aggregated to the monthly frequencies consistent with the dependent variable. The number of lags of the dependent variable (Q) and the shock (M) are selected by the AIC criteria for up to 4 periods. The dashed ribbons are the 90 percent confidence intervals generated based on the Newey-West standard errors.

4.3 Cleanliness of Firms

The decline in clean investment following a tightening is also supported by firm-level evidence, and it particularly impacts environmentally friendly firms. The first step for

the central bank interest rate to impact the firms is to pass to the firms' capital cost. For each firm in each month, I use the Analyst-forecast-based Implied Cost of Capital (ICCA) calculated by Lee et al. (2021), which is suitable for time-series analysis. The identification is as follows.

$$\text{ICCA}_{t+h} - \text{ICCA}_{t-1} = \phi^{(h)} \Delta\text{ICCA}_{t-1} + \beta^{(h)} x_t + u_{t+h|t} \tag{2}$$

The parameter estimate to look at is $\beta^{(h)}$.

As shown in Figure 15, the tightening impact passes to capital cost in 8 months, and its impact continues for another 8 months. The transmission is sufficiently quick to identify the tightening impact on investment concurrently at an annual frequency, as the response turns significantly positive within one year.

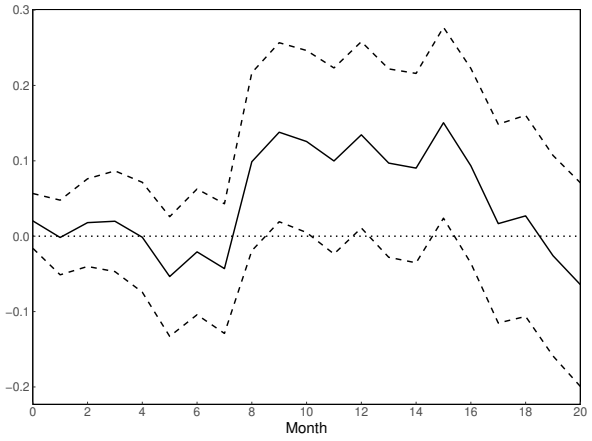

Figure 15: ICCA Response to US MPs

Notes: The dashed ribbons are the 90 percent confidence intervals generated based on standard errors clustered to firm and year.

Moreover, the response to the tightening is more sensitive for environmentally friendlier firms. I apply the following identification to estimate the heterogeneous effect across firms' cleanliness.

$$\text{ICCA}_{i,t+h} - \text{ICCA}_{i,t-1} = \phi^{(h)} \Delta\text{ICCA}_{i,t-1} + \beta_1^{(h)} s_{i,t-L} + \beta_2^{(h)} x_t s_{i,t-L} + \alpha_i^{(h)} + \tau_t^{(h)} + u_{i,t+h|t} \tag{3}$$

Here, I proxy environmental friendliness by four indices: renewable energy ratio, CO2 equivalent per unit of revenue, emission score, and resource use score. Note that I use

last year's indice, $s_{i,t-L}$, for each firm i to exclude potential endogeneity issues. The interaction terms of MPs and the indices, β_2, reflect the sensitivity of firm environmental friendliness to the response to MPs, and their results are shown in Figure C.4.

The environmentally friendlier firms are more likely to quit after a tightening. I identify the probability of a listed firm in the US exiting the market as dependent on the cost of capital interacting with the environmental friendliness indicator, and the interaction term captures the sensitivity of raising capital cost by environmental friendliness. The identification is the following logit regression.

$$\log\left(\frac{1}{1-\Pr(\text{Exit}_{i,t})}-1\right)=\beta_0+\beta_1 s_{i,t}+\beta_2 x_t s_{i,t}+\gamma W_{i,t}+u_{i,t} \tag{4}$$

Controls, W, include the number of years the firms exist in the market. Using the logit regression, Table 1 shows that environmentally friendlier firms are more likely to quit after a tightening. When environmentally friendly firms exit disproportionally after tightening, existing firms' average environmental awareness declines, negatively impacting clean energy adoption and clean investment and, subsequently, air pollution.

Table 1: Firm Exit Probability, Logit Regression

	Original	Renewable Energy Ratio	CO2 Equivalent / Revenue	Emission Score	Resource Use Score
ICCA	5.8766***	-8.8430	12.3992***	5.2579***	4.3996***
	(0.2355)	(7.1787)	(2.1817)	(1.3596)	(1.4037)
Indicator		-1.6283+	2.1941***	-2.8786***	-2.9768***
		(1.1348)	(0.6433)	(0.4546)	(0.4549)
ICCA × Indicator		21.7395**	-6.6377+	5.8759*	8.2521**
		(10.1555)	(4.5306)	(3.4717)	(3.4581)
N	70670	6241	19241	34980	34980
AIC	31571	522	1501	4248	4263

Notes: Significance Codes: ***: 0.01, **: 0.05, *: 0.1, +: 0.2.

Then, I look at firms' pollution emission responses to a tightening using the following identifications.

$$y_{i,t} = \beta x_t + \gamma W_{i,t} + \alpha_i + u_{i,t} \tag{5a}$$

$$y_{i,t} = \beta_1 s_{i,t} + \beta_2 x_t s_{i,t} + \alpha_i + \tau_t + u_{i,t} \tag{5b}$$

Here Equation 5a is the original specification of firm emission to the tightening, and Equation 5b is used to look at heterogeneous responses across firms' cleanliness.

From the firm-level emission record, a tightening also degrades air cleanliness, and the impact is partly through leaving a stronger impact on environmentally friendlier firms. Using CO2 equivalent (Scope 1 and 2, which includes direct emission) as the proxy for pollution, a tightening increases pollution, as shown in the first column of Table 2. The result is in line with Hartzmark and Shue (2023). In the other columns, the interaction term captures the sensitivity of pollution to environmental friendliness after the tightening, and the environmentally friendlier firms respond more to the tightening.[14]

To exclude the impact of potential noise in the firm-level indicators, I replace the cleanliness indicator with the dummy of whether the cleanliness ranking of the firm is above the 80th percentile (or below the 20th percentile) and look at the interaction term of the dummy with the MPs. The results suggest more responses by the cleanest fifth and fewer responses by the least clean fifth of all firms, as in Table C.1. The results align with the baseline, suggesting that the firm's clean investment change is an important source of the channel from MPs to air pollution.

[14] I include Year FE as I intend to capture the variation by MPs after controlling for firm and year fixed effects.

Table 2: Firm Pollution Responses to MPs and Cleanliness

	Original	Renewable Energy Ratio	Emission Score	Resource Use Score
MPs	0.3060**			
	(0.1307)			
Indicator		0.0566	0.0187	0.0816
		(0.1000)	(0.0765)	(0.0768)
Indicator × MPs		1.4664**	1.5413*	2.0115**
		(0.6344)	(0.8016)	(0.8583)
Firm FE	Yes	Yes	Yes	Yes
Year FE		Yes	Yes	Yes
N	5,093	1,132	4,716	4,716
Adjusted R^2	0.9795	0.9771	0.9812	0.9809

Notes: Significance levels are based on Firm standard-errors. For specifications with Year FE, they are based on Firm and Year standard-errors. Significance Codes: ***: 0.01, **: 0.05, *: 0.1, +: 0.2.

4.4 Cleanliness of Regions

Taking advantage of the geospatial data, I study the heterogeneous pollution responses across regions. By applying the baseline identification to each mesh, I obtain the IRF for each mesh. I apply the same equation as Equation 1 to each region i that can be mesh, and the specification is as follows.

$$y_{i,t+h} - y_{i,t-1} = \sum_{q=1}^{Q} \phi_{i,q}^{(h)} \Delta y_{i,t-q} + \sum_{m=0}^{M} \beta_{i,m}^{(h)} x_{t-m} + \sum_{r=1}^{R} \gamma_{i,r}^{(h)} W_{i,t-r} + u_{i,t+h|t} \tag{6}$$

Then, I take the average of the responses across months, and the map showing the average response at mesh level is in Figure 16. While the pollution response is predominantly positive across states, it is driven by the West and the Midwest, which are characterized by more stringent environmental policies and higher clean energy depen-

dency compared to other US regions. Most pollution declines come from west Texas, where traditional energy facilities are concentrated. In California, the strongest pollution increase comes from the most polluted Greater Los Angeles area, suggesting that the recorded response is not driven by noise in humanless places. Then, I aggregate the mesh-level pollution data to state level and obtain the IRF for each state. The map showing the average response by each state is in Figure C.5.

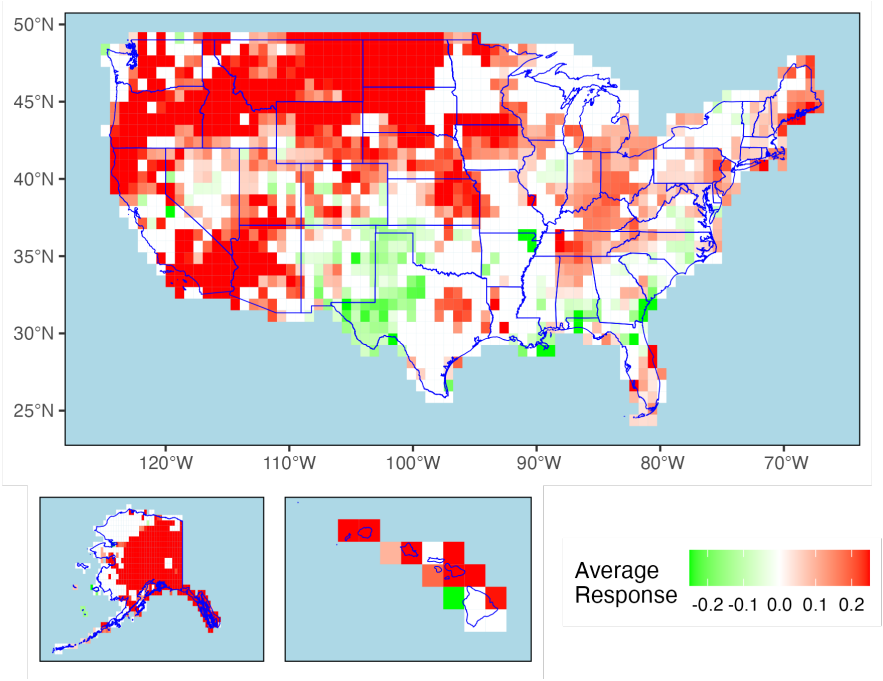

Figure 16: Average Pollution Response to MPs by Mesh

Notes: MPs is aggregated to the monthly frequencies consistent with the dependent variable. The number of lags of the dependent variable (Q) and the shock (M) are selected by the AIC criteria for up to 4 periods. When taking the average across the time horizon from the month the MPs is realized to 20 months later, insignificant values at a 90 percent confidence level are treated as zero. If the region has both significantly positive and significantly negative responses, the average response by the region is interpreted as zero. Extreme values with absolute values greater than 0.25 are winsorized on the map.

Intuitively, in states with more stringent environmental policies, firms invest more in clean energy, and the green premium, as defined by the difference in capital cost of environmentally friendly and environmentally hazardous firms, is lower. Consequently,

firms try to become environmentally friendlier for a lower capital cost, partly by cleaning up their investment. Therefore, these states are more sensitive to tightening, as clean investment accounts for a greater share of total investment. To test this hypothesis, I use the following identification.

$$y_{i,t+h} - y_{i,t-1} = \beta_1^{(h)} s_{i,t-L} + \beta_2^{(h)} x_t s_{i,t-L} + \gamma^{(h)} W_{i,t-1} + \alpha_i^{(h)} + \tau_t^{(h)} + u_{i,t+h|t} \tag{7}$$

Here $y_{i,t}$ is pollution in state i in year-month t. x_t is MPs in year-month t. $s_{i,t}$ is the regional indicator (e.g., environmental friendliness) in state i in month t.[15] W includes controls, such as weather. α and τ are state and month fixed effects, respectively. To exclude potential endogeneity, the regional indicator I use in the regression is lagged by L. I choose the length of the lag as one year in the baseline. The key coefficients to estimate are $\beta_2^{(h)}$, corresponding to the interaction term.

To look at the impact of environmental friendliness on the pollution response to MPs, I firstly define the green premium indicator. For each state, I group all firms according to an environmental indicator, such as the renewable energy usage ratio. The firms ranking in the top 20 percent are the high-value firms, and those ranking in the bottom 20 percent are the low-value firms. Then, I calculate the average capital costs of high-value and low-value firms. Their difference is the green premium. I use the green premium as the regional indicator in the interaction term identification, and the IRFs of the interaction term are in Figure 17.[16]. The interaction term of green premium and MPs is constantly negative using the renewable energy ratio as the grouping factor, implying that when a state imposes a more stringent environmental policy, defined as having a lower green premium, the air pollution response to tightening increases.

[15] The regional indicators are at annual frequency. Therefore, the value used depends on the year corresponding to year-month t.

[16] For each facet in the figure, if the indicator has positive upward polarity for environmental friendliness, I color the facet title in green, otherwise I color it in red.

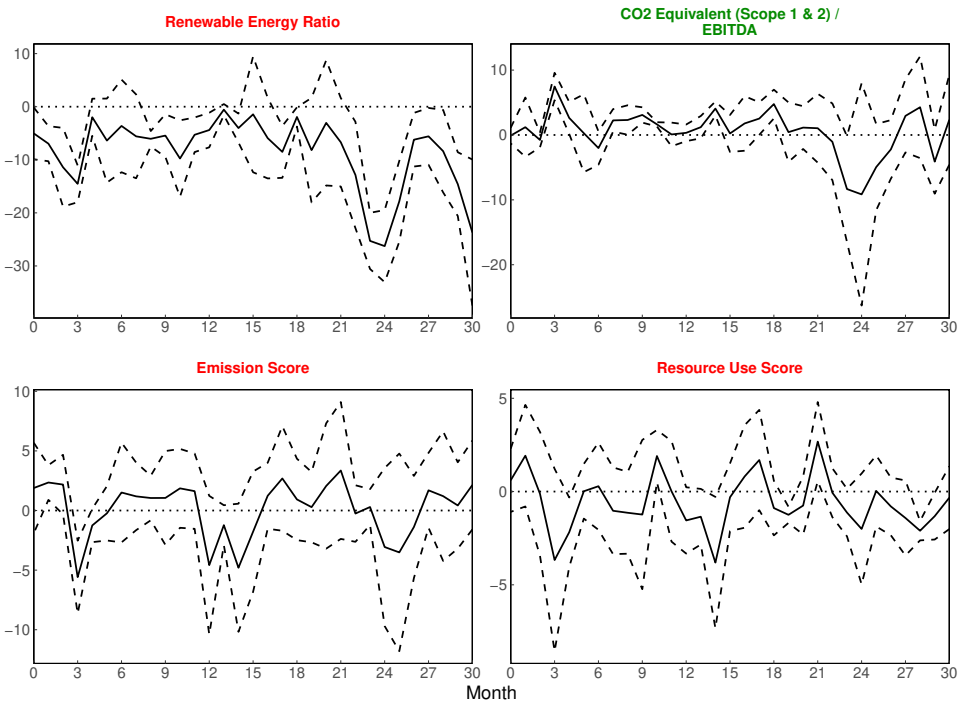

Figure 17: Pollution Response to Interaction of US MPs and Clean Energy Credit Support, State level

Notes: The dashed ribbons are the 90 percent confidence intervals generated based on standard errors clustered to region and year.

Then, I use clean investment share in GDP as the proxy for the environmental friendliness indicator. Intuitively, places with higher environmental policy stringiness are more inclined to clean investments. The IRFs of the interaction terms are in Figure C.6. The increase in air pollution is stronger in states with a higher clean investment share in GDP, especially retail clean investment share, suggesting clean investment as a channel for the pollution response to tightening.

Then, I use the clean energy dependency ratio as the regional indicator. For each state, the clean energy dependence ratio is the clean energy power plant capacity divided by the total power plant capacity. The IRFs of the interaction terms are in Figure 18. The pollution response increases with the share of clean energy and declines with the dependency on coal, oil and gas. As clean investment, including capital-intensive investment in clean power plants, is more prominent in states with a higher clean energy

dependency ratio, tightening has a stronger impact in these states.

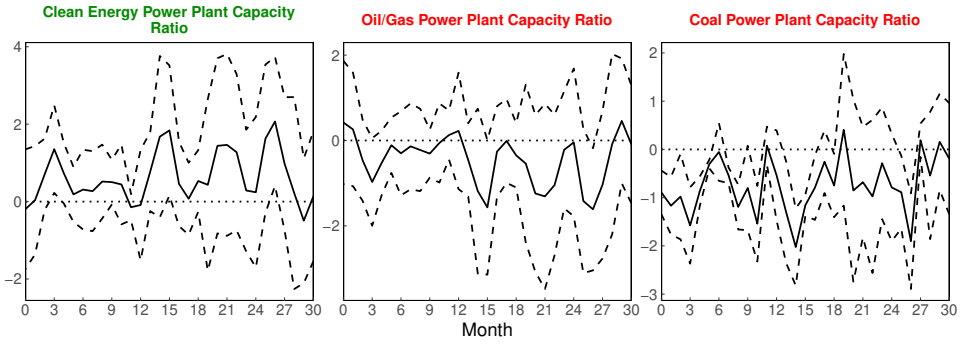

Figure 18: Pollution Response to Interaction of US MPs and Clean Energy New Commission Share, State level

Notes: The dashed ribbons are the 90 percent confidence intervals generated based on standard errors clustered to region and year.

As a further step, I directly study the heterogeneous responses at the mesh level. To match the firms with the meshes, I geocode the location of the address of the headquarters of each firm and locate the mesh of the location. Then, I calculate the average of the firm-level indicators (e.g., renewable energy usage ratio) of all firms within each mesh. As an illustration, the average renewable energy usage ratio at the mesh level is shown in Figure C.7.

By applying the interaction term identification at the mesh level, the results using the green premium as the regional indicator are shown in Figure C.8. By including at least the first-degree neighboring meshes, the results are consistent with my hypothesis that environmental stringiness induces more clean energy investment and exposes a region under a higher pollution sensitivity to tightening.[17]

Likewise, I use the clean energy dependency ratio as the regional indicator at mesh level. The map showing the cleanliness of power plants within each mesh is in Figure C.9.

[17] At least the first-degree neighboring meshes should be included when measuring the pollution impact of a tightening. Assume pollution to be evenly spread across each direction. When the firm is located in a corner of the mesh, only a quarter of the pollution is recorded within the mesh. Overall, $\frac{7}{16}$ of the pollution sourced within a mesh impacts the area outside the mesh.

The clean power plants are more sparsely distributed than traditional energy-based power plants. The IRFs of the interaction term between the regional indicator and the MPs are shown in Figure C.10. In line with state-level findings, places with a higher clean energy dependency are exposed to more pollution increases after a tightening.

5 Optimal Policy Coordination

In this section, I present the E-DSGE model used to simulate previous empirical findings. Firstly, I quantitatively sketch the agents' behaviors in the economy, including the behaviors of households, firms, the government, and the central bank. Secondly, I calibrate the model with parameters based on previous literature before estimating the new parameters using Bayesian estimation. Thirdly, I find the optimal coordination of fiscal and monetary policies that maximizes consumer welfare after a monetary tightening.

Based on Annicchiarico and Di Dio (2015), I introduce a household utility function with pollution, two types of capital (clean and traditional), a pollution factor dependent on environmental capital, and a pollution tax invested in environmental capital. The model starts with a representative agent whose utility is determined by a composite consumption, cash holding, and labor. The composite consumption consists of consumption (good) and pollution (bad). The price dynamics follow the New Keynesian framework with Calvo price adjustment. Capital consists of traditional capital and environmental capital. Firm factors of production include traditional capital and labor. It produces goods with pollution, and the pollution factor (intensity per unit of good) depends on clean technology. Clean technology is improved with environmental capital. The representative firm also chooses the abatement effort, where the cost of abatement increases with the effort, and the pollution declines with the effort. The government charges a pollution tax on firms proportional to pollution, and invests all the tax income on environmental capital. The central bank sets the interest rate following a Taylor rule linearly dependent on inflation and the output gap. The flowchart of the model is in Figure 19.

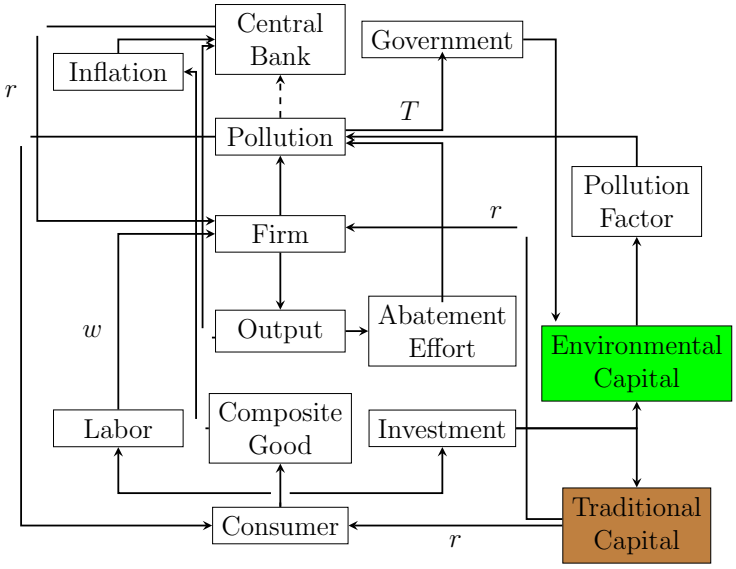

Figure 19: Flowchart of the Model

5.1 Model Setting

5.1.1 Household

The representative household maximizes its utility across periods, V.

$$\max_{C_t, M_t, L_t, B_t, I_t} V_t = \mathcal{U}_t + \beta \mathbb{E}_t V_{t+1} \tag{8}$$

It chooses the good C, cash holding M, labor L, bond holding B, and investment I, in each period t. The time discount factor per period is β.

The utility per period, $\mathcal{U}$, is determined by:

$$\mathcal{U}_t = \frac{\tilde{C}_t^{1-\sigma}}{1-\sigma} + \frac{\gamma}{1-b}\left(\frac{M_t}{P_t}\right)^{1-b} - \chi \frac{L_t^{1+\eta}}{1+\eta} \tag{9}$$

The household derives utility from the composite good, $\tilde{C}$, and utility from cash holding is derived from the real value deflated by price P. It has a disutiliy of labor.

The composite good consists of a combination of the material good and the pollution Z, which is a bad that negatively contributes to the composite good.

$$\tilde{C}_t = \left[a C_t^{1-\phi} + (1-a)(Z_t^{-1})^{1-\phi}\right]^{\frac{1}{1-\phi}} \tag{10}$$

The household faces the budget constraint:

$$\begin{aligned}&\frac{M_t}{P_t}+\frac{B_t}{P_t}+C_t+\frac{K_t}{1-g}+\frac{\Phi}{2}\left(\frac{I_t}{K_{t-1}}-\frac{\delta}{1-g}\right)^2 K_{t-1}+\mathcal{CA}_t\\&\leq\frac{M_{t-1}}{P_t}+\frac{B_{t-1}R_{t-1}}{P_t}+w_tL_t+\left(r_t+\frac{1-\delta}{1-g}\right)K_{t-1}+\Pi_t\end{aligned}\tag{11}$$

Bond holding competes with cash holding with a gross interest rate of $R>1$. Traditional capital K is associated with a capital adjustment cost. At the steady state, investment partly (g) goes to traditional capital and barely compensates for the depreciation in the steady state, where the capital adjustment cost is zero. The cost of abatement $\mathcal{CA}$ depends on the pollution abatement effort U. The wage per unit of labor is w, and the return to one unit of traditional capital is r. The firms' profit Π is zero in the competitive market equilibrium.

The traditional capital dynamics consists of depreciation and non-clean investment, I^K.

$$K_t=(1-\delta)K_{t-1}+I_t^K\tag{12}$$

5.1.2 Firm

The representative firm's production function is:

$$Y_t=(1-\Gamma)A_tK_{t-1}^{\alpha}L_t^{1-\alpha}\tag{13}$$

Output Y depends on Total Factor Productivity (TFP) A and capital and labor inputs. It is negatively impacted by pollution, and the lost portion is Γ, which follows:

$$\Gamma(M)=\gamma_0+\gamma_1M+\gamma_2M^2\tag{14}$$

Here I assume M, the global pollution stock, to be fixed, as its change is of substantially lower order of magnitude than the dynamics we study.[18] The output can be derived from

[18]Using the calibration in AD2015, $d(M_t)=1.4647\times10^{-8}M_t^2-6.6722\times10^{-6}M_t+1.3950\times10^{-3}$, $M_t=.9979M_{t-1}+Z_t+Z_t^*$, $M=800\Rightarrow D=0.0054$. When Z increases by 1%, M increases by only 0.0021%. From log-linearlization on $d(M_t)=d_t=\gamma_0+\gamma_1M_t+\gamma_2M_t^2$, $\hat{d}_t=\frac{2\gamma_2M^2+\gamma_1M}{d}\hat{M}_t=2.4691\hat{M}_t$, $\hat{\Gamma}_t=-\frac{d}{1-d}\hat{d}_t=-0.0055\hat{d}_t=-0.0135\hat{M}_t$. Therefore, Γ declines by 0.0000418%, which is ignorable.

a continuum of Dixit-Stigliz intermediate goods:

$$Y_t = \left[\int_0^1 Y_{jt}^{\frac{\theta-1}{\theta}} dj \right]^{\frac{\theta}{\theta-1}}, \ \theta > 1 \tag{15}$$

The firm maximizes profit, which is zero in the competitive equilibrium, by choosing capital input, labor input, and abatement effort.

$$\max_{K,L,U} \Pi_t = P_t Y_t - w_t L_t - r_t K_t - T_t - \mathcal{CA}_t = 0 \tag{16}$$

The government taxes the firms with the amount T due to the pollution. In each period, only a fraction (ω) of the firms change their prices, while the remaining firms have sticky prices.

5.1.3 Pollution

Pollution Z is determined by the abatement effort, the pollution factor φ, and the output.

$$Z_t = (1 - U_t)\varphi_t Y_t \tag{17}$$

The abatement effort can be considered as the effort paid by firms, and the pollution factor reflects clean energy technology.

The tax is proportional to pollution emissions with a fixed tax rate τ.

$$T_t = \tau Z_t \tag{18}$$

The environmental capital dynamics consists of depreciation, government spending, and clean investment, I^N.

$$N_t = (1 - \delta_N)N_{t-1} + T_t + I_t^N \tag{19}$$

Clean investment is funded by both the government through tax and the households through investment.

The pollution factor, which represents clean technology advancement, is determined by the environmental capital.

$$\varphi_t = \omega_\varphi \tilde{\varphi}_t + (1 - \omega_\varphi)\varphi_{t-1} \tag{20}$$

The technology is also sticky, as its adoption requires some time to be put into use. I assume that a portion (ω_φ) of the new technology is realized in each period. The pollution factor with out sticky technology, $\tilde{\varphi}$, is a function of environmental capital. When clean investment increases, the pollution factor decreases.

$$\tilde{\varphi}_t = \varphi^f \left(\frac{\mu}{\mu + N_t} \right)^h \tag{21}$$

The cost of abatement effort is determined by abatement effort and output.

$$\mathcal{CA}_t = \phi_1 U_t^{\phi_2} Y_t \tag{22}$$

5.1.4 Monetary Policy

The monetary policy follows a Taylor-type rule targeting inflation and output gap with policy stickiness.

$$\log(R_t) = \rho_R \log(R_{t-1}) + (1 - \rho_R)(\log(R^n) + \psi_\pi(\widehat{\pi}_t - \widehat{\bar{\pi}}) + \psi_Y(\widehat{Y}_t - \widehat{\bar{Y}})) + \varepsilon_{R,t} \tag{23}$$

The targeted inflation and output are the steady-state values. The MPs ε_R follows an i.i.d. distribution with volatility σ_R.

$$\varepsilon_{R,t} = \nu_{R,t},\ \nu_R \sim \text{iid}(0, \sigma_R^2) \tag{24}$$

5.1.5 Market Clearing Conditions

Productivity follows a sticky path with a productivity shock ε_A in each period.

$$\log(A_t) = \rho_A \log(A_{t-1}) + \varepsilon_{A,t} \tag{25}$$

The shock follows an i.i.d. distribution with volatility σ_A.

$$\varepsilon_{A,t} = \nu_{A,t},\ \nu_A \sim \text{iid}(0, \sigma_A^2) \tag{26}$$

The goods market clears.

$$Y_t = C_t + I_t + \frac{\Phi}{2} \left(\frac{I_t}{K_{t-1}} - \frac{\delta}{1-g} \right)^2 + \mathcal{CA}_t \tag{27}$$

5.1.6 Clean Investment Sensitivity

While the steady-state clean investment share is g, the sensitivities of clean and non-clean investment are different, generating different investment responses to a monetary tightening when the economy deviates from the steady state. The empirical results suggest a higher investment response by clean than non-clean investments due to a longer investment horizon. My model setting incorporates this fact, as clean technology adoption is a gradual process, and the payback period of clean investment is longer than non-clean investment. To calculate the relative sensitivity of clean versus non-clean investment after a MPs, I calculate the durations of the two types of investment based on the marginal cash flow from one additional unit of clean and non-clean investment, respectively.

The marginal cash flow for traditional capital, MPI^K, comes from higher productivity.

$$MPI_t^K = \mathbb{E}_t \sum_{n=1}^{\infty} \frac{1}{(1+r_t)^n} \frac{d\Pi_{t+n}}{dK_{t+n-1}} \frac{dK_{t+n-1}}{dK_{t-1}} \tag{28}$$

The marginal cash flow for environmental capital, MPI^N, comes from less pollution tax and abatement cost.

$$MPI_t^N = \mathbb{E}_t \sum_{n=1}^{\infty} \frac{1}{(1+r_t)^n} \frac{d\Pi_{t+n}}{d\varphi_{t+n}} \frac{d\varphi_{t+n}}{dN_t} \tag{29}$$

Using the duration formula, the Macaulay durations of the marginal cash flows for traditional and environmental capital are respectively:

$$Dur_t^K = \frac{1-\delta}{r_t+\delta} \tag{30}$$

$$Dur_t^N = \frac{1}{\omega_\varphi - \delta_N} \left[\frac{(1-\delta_N)(r_t+\omega_\varphi)}{r_t+\delta_N} - \frac{(1-\omega_\varphi)(r_t+\delta_N)}{r_t+\omega_\varphi} \right] - 1 \tag{31}$$

The relative sensitivity to investment by environmental versus traditional capital, $\frac{\varepsilon_{NI}}{\varepsilon_{KI}}$, is:

$$\left(\frac{\varepsilon_{NI}}{\varepsilon_{KI}} \right)_t = \frac{Dur_t^K}{Dur_t^N} \tag{32}$$

The property can be used to generate responses after a deviation from the steady state. The derivation is in Appendix D.1.4.

From the duration of clean investment (environmental capital), I have the following prediction.

Prediction 1. *The Macaulay duration of environmental capital investment increases when the adoption rate of clean technology decreases.*

When the speed of clean technology decreases, it takes more months for the pollution factor to fully realize the technological benefit of clean investment. The property empirically matches the longer investment horizon of clean investment relative to non-clean investment. The proof is in Appendix D.1.5.

Using the same duration formula, I obtain that the duration of environmental capital tends to be longer than traditional capital's.

Prediction 2. *The Macaulay duration of environmental capital investment is longer than that of traditional capital investment.*

Therefore, clean investment has a longer horizon than non-clean investment in terms of financial payback. The condition holds for conventional calibration.

The impact of pollution increase emerges after several months when the negative output impact by the MPs dies out, but the regression in pollution-control technology persists. I prove that the magnitude of the increase in pollution after a positive MPs increases if the clean investment share increases.

Prediction 3. *Pollution increases more after a monetary tightening when the clean investment share increases.*

The proof is in Appendix D.1.6. Like the previous prediction, this one also holds for conventional calibration, as I will show next.

5.2 Calibration

The calibration of a parameter follows previous literature if it exists. To match the empirical baseline, I calibrate the model using a monthly frequency. Common parameters follow the general literature in New Keynesian DSGE, and those related to the environment follow Annicchiarico and Di Dio (2015). The values used in the calibration are shown in Table 3. Key steady-state values derived from the parameter calibration are also shown.

Table 3: Calibration of parameters

Variable	Description	Value
Parameters		
σ	Consumer relative risk aversion	1
ϕ	Elasticity of substitution between consumption and pollution	0.5
β	Time discount factor	0.9983
δ	Capital depreciation rate	0.0083
Φ	Capital adjustment cost factor	20
α	Capital share in production	0.33
η	Inverse Frisch elasticity of labor supply	1
ω	Speed of price change per period	0.7
b	Consumer relative risk aversion in cash	0.5
ρ_R	Persistence of monetary policy shock	0.9
σ_R	Volatility of monetary policy shock	0.1
ψ_π	Monetary policy response to inflation	1.5
ψ_Y	Monetary policy response to output	0.0416667
ρ_A	Persistence of TFP shock	0.97
σ_A	Volatility of TFP shock	0.1
χ	Disutility factor of labor	5
γ	Utility factor of cash	0.003
γ_0	Pollution damage function: constant term	0.001395
γ_1	Pollution damage function: linear term	-6.6722e-06
γ_2	Pollution damage function: quadratic term	1.4647e-08
ϕ_1	Factor of effort cost on abatement effort	0.185
ϕ_2	Curvature of effort cost on abatement effort	2.8
φ_f	Pollution factor without clean technology	0.45
$\bar{M}$	Global pollution reservation	800
Steady state		
κ	NKPC inflation response to MCP	0.1291
Γ	Pollution damage ratio	0.0054
$\frac{K}{L}$	Steady state capital-labor ratio	129.9134
s_I	Steady state investment ratio	0.2720
$\frac{\varepsilon_{NI}}{\varepsilon_{KI}}$	Relative investment elasticity of environmental versus traditional capital	1.3836
$\frac{\varepsilon_{I^N,MP}}{\varepsilon_{I^K,MP}}$	Relative MPs elasticity of clean versus non-clean investment	2.4603

Notes: The steady state values are based on arbitrarily assigned values of parameters to be estimated.

The IRFs of key variables in the model are in Figure 20. After MPs, FFR increases. Output, consumption, and CPI decline due to fewer investment activities. The decline in environmental capital is greater than in traditional capital, and pollution increases after several periods when output gradually recovers. The pollution increase is due to the regression of clean technology, represented by an increase in the pollution factor. Long-term household utility declines due to lower consumption and higher pollution.

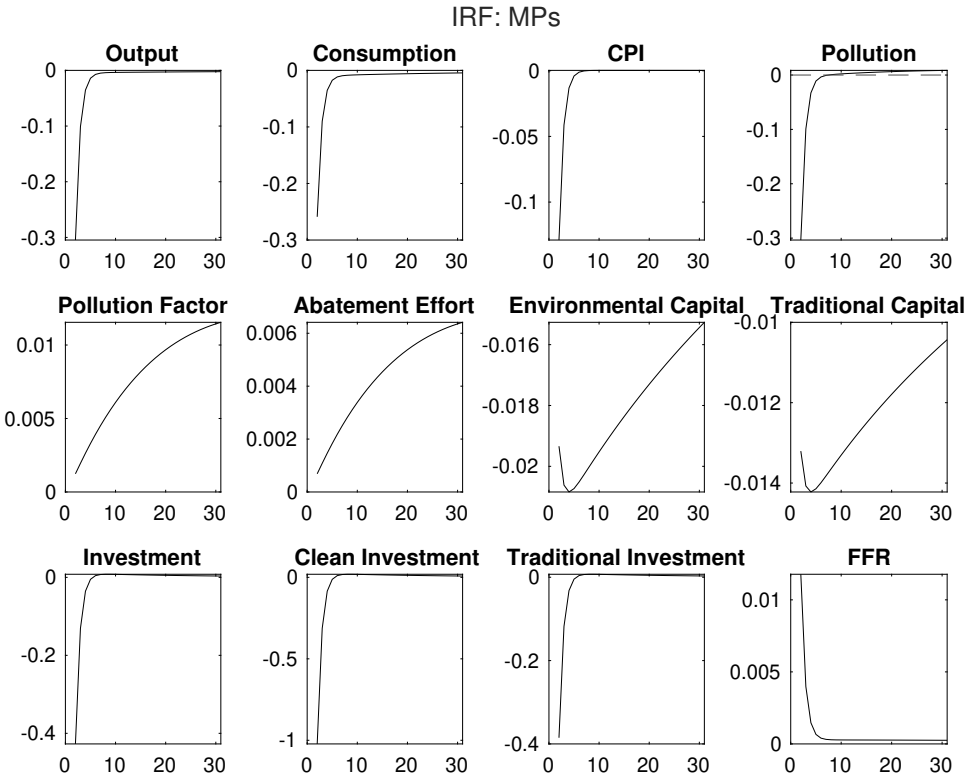

Figure 20: Model IRF to MPs: Initial Value Calibration

Notes: For the parameters to be estimated, the steady-state values are the initial values in the estimations.

By varying the clean investment share, the dynamics change and pollution increases more after the MPs when the share increases. As in Figure D.2, the pollution increase is stronger when the environmental capital share increases. This is consistent with Prediction 3. The difference comes from the faster decaying impact on environmental capital for the higher environmental capital share after a tightening, which causes a stronger impact on pollution reduction technology, as reflected by the pollution factor change.

The result is consistent with the empirical evidence.

5.3 Estimation

Several parameters are novel in the model setting without reference to previous literature. Therefore, their values need to be estimated. I estimate their values by matching the model IRF with the empirical baseline IRFs regarding pollution and output responses for a selected period after the shock. I estimate the parameters x that minimize the standard-error-weighted sum of the squared distances between the model and empirical IRFs across the selected periods as follows.[19]

$$x = \text{argmin} \sum_{y\in\{Z,Y\}} \sum_{h=H_{\min}}^{H_{\max}} \left(\frac{\frac{dy(x;h)}{d\varepsilon_R} - \beta_{y,0}^{(h)}}{\text{se}(\beta_{y,0}^{(h)})} \right)^2 + M \sum_{y\in\{I_K,I_N\}} \left(\frac{\min_h(\frac{dy(x;h)}{d\varepsilon_R}) - \min_{h=h^*}(\beta_{y,0}^{(h)})}{\text{se}(\beta_{y,0}^{(h^*)})} \right)^2 \tag{33}$$

The indicators to be matched, y, include pollution and output. $y(x;h)$ is the log deviation of y from the steady state h months after the shock when the parameters are x. $\beta_{y,0}^{(h)}$ is the empirical IRF of h months after the shock. I set $H_{\min}$ to 5 months and $H_{\max}$ to 30 months. Additionally, I match traditional and clean investment using peak-to-peak matching with a multiplier M of 10.

I estimate the parameters of interest using both the gradient-based optimization algorithm[20] and the Bayesian estimation. The estimation results are shown in Table 4. The details of the estimation are given in Figure D.1. The statistics of the estimation are in Table D.1.

[19] As the MPs in the empirical identification is unit based, I rescale the model IRFs by dividing original magnitudes by the interest rate R's response to ε_R in the first period.

[20] The MATLAB function I use is `fmincon` with the interior point algorithm.

Table 4: Estimation of parameters

Variable	Description	Initial value	Optimized value	Bayesian optimum
Parameters				
a	Consumer utility weight on consumption	0.9	0.7851	0.7953
δ_N	Environmental capital depreciation rate	0.0083	0.0100	0.0093
h	Curvature of pollution factor on environmental capital	1	1.0000	0.9902
μ	Buffer of pollution factor on environmental capital	1	1.0000	1.0055
ω_φ	Speed of technology adoption per period	0.04	0.0976	0.1330
τ	Pollution tax rate	0.2	0.0100	0.1716
g	Ratio of environmental capital investment	0.2	0.0821	0.0566
$\frac{\varepsilon_{I^N,MP}}{\varepsilon_{I^K,MP}}$	Relative MPs elasticity of clean versus non-clean investment	2.4603	2.0845	2.0697
Likelihood				
$(\text{distance})^2$	Sum of squared distances between SLP and model IRF	19.0261	10.8981	11.5171

Notes: (a) I apply the Metropolis-Hastings algorithm with Random Walk draws. The first 100,000 draws use the identity matrix to draw shifts from a multivariable normal distribution. After the 100,000 draws, I calculate the covariance matrix of the generated chains of parameters and use it as the covariance matrix of the random draw for the next 250,000 draws.

(b) As in Uribe and Schmitt-Grohe (2017), I assign each estimated parameter a uniform prior with an upper bound and a lower bound using reasonable values, and I skip a draw if any of the resulting parameters is out of the boundary, or if there is no stable steady state based on the generated parameters.

The estimated model IRFs reasonably match the empirical baseline IRF, as shown in Figure 21, especially the pollution and GDP, since I estimate the parameters based on the two indicators.

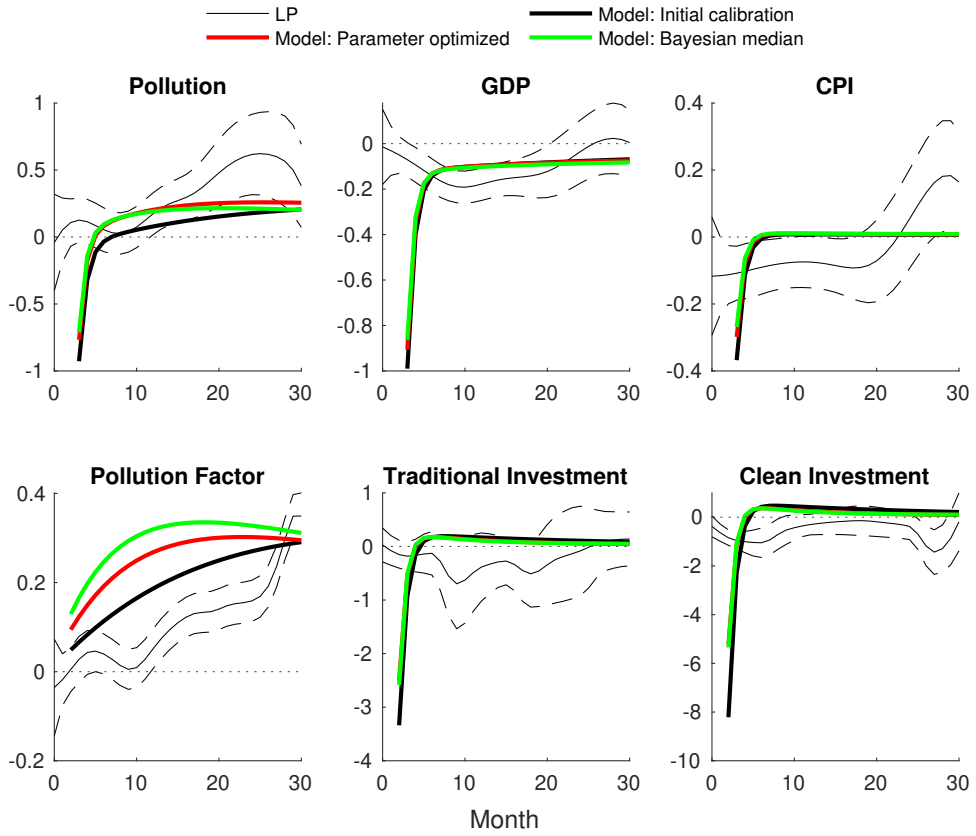

Figure 21: IRF Matching, SLP and E-DSGE

Notes: MPs is aggregated to the monthly frequencies consistent with the dependent variable. The number of lags of the dependent variable (Q) and the shock (M) are selected by the AIC criteria for up to 4 periods. The dashed ribbons are the 90 percent confidence intervals generated based on the Newey-West standard errors.

The distributions of the generated chains of parameters in the Bayesian estimation imply the range of the values of the parameters of interest, as shown in Figure 22. The depreciation rate of environmental capital, δ_N, is not very different from that of traditional capital. The curvature of the pollution factor function on environmental capital, h, is low, as its value is close to one. The clean technology adoption is sticky, as implied by a ω_φ peaking at somewhere substantially below one. Pollution estimated by the gradient algorithm peaks at 25 months after the shock, which exactly matches the empirical baseline.[21] The pollution tax is low, consistent with the current situation in

[21]The estimated pollution factor peaks 23 months after the shock. The model assumes that technology adoption in each period only varies with the environmental capital in the period. As envi-

the US. Finally, the proportion of investment in environmental capital is less than the initially calibrated 20 percent. The Bayesian median is close to the 10 percent implied by the clean investment divided by the concurrent structure and equipment investments in the US in 2023. The empirical clean investment ratio is also close to the 8.2 percent estimated by the gradient algorithm. However, the incompleteness of the clean investment data provided by the Clean Investment Monitor implies the actual clean investment percentage is potentially higher.

---

ronmental capital gradually recovers from the initial large decline, the magnitude of technological adoption on the pollution factor declines, and the pollution factor peaks just before the new round of technology adopted is less advanced than the existing technology. That is, the peak h^* arrives when: $\begin{cases} \tilde{\varphi}_{t+h^*} > \varphi_{t+h^*-1} \\ \tilde{\varphi}_{t+h^*+1} < \varphi_{t+h^*} \end{cases}$, and $\tilde{\varphi}_{t+h+1} < \tilde{\varphi}_{t+h}$ for sufficiently large h. Therefore, such a h^* exists.

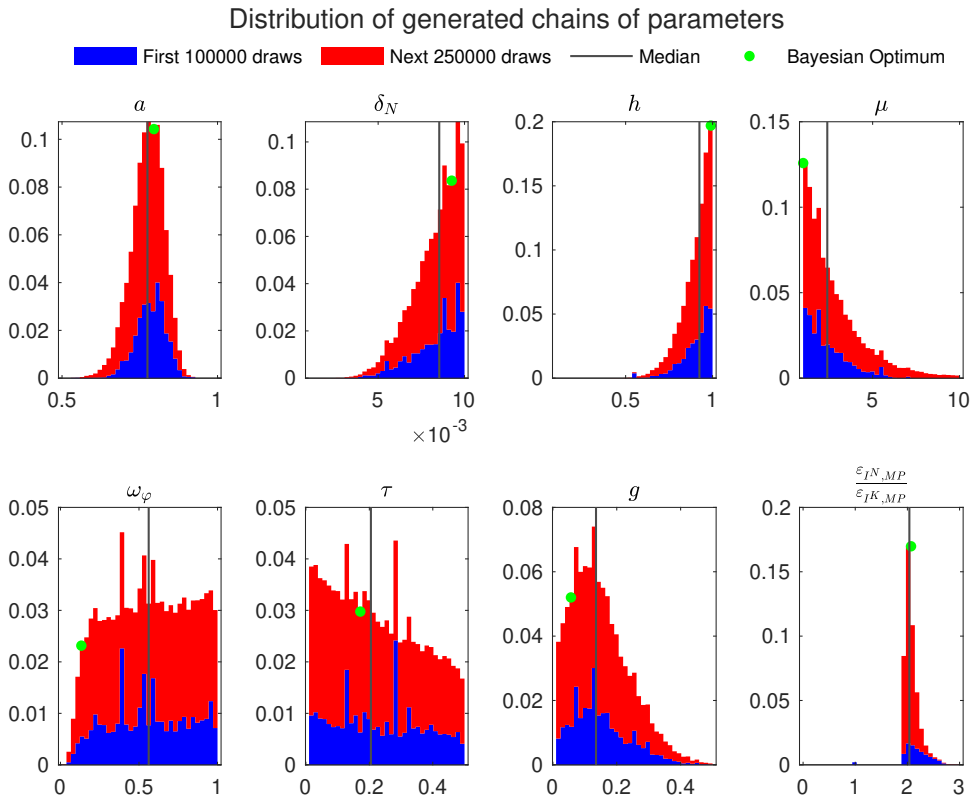

Figure 22: Bayesian Estimation of the Model: Parameters Distributions

Notes: (a) I apply the Metropolis-Hastings algorithm with Random Walk draws. The first 100,000 draws use the identity matrix to draw shifts from a multivariable normal distribution. After the 100,000 draws, I calculate the covariance matrix of the generated chains of parameters and use it as the covariance matrix of the random draw for the next 250,000 draws.

(b) As in Uribe and Schmitt-Grohe (2017), I assign each estimated parameter a uniform prior with an upper bound and a lower bound using reasonable values, and I skip a draw if any of the resulting parameters is out of the boundary, or if there is no stable steady state based on the generated parameters.

5.4 Optimal Policy

The economic turbulence after a MPs declines household utility. To optimize household utility or to minimize utility loss by stabilizing consumption and pollution after the shock, the central bank potentially helps by targeting pollution in addition to inflation and output. By modifying the monetary policy to add a pollution target in the Taylor

function:

$$\log(R_t) = \rho_R \log(R_{t-1}) + (1-\rho_R)(\log(R^n) + \psi_\pi(\widehat{\pi}_t - \widehat{\bar{\pi}}) + \psi_Y(\widehat{Y}_t - \widehat{\bar{Y}}) + \psi_{Z,\text{mp}}(\widehat{Z}_t - \widehat{\bar{Z}})) + \varepsilon_{R,t} \tag{34}$$

Here $\psi_{Z,\text{mp}}$ is the response to change in pollution. With positive responses to pollution, pollution is more stabilized, whereas consumption becomes less stabilized. Observing the initial pollution decline, the central bank more aggressively lowers the interest rate than the pollution-neutral case to prevent the loss of environmental capital.

Utility response to the shock is:

$$\frac{d\mathcal{U}_{t+h}}{d\varepsilon_{R,t}} = \tilde{C}^{1-\sigma} \frac{d \log \tilde{C}_{t+h}}{d\varepsilon_{R,t}} + \gamma \left(\frac{M}{P}\right)^{1-b} \frac{d \log \frac{M_{t+h}}{P_{t+h}}}{d\varepsilon_{R,t}} - \chi L^{1+\eta} \frac{d \log L_{t+h}}{d\varepsilon_{R,t}} \tag{35}$$

When varying the monetary policy response to pollution, $\psi_{Z,\text{mp}}$, the change in household utility after a MPs is shown in Figure 23. More aggressive responses to pollution at sufficiently low levels help stabilize the utility change after a shock. The stabilization effect comes from reduced consumption and pollution factor volatility, as shown in Figure D.3. The latter comes from lower financial costs after the initial tightening, helping defend environmental capital from further depreciation.

Besides monetary policy, changing the fiscal policy by varying the pollution tax with the overall pollution level also helps stabilize the utility change after a MPs. Instead of a fixed tax rate, allowing the rate, τ, to change with pollution:

$$\tau_t = \tau Z_t^{\psi_Z} \tag{36}$$

When varying the fiscal policy response to pollution, ψ_Z, the change in household utility after a MPs is shown in Figure 24. A negative ψ_Z implies credit for the firm emission after a tightening, which helps stabilize the utility change after a shock. The effectiveness increases when the magnitude of adjustment increases within sufficiently low levels. The stabilization effect comes from relaxing the financial cost of investing in environmental capital, as shown in Figure D.4. When the credit expands, the environmental capital loss is partly recovered, preventing the pollution factor from increasing and, subsequently,

increasing air pollution.

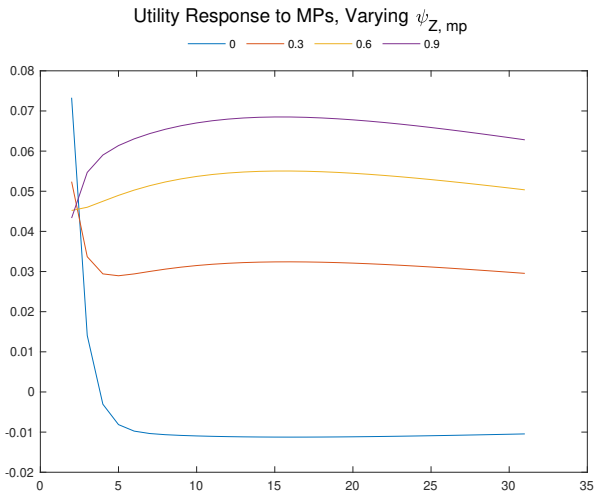

Figure 23: Consumer Welfare Response to MPs, by Monetary Policy Regimes

Notes: All the parameter calibrations follow the values that minimize the sum of distances between SLP and E-DSGE at each selected horizon.

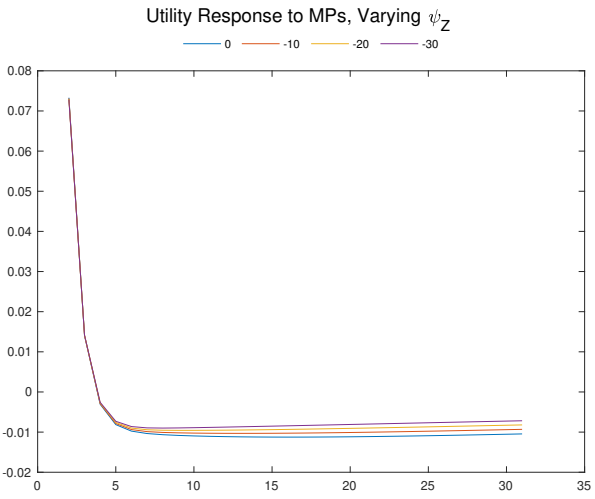

Figure 24: Consumer Welfare Response to MPs, by Fiscal Policy Regimes

Notes: All the parameter calibrations follow the values that minimize the sum of distances between SLP and E-DSGE at each selected horizon.

As both fiscal and monetary policies can be revised from the baseline model to better stabilize household utility after a MPs, their coordination potentially benefits the households more. To investigate the benefit of coordination, I vary both ψ_Z and $\psi_{Z,\text{mp}}$ to find the optimal policy mix that minimizes the utility loss from volatility after a MPs. The optimization problem is:

$$\min_{\psi_{Z,\text{mp}},\psi_Z} \int_{H_{\min}}^{H_{\max}} \left(\frac{d\mathcal{U}_{t+h}}{d\varepsilon_{R,t}} \right)^2 dh \tag{37}$$

The results are shown in Figure 25, implying the optimal policy mix to be $\psi_Z = -19.5$ and $\psi_{Z,\text{mp}} = 0.55$. At this point, after a monetary tightening, tax credits are imposed on firms to prevent their further loss and subsequent loss in environmental capital investment. Concurrently, the interest rate will be lowered following the initial output and pollution drops, which prevents environmental capital loss that induces a long-term pollution increase. Lowering the initial turbulence in environmental capital

prevents long-term pollution deviation and utility instability.

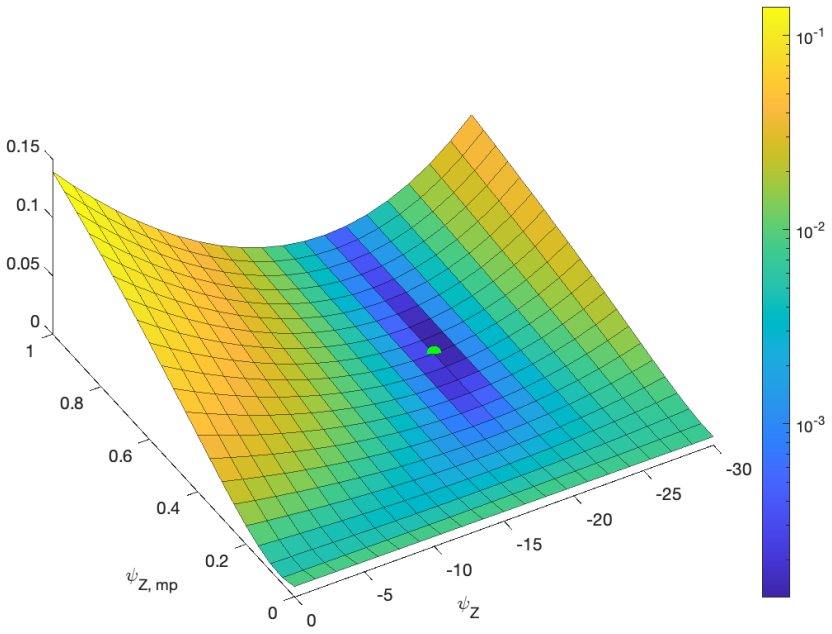

Figure 25: Optimal Fiscal and Monetary Policy Coordination for Consumer Welfare Maximization after a MPs

Notes: The interval of $\psi_{Z,\text{mp}}$ is 0.05, and the interval of ψ_Z is 1.5. The optimal point is denoted with the green dot. All the parameter calibrations follow the values that minimize the sum of distances between SLP and E-DSGE at each selected horizon.

Note that the negative response of pollution tax rate to pollution can also be interpreted as a regulation relaxation after an increase in pollution. When regulation relaxes, the aggregated pollution tax rate should decrease. Such policy benefits consumers, who care about both material consumption and environmental amenities.

6 Extension

In this section, I extend the results to other countries and study the global spillover of the US MPs. I also present the recent global pollution trend and investigate the role of US monetary policy in influencing it.

6.1 The Global Spillover

The decline in air pollution since the GFC is mainly driven by advanced economies, as shown in Figure E.1, particularly the EU. Pollution reduction in the US is also remarkable, except in the late 2010s when the US withdrew from the Paris Agreement. Compared to AE, pollution in emerging markets (EM) barely declines.[22]

Looking at the pollution change by countries and regions in the US and China, as shown in Figure E.2, the European countries have experienced the most remarkable pollution decline since the GFC. The decline is also substantial in the US, Canada, Australia, and Japan. For EM economies, pollution in China declines after increasing policy attention during the period. The observation is consistent with the clean energy dependency ratio of the newly opened power plants, as shown in Figure E.3. The cleanness of new power plants is substantially higher in the US, Europe, and other AE economies compared to the EM economies.

As an extension to the baseline identification, I add the aggregated output, pollution and CPI of EM economies to the baseline LP specification, and the IRFs are shown in Figure E.4. Here, due to data concerns, I use nighttime light (NTL) as a proxy for economic activities in EM. The CPI of EM is calculated by the US inflation and the change in the real exchange rate for each country.[23] While the output decline and pollution increase still hold for the US, the output decline in the EM is accompanied by a weak pollution decline, implying co-movement. CPI in EM also declines in line with the output decline.

I apply the baseline identification to each country and US/China regions, and the average responses are shown in Figure 26. Among EM economies, the pollution decline mainly appears in China. While clean investment is vastly domestic for AE, the overall

[22] EM here includes all OECD members except Chile, Colombia, Costa Rica, Latvia, Lithuania, Mexico, and Turkey. I also add Hong Kong, Singapore, and Taiwan to AE.

[23] For each country in each year, I calculate the inflation as the US inflation plus the percentage change of the PPP conversion ratio (real exchange rate over nominal exchange rate, quoted in domestic currency per USD). Then, I calculate the average inflation across the EM economies weighted by the population of each country in the corresponding year.

response by EM economies shows that the channel is weak for them. The economic activities of the EM economies, as proxied by NTL in Figure E.5, imply a comovement between output and pollution in these countries, notably India, Brazil, and most African countries. Moreover, the output decline in EM is unlikely to be related to the US dollar appreciation after the US MPs, as shown by the exchange rate of the US dollar after the MPs in Figure E.6.

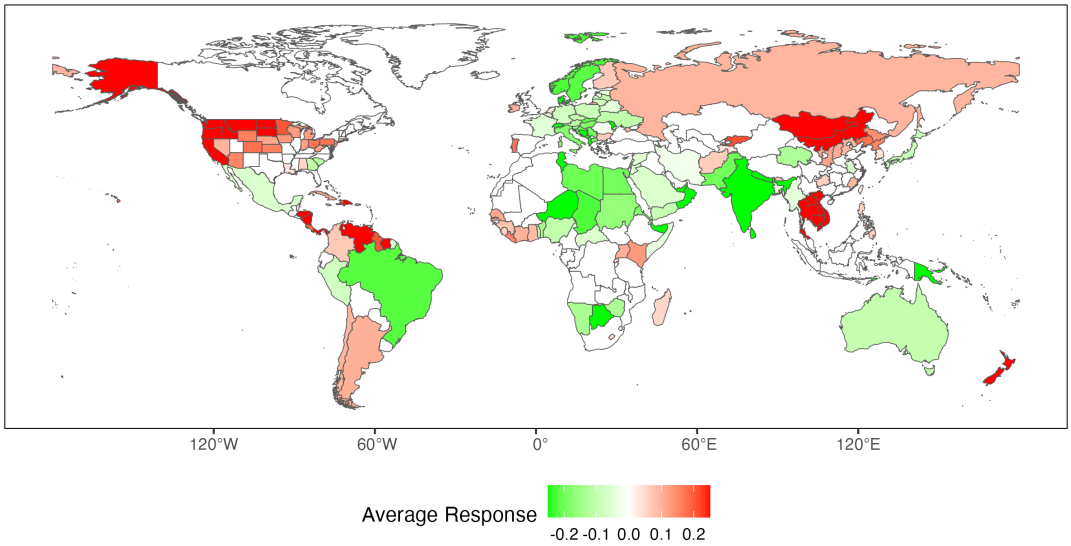

Figure 26: Average Pollution Response to MPs by Country and Region

Notes: MPs is aggregated to the monthly frequencies consistent with the dependent variable. The number of lags of the dependent variable (Q) and the shock (M) are selected by the AIC criteria for up to 4 periods. When taking the average across the time horizon from the month the MPs is realized to 20 months later, insignificant values at a 90 percent confidence level are treated as zero. If the region has both significantly positive and significantly negative responses, the average response by the region is interpreted as zero. Extreme values with absolute values greater than 0.25 are winsorized on the map.

7 Conclusion

This paper studies the environmental externalities of the US monetary policy shock by looking at the air pollution responses after the shock. Surprisingly, output declines, but

air pollution increases after a monetary tightening. The divergent path is explained by a clean investment channel, where the tightening passes to firms' capital cost, diverting their funding away from investment in clean technology and subsequently increasing air pollution. The channel is supported by firm-level evidence, as environmentally friendlier firms are more sensitive to tightening. It is also consistent with heterogeneous responses at the regional level. Finally, the quantitative results imply that if the monetary policy targets pollution in addition to inflation and output, the environment-augmented household utility will further stabilize. The effectiveness of pollution targeting improves when coordinating with pollution tax relief that prevents environmental capital loss.

The data used in the study are also useful for related research questions. Firstly, environmental policy in developing countries potentially changes following a US monetary tightening. Secondly, firm behavior on clean investment after a capital cost increase potentially differs across industries. Moreover, the study only points out one of the channels for the increase in pollution after tightening, and there are potentially other channels that lead to similar environmental impacts.

References

Almond, D., Du, X., Karplus, V. J., & Zhang, S. (2021). Ambiguous Air Pollution Effects of China's COVID-19 Lock-down. *AEA Papers and Proceedings*, *111*, 376–380. https://doi.org/10.1257/pandp.20211032

Angelopoulos, K., Economides, G., & Philippopoulos, A. (2013). First-and second-best allocations under economic and environmental uncertainty. *International Tax and Public Finance*, *20*(3), 360–380. https://doi.org/10.1007/s10797-012-9234-z

Annicchiarico, B., & Di Dio, F. (2015). Environmental policy and macroeconomic dynamics in a new Keynesian model. *Journal of Environmental Economics and Management*, *69*, 1–21. https://doi.org/10.1016/j.jeem.2014.10.002

Annicchiarico, B., & Di Dio, F. (2017). GHG Emissions Control and Monetary Policy. *Environmental and Resource Economics*, *67*(4), 823–851. https://doi.org/10.1007/s10640-016-0007-5

Attílio, L. A., Faria, J. R., & Rodrigues, M. (2023). Does monetary policy impact CO2 emissions? A GVAR analysis. *Energy Economics*, *119*, 106559. https://doi.org/10.1016/j.eneco.2023.106559

Axbard, S. (2016). Income Opportunities and Sea Piracy in Indonesia: Evidence from Satellite Data. *American Economic Journal: Applied Economics*, *8*(2), 154–194. https://doi.org/10.1257/app.20140404

Barnichon, R., & Brownlees, C. (2019). Impulse Response Estimation by Smooth Local Projections. *The Review of Economics and Statistics*, *101*(3), 522–530. https://doi.org/10.1162/rest_a_00778

Bräuning, F., & Ivashina, V. (2020). U.S. monetary policy and emerging market credit cycles. *Journal of Monetary Economics*, *112*, 57–76. https://doi.org/10.1016/j.jmoneco.2019.02.005

Burney, J. A. (2020). The downstream air pollution impacts of the transition from coal to natural gas in the United States. *Nature Sustainability*, *3*(2), 152–160. https://doi.org/10.1038/s41893-019-0453-5

Cai, X., Lu, Y., Wu, M., & Yu, L. (2016). Does environmental regulation drive away inbound foreign direct investment? Evidence from a quasi-natural experiment in China. *Journal of Development Economics*, *123*, 73–85. https://doi.org/10.1016/j.jdeveco.2016.08.003

Camara, S., Christiano, L., & Dalgic, H. (2024, July). *The International Monetary Transmission Mechanism* (tech. rep.). NBER. https://www.nber.org/books-and-chapters/nber-macroeconomics-annual-2024-volume-39/international-monetary-transmission-mechanism

Center For International Earth Science Information Network-CIESIN-Columbia University. (2018). Gridded Population of the World, Version 4 (GPWv4): Population Count, Revision 11. https://doi.org/10.7927/H4JW8BX5

Chan, Y. T. (2020). Are macroeconomic policies better in curbing air pollution than environmental policies? A DSGE approach with carbon-dependent fiscal and monetary policies. *Energy Policy*, *141*, 111454. https://doi.org/10.1016/j.enpol.2020.111454

Chen, S.-S., & Lin, T.-Y. (2024). Monetary policy and renewable energy production. *Energy Economics*, *132*, 107495. https://doi.org/10.1016/j.eneco.2024.107495

Chor, D., & Li, B. (2024). Illuminating the effects of the US-China tariff war on China's economy. *Journal of International Economics*, *150*, 103926. https://doi.org/10.1016/j.jinteco.2024.103926

Christiano, L. J., Eichenbaum, M., & Evans, C. L. (2005). Nominal Rigidities and the Dynamic Effects of a Shock to Monetary Policy. *Journal of Political Economy*, *113*(1), 1–45. https://doi.org/10.1086/426038

Clarida, R., Galí, J., & Gertler, M. (2002). A simple framework for international monetary policy analysis. *Journal of Monetary Economics*, *49*(5), 879–904. https://doi.org/10.1016/S0304-3932(02)00128-9

Clay, K., Muller, N. Z., & Wang, X. (2021). Recent Increases in Air Pollution: Evidence and Implications for Mortality. *Review of Environmental Economics and Policy*, *15*(1), 154–162. https://doi.org/10.1086/712983

Coibion, O., & Gorodnichenko, Y. (2011). Monetary Policy, Trend Inflation, and the Great Moderation: An Alternative Interpretation. *American Economic Review*, *101*(1), 341–370. https://doi.org/10.1257/aer.101.1.341

Coibion, O., & Gorodnichenko, Y. (2012). Why Are Target Interest Rate Changes so Persistent? *American Economic Journal: Macroeconomics*, *4*(4), 126–162. https://doi.org/10.1257/mac.4.4.126

Colmer, J. (2021). Temperature, Labor Reallocation, and Industrial Production: Evidence from India. *American Economic Journal: Applied Economics*, *13*(4), 101–124. https://doi.org/10.1257/app.20190249

Colorado School of Mines. (n.d.). Earth Observation Group - Payne Institute for Public Policy. https://payneinstitute.mines.edu/eog/

Copernicus Climate Change Service. (2021). Temperature and precipitation gridded data for global and regional domains derived from in-situ and satellite observations. https://doi.org/10.24381/CDS.11DEDF0C

Creutzig, F., Agoston, P., Goldschmidt, J. C., Luderer, G., Nemet, G., & Pietzcker, R. C. (2017). The underestimated potential of solar energy to mitigate climate change. *Nature Energy*, *2*(9), 17140. https://doi.org/10.1038/nenergy.2017.140

Dedola, L., Karadi, P., & Lombardo, G. (2013). Global implications of national unconventional policies. *Journal of Monetary Economics*, *60*(1), 66–85. https://doi.org/10.1016/j.jmoneco.2012.12.001

Drudi, F., Moench, E., Holthausen, C., Weber, P.-F., Ferrucci, G., Setzer, R., Nino, V. D., Barbiero, F., Faccia, D., Breitenfellner, A., Faiella, I., Farkas, M., Bun, M., Fornari, F., Ciccarelli, M., Matthieu, D. P., Giovannini, A., Papadopoulou, N., Parker, M., … Ouvrard, J.-F. (2021, September). *Climate Change and Monetary Policy in the Euro Area* (tech. rep. No. 2021/271). https://ssrn.com/abstract=3928292

Eurostat. (n.d.). Eurostat. https://ec.europa.eu/eurostat

Fan, Y., Gao, Q., & Tang, C. K. (2023). The Unintended Consequences of Coal-fired Power Plant Closures: Evidence from China. *SSRN Electronic Journal*. https://doi.org/10.2139/ssrn.4651899

Fischer, C., & Springborn, M. (2011). Emissions targets and the real business cycle: Intensity targets versus caps or taxes. *Journal of Environmental Economics and Management*, *62*(3), 352–366. https://doi.org/10.1016/j.jeem.2011.04.005

Fornaro, L., Guerrieri, V., & Reichlin, L. (2024, July). *Monetary Policy for the Energy Transition* (tech. rep.). Deutsche Bundesbank. https://www.bundesbank.de/resource/blob/829620/3c110e66dda94a604b789787a97097d8/mL/2024-06-26-eltville-fornaro-data.pdf

GADM. (n.d.). GADM maps and data. https://gadm.org

Global Energy Monitor contributors. (2023, September). Global Energy Monitor Wiki. Retrieved December 29, 2023, from https://www.gem.wiki/w/index.php?title=Main_Page&oldid=482224

Gordo, N., Hunt, A., & Morley, B. (2024). Alternative monetary policies and renewable energy stock returns. *Energy Economics*, *136*, 107740. https://doi.org/10.1016/j.eneco.2024.107740

Gorodnichenko, Y., & Shapiro, M. D. (2007). Monetary policy when potential output is uncertain: Understanding the growth gamble of the 1990s. *Journal of Monetary Economics*, *54*(4), 1132–1162. https://doi.org/10.1016/j.jmoneco.2006.03.004

Gürkaynak, R., Karasoy-Can, H. G., & Lee, S. S. (2022). Stock Market's Assessment of Monetary Policy Transmission: The Cash Flow Effect. *The Journal of Finance*, *77*(4), 2375–2421. https://doi.org/10.1111/jofi.13163

Halkos, G., & Paizanos, E. (2015, February). *Effects of Macroeconomic Policy on Air Quality: Evidence from the US* (tech. rep. No. 62001). https://mpra.ub.uni-muenchen.de/62001/

Hartzmark, S. M., & Shue, K. (2023). Counterproductive Sustainable Investing: The Impact Elasticity of Brown and Green Firms. *SSRN Electronic Journal*. https://doi.org/10.2139/ssrn.4359282

Hashmi, S. M., Syed, Q. R., & Inglesi-Lotz, R. (2022). Monetary and energy policy interlinkages: The case of renewable energy in the US. *Renewable Energy*, *201*, 141–147. https://doi.org/10.1016/j.renene.2022.10.082

Heutel, G. (2012). How should environmental policy respond to business cycles? Optimal policy under persistent productivity shocks. *Review of Economic Dynamics*, *15*(2), 244–264. https://doi.org/10.1016/j.red.2011.05.002

Heyes, A., & Saberian, S. (2022). Hot Days, the ability to Work and climate resilience: Evidence from a representative sample of 42,152 Indian households. *Journal of Development Economics*, *155*, 102786. https://doi.org/10.1016/j.jdeveco.2021.102786

Hirth, L., & Steckel, J. C. (2016). The role of capital costs in decarbonizing the electricity sector. *Environmental Research Letters*, *11*(11), 114010. https://doi.org/10.1088/1748-9326/11/11/114010

Hirth, L., Ueckerdt, F., & Edenhofer, O. (2015). Integration costs revisited – An economic framework for wind and solar variability. *Renewable Energy*, *74*, 925–939. https://doi.org/10.1016/j.renene.2014.08.065

Inness, A., Ades, M., Agustí-Panareda, A., Barré, J., Benedictow, A., Blechschmidt, A.-M., Dominguez, J. J., Engelen, R., Eskes, H., Flemming, J., Huijnen, V., Jones, L., Kipling, Z., Massart, S., Parrington, M., Peuch, V.-H., Razinger, M., Remy, S., Schulz, M., & Suttie, M. (2019). The CAMS reanalysis of atmospheric composition. *Atmospheric Chemistry and Physics*, *19*(6), 3515–3556. https://doi.org/10.5194/acp-19-3515-2019

International Energy Agency. (2021, December). The Cost of Capital in Clean Energy Transitions. Retrieved October 21, 2024, from https://www.iea.org/articles/the-cost-of-capital-in-clean-energy-transitions

Jarociński, M. (2024). Estimating the Fed's unconventional policy shocks. *Journal of Monetary Economics*, *144*, 103548. https://doi.org/10.1016/j.jmoneco.2024.01.001

Jordà, Ò. (2005). Estimation and Inference of Impulse Responses by Local Projections. *American Economic Review*, *95*(1), 161–182. https://doi.org/10.1257/0002828053828518

Känzig, D. (2023, May). *The Unequal Economic Consequences of Carbon Pricing* (tech. rep. No. w31221). National Bureau of Economic Research. Cambridge, MA. https://doi.org/10.3386/w31221

Khan, A., King, R. G., & Wolman, A. L. (2003). Optimal Monetary Policy. *Review of Economic Studies*, *70*(4), 825–860. https://doi.org/10.1111/1467-937X.00269

Kolasa, M., & Wesołowski, G. (2020). International spillovers of quantitative easing. *Journal of International Economics*, *126*, 103330. https://doi.org/10.1016/j.jinteco.2020.103330

Lakdawala, A., Moreland, T., & Schaffer, M. (2021). The international spillover effects of US monetary policy uncertainty. *Journal of International Economics*, *133*, 103525. https://doi.org/10.1016/j.jinteco.2021.103525

Lee, C. M. C., So, E. C., & Wang, C. C. Y. (2021). Evaluating Firm-Level Expected-Return Proxies: Implications for Estimating Treatment Effects (W. Jiang, Ed.). *The Review of Financial Studies*, *34*(4), 1907–1951. https://doi.org/10.1093/rfs/hhaa066

Lelieveld, J., Klingmüller, K., Pozzer, A., Burnett, R. T., Haines, A., & Ramanathan, V. (2019). Effects of fossil fuel and total anthropogenic emission removal on public health and climate. *Proceedings of the National Academy of Sciences*, *116*(15), 7192–7197. https://doi.org/10.1073/pnas.1819989116

Liu, R. A., Wei, Y., Qiu, X., Kosheleva, A., & Schwartz, J. D. (2022). Short term exposure to air pollution and mortality in the US: A double negative control analysis. *Environmental Health*, *21*(1), 81. https://doi.org/10.1186/s12940-022-00886-4

Liu, Z., & Lu, Q. (2024). Carbon dioxide fertilization, carbon neutrality, and food security. *China Economic Review*, *85*, 102177. https://doi.org/10.1016/j.chieco.2024.102177

Lupu, I., Criste, A., Ciumara, T., Milea, C., & Lupu, R. (2024). Addressing the Renewable Energy Challenges through the Lens of Monetary Policy—Insights from the Literature. *Energies*, *17*(19), 4820. https://doi.org/10.3390/en17194820

Michler, J. D., Josephson, A., Kilic, T., & Murray, S. (2022). Privacy protection, measurement error, and the integration of remote sensing and socioeconomic survey data. *Journal of Development Economics*, *158*, 102927. https://doi.org/10.1016/j.jdeveco.2022.102927

Miranda-Agrippino, S., & Nenova, T. (2022). A tale of two global monetary policies. *Journal of International Economics*, *136*, 103606. https://doi.org/10.1016/j.jinteco.2022.103606

Miranda-Agrippino, S., & Rey, H. (2020). U.S. Monetary Policy and the Global Financial Cycle. *The Review of Economic Studies*, *87*(6), 2754–2776. https://doi.org/10.1093/restud/rdaa019

Mughal, N., Kashif, M., Arif, A., Guerrero, J. W. G., Nabua, W. C., & Niedbała, G. (2021). Dynamic effects of fiscal and monetary policy instruments on environmental pollution in ASEAN. *Environmental Science and Pollution Research*, *28*(46), 65116–65126. https://doi.org/10.1007/s11356-021-15114-8

National Institute for Environmental Studies. (2023). ODIAC Fossil Fuel Emission Dataset. Retrieved December 29, 2023, from https://db.cger.nies.go.jp/dataset/ODIAC/

Noailly, J., Nowzohour, L., Van Den Heuvel, M., & Pla, I. (2024). Heard the news? Environmental policy and clean investments. *Journal of Public Economics*, *238*, 105190. https://doi.org/10.1016/j.jpubeco.2024.105190

Obstfeld, M., & Rogoff, K. (2002). Global Implications of Self-Oriented National Monetary Rules. *The Quarterly Journal of Economics*, *117*(2), 503–535. https://doi.org/10.1162/003355302753650319

Pinkovskiy, M., & Sala-i-Martin, X. (2016). Lights, Camera … Income! Illuminating the National Accounts-Household Surveys Debate. *Quarterly Journal of Economics*, *131*(2), 579–631. https://doi.org/10.1093/qje/qjw003

Ravn, M. O., & Uhlig, H. (2001). On Adjusting the Hp-Filter for the Frequency of Observations. *SSRN Electronic Journal*. https://doi.org/10.2139/ssrn.273355

Refinitiv. (n.d.). Product: Refinitiv ESG Data (tr_esg). https://wrds-www.wharton.upenn.edu/data-dictionary/tr_esg/

Rhodium Group and MIT. (2023). The Clean Investment Monitor. https://www.cleaninvestmentmonitor.org

Roback, J. (1982). Wages, Rents, and the Quality of Life. *Journal of Political Economy*, *90*(6), 1257–1278. https://doi.org/10.1086/261120

Rossi, B., & Zubairy, S. (2011). What Is the Importance of Monetary and Fiscal Shocks in Explaining U.S. Macroeconomic Fluctuations? *Journal of Money, Credit and Banking*, *43*(6), 1247–1270. https://doi.org/10.1111/j.1538-4616.2011.00424.x

Shrimali, G., & Kniefel, J. (2011). Are government policies effective in promoting deployment of renewable electricity resources? *Energy Policy*, *39*(9), 4726–4741. https://doi.org/10.1016/j.enpol.2011.06.055

Shukla, K., Seppanen, C., Naess, B., Chang, C., Cooley, D., Maier, A., Divita, F., Pitiranggon, M., Johnson, S., Ito, K., & Arunachalam, S. (2022). ZIP Code-Level Estimation of Air Quality and Health Risk Due to Particulate Matter Pollution in New York City. *Environmental Science & Technology*, *56*(11), 7119–7130. https://doi.org/10.1021/acs.est.1c07325

S&P Global Market Intelligence. (n.d.). Product: S&P Compustat North America - annual update (current + historical data) (comp_na_annual_all). https://wrds-www.wharton.upenn.edu/data-dictionary/comp_na_annual_all/

Steckel, J. C., & Jakob, M. (2018). The role of financing cost and de-risking strategies for clean energy investment. *International Economics*, *155*, 19–28. https://doi.org/10.1016/j.inteco.2018.02.003

Swanson, E. T. (2021). Measuring the effects of federal reserve forward guidance and asset purchases on financial markets. *Journal of Monetary Economics*, *118*, 32–53. https://doi.org/10.1016/j.jmoneco.2020.09.003

Tang, W., Llort, J., Weis, J., Perron, M. M. G., Basart, S., Li, Z., Sathyendranath, S., Jackson, T., Sanz Rodriguez, E., Proemse, B. C., Bowie, A. R., Schallenberg, C., Strutton, P. G., Matear, R., & Cassar, N. (2021). Widespread phytoplankton blooms triggered by 2019–2020 Australian wildfires. *Nature*, *597*(7876), 370–375. https://doi.org/10.1038/s41586-021-03805-8

Tenreyro, S., & Thwaites, G. (2016). Pushing on a String: US Monetary Policy Is Less Powerful in Recessions. *American Economic Journal: Macroeconomics*, *8*(4), 43–74. https://doi.org/10.1257/mac.20150016

Tufail, S., Alvi, S., Hoang, V.-N., & Wilson, C. (2024). The effects of conventional and unconventional monetary policies of the US, EU, and China on global green investment. *Energy Economics*, *134*, 107549. https://doi.org/10.1016/j.eneco.2024.107549

Ullah, S., Ozturk, I., & Sohail, S. (2021). The asymmetric effects of fiscal and monetary policy instruments on Pakistan's environmental pollution. *Environmental Science and Pollution Research*, *28*(6), 7450–7461. https://doi.org/10.1007/s11356-020-11093-4

United States Environmental Protection Agency. (n.d.). Air Data: Air Quality Data Collected at Outdoor Monitors Across the US. https://www.epa.gov/outdoor-air-quality-data

Uribe, M., & Schmitt-Grohe, S. (2017). *Open economy macroeconomics*. Princeton University Press.

Vazquez Santiago, J., Hata, H., Martinez-Noriega, E. J., & Inoue, K. (2024). Ozone trends and their sensitivity in global megacities under the warming climate. *Nature Communications*, *15*(1), 10236. https://doi.org/10.1038/s41467-024-54490-w

Wang, C., Lin, Q., & Qiu, Y. (2022). Productivity loss amid invisible pollution. *Journal of Environmental Economics and Management*, *112*, 102638. https://doi.org/10.1016/j.jeem.2022.102638

Wang, X. (n.d.). Historical data of air quality and weather in China. https://quotsoft.net/air/

Wong, D. W., Yuan, L., & Perlin, S. A. (2004). Comparison of spatial interpolation methods for the estimation of air quality data. *Journal of Exposure Science & Environmental Epidemiology*, *14*(5), 404–415. https://doi.org/10.1038/sj.jea.7500338

Woodford, M. (2001). The Taylor Rule and Optimal Monetary Policy. *American Economic Review*, *91*(2), 232–237. https://doi.org/10.1257/aer.91.2.232

Zhang, D., Wang, Y., & Peng, X. (2023). Carbon Emissions and Clean Energy Investment: Global Evidence. *Emerging Markets Finance and Trade*, *59*(2), 312–323. https://doi.org/10.1080/1540496X.2022.2099270

Appendix A Data

A.1 Baseline Panel Summary Statistics

Table A.1: Summary Statistics: Monthly Panel Data

	N	Time range	Mean	SD	Min	Max
Pollution (Satellite)	252	2003M1:2023M12	0.0000	0.2576	-0.4278	0.7933
Pollution (EPA)	252	2003M1:2023M12	-0.0000	0.4956	-0.8213	0.8270
PM10	252	2003M1:2023M12	-17.6725	0.2677	-18.2347	-16.6355
PM2.5	252	2003M1:2023M12	-18.0152	0.2703	-18.6031	-16.9726
CO	252	2003M1:2023M12	-7.0439	0.0702	-7.2219	-6.8343
NO2	252	2003M1:2023M12	-12.3019	0.2282	-12.6444	-11.7613
O3	252	2003M1:2023M12	-5.0072	0.0244	-5.0815	-4.9045
SO2	252	2003M1:2023M12	-12.6920	0.3287	-13.1481	-11.9983
CO2	240	2003M1:2022M12	18.5939	0.0790	18.2939	18.7851
MPs: MP1	252	2003M1:2023M12	-0.0025	0.0458	-0.5725	0.1574
MPs: Acosta FF0	252	2003M1:2023M12	-0.0012	0.0244	-0.2000	0.1300
MPs: Swanson FFR	252	2003M1:2023M12	-0.0002	0.0096	-0.0551	0.0537
MPs: Forward Guidance	252	2003M1:2023M12	-0.0539	0.8466	-3.0408	4.0094
MPs: LSAP	252	2003M1:2023M12	-0.0243	0.9626	-11.2674	2.5469
MPs: Information	252	2003M1:2023M12	0.0346	0.7154	-4.8446	2.7570
GDP	252	2003M1:2023M12	9.8110	0.1190	9.5897	10.0442
CPI	252	2003M1:2023M12	5.4448	0.1315	5.2073	5.7325
Indistrial Production	252	2003M1:2023M12	4.5832	0.0485	4.4388	4.6454
Temperature	204	2003M1:2019M12	3.1918	0.0468	3.0450	3.3357

Notes: MPs are aggregated to monthly level. For MPs, a month includes at most one shock, so the value for the month is either zero or the shock in that month.

Table A.2: Summary Statistics: Quarterly Panel Data

	N	Time range	Mean	SD	Min	Max
Pollution (Satellite)	84	2003Q1:2023Q4	0.0000	0.2534	-0.3905	0.5774
Pollution (EPA)	84	2003Q1:2023Q4	-0.0000	0.4954	-0.7437	0.8065
MPs: MP1	84	2003Q1:2023Q4	-0.0075	0.0670	-0.4151	0.1480
GDP	84	2003Q1:2023Q4	9.8092	0.1194	9.5897	10.0415
Gross Fixed Capital Formation	84	2003Q1:2023Q4	8.2155	0.1575	7.9692	8.4906
Private Domestic Investment	84	2003Q1:2023Q4	8.0180	0.2034	7.5740	8.3548
Private Fixed Investment	68	2007Q1:2023Q4	8.0407	0.1960	7.6845	8.3345
All Clean Investment	26	2018Q1:2024Q2	24.2658	0.4599	23.6236	25.0605
Manufacturing Clean Investment	26	2018Q1:2024Q2	21.5886	1.1988	19.7880	23.6790
Retail Clean Investment	26	2018Q1:2024Q2	23.6158	0.4228	22.8950	24.2615
Other Clean Investment	26	2018Q1:2024Q2	23.2946	0.4050	22.5075	23.9562

Notes: MPs are aggregated to quarterly level.

A.2 Details of Pollution Data

A.2.1 Geospatial Data

Data Source The monthly air pollution dataset is derived from CAMS global reanalysis (EAC4) monthly averaged fields, the fourth generation of the ECMWF global reanalysis of atmospheric composition. The data period begins in January 2003. The data assimilation principle the source data uses is based on the method used to forecast weather and air quality (CAMS2020). Public access is available from the Atmosphere Data Store of the Atmosphere Monitoring Service implemented by the ECMWF, Copernicus, the Earth Observation component of the European Union's space programme.

Alternatively, the source provides the tri-hourly version of CAMS global reanalysis (EAC4) with the same set of indicators. The high-frequency version is potentially useful for further economic analysis requiring more frequent pollution dynamics than the monthly observations.

Panel Construction The six indicators I use from the dataset include: PM2.5 (kg per cubic meter), PM10 (kg per cubic meter), total column carbon monoxide (kg per square meter), total column nitrogen dioxide (kg per square meter), total column ozone (kg per square meter), and total column sulfur dioxide (kg per square meter). All the indicators are single-level variables, with the total column variables being the sum of the values across altitudes.

The shape files I use for countries and US states are from GADM.[24] In each geospatial map file, I crop the target region using each shape file by including all meshes that touch any polygon within the shape file. The resolution of the geospatial data, 0.75 degrees (about 75km at the equator), is sufficiently accurate to capture the area of each US state. As an illustration, I show the PM10 geospatial map of the selected North American region with the shape files of the US states in Figure A.1.

[24]The shape files are publicly available on the website of GADM.

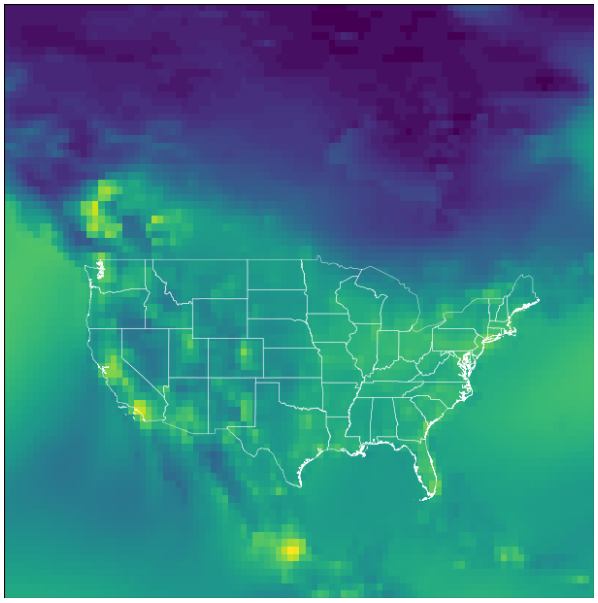

Figure A.1: Pollution Data from Satellite Image: US PM10, January 2003

For each US state, I select all meshes that touch or lay within the shape file of the state. Then, I sum up the values of all selected meshes and label the summation as PM10 in the selected state in the month that corresponds to the map file.

Principle Component Analysis For each pollutant, I take the logarithm of the original value. In the baseline, I apply the PCA to the time series of the population-weighted average of air pollutants of the US. The percentage of variation explained by each component indexed by descending power is shown in Figure A.2.

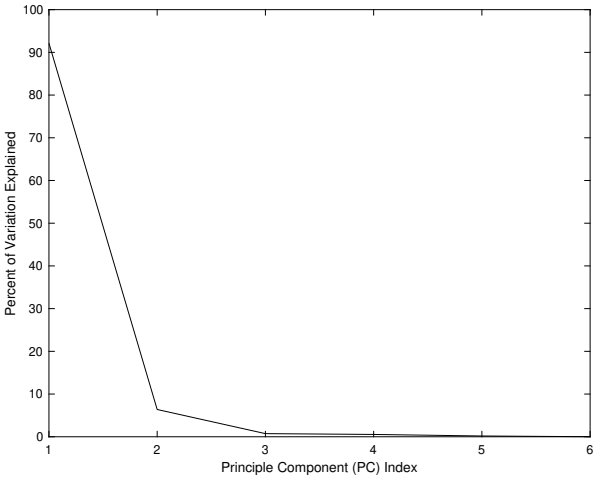

Figure A.2: Explanatory Power of Each Component Derived from the Principle Component Analysis on Air Pollution Indicators

Then, I compare the original series with the PCA-fitted series for each pollutant. I only show the fitted series for the first two principal components, as they jointly explain more than 95 percent of the variation. As shown in Figure A.3, the first principal component,

PC1, explains most of the variations in the two comprehensive indicators (PM10 and PM2.5), NO2, and SO2, including the trend. It also explains some variations in CO, especially the overall trend. The second principal component (PC2) partly explains the detrended variation. The variation in O3 is seldom explained by the first two principal components.

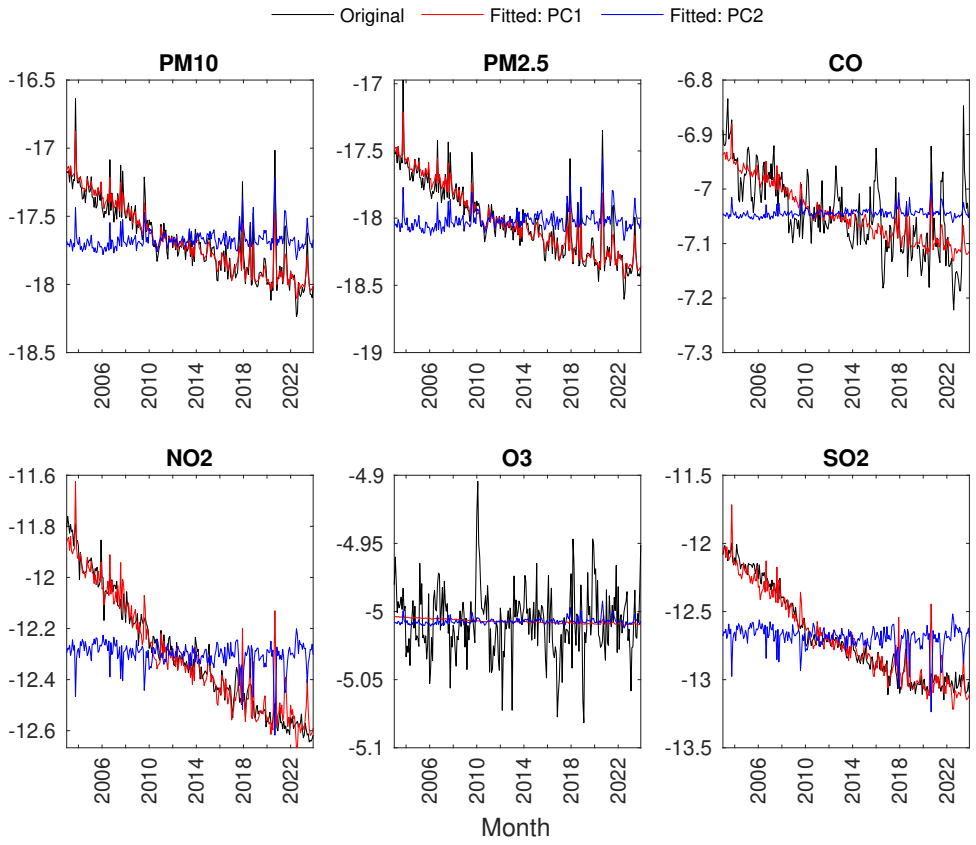

Figure A.3: Explanatory Power of Each Component Derived from the Principle Component Analysis on Air Pollution Indicators

After PCA, I normalize the scale of the first principal component (PC1) so that one unit of change in PC1 corresponds to one log-point change in pollution.

A.2.2 Monitoring Stations

The air pollution data from US monitor stations are publicly available on the USEPA website. I download the data from the pre-generated data files. In the Tables of Daily Summary Data, available since 1980, I use PM2.5 non FRM/FEM Mass (88502), PM10 Mass (81102), CO (42101), NO2 (42602), Ozone (44201), and SO2 (42401) to construct the pollution (PC1) time series using the same method as I do for the geospatial data. As an illustration, I show selected observations of the PM2.5 data in Table A.3.

Table A.3: Air Pollution Data from US EPA: PM2.5 Sample

State Code	County Code	Site Number	Paremeter Code	POC	Method Code	Arithmetic Mean
19	013	0009	88502	3	731	7.1
19	013	0009	88502	4	731	4.6
19	137	0002	88502	3	731	2.8
19	137	0002	88502	4	731	4.5
53	003	0004	88502	4	771	14.6
53	003	0004	88502	8	171	19.5

Notes: The data are from the Daily Summary Data of the Pre-Generated Data Files of the United States Environmental Protection Agency. The selected rows are for the date 2024-01-01. Paremeter Code 88502 represents PM2.5 non FRM/FEM Mass. Method Code 171 represents Met-one BAM-1022 W/PM2.5 SCC - Beta Attenuation. Method Code 731 represents Met-One BAM-1020 W/PM2.5 SCC - Beta Attenuation. Method Code 771 represents Correlated Radiance Research M903 With Heated Inlet - Nephelometry.

For each row in the data, I can identify the state and the date. The longitude and latitude of each monitoring station are also publicly available on the website.

From the longitude and latitude of all stations, I aggregate them to match the meshes in the geospatial data. The matching statistics are in Table A.4. Note that there are 2344 meshes for the US. Within each mesh, I aggregate the observation of each station weighted by the inverse of the distance between the station and the centroid of the mesh, following the invese distance weighting (IDW) approach (Wong et al., 2004). The aggregation from mesh to nation follows the same process as the aggregation in the geospatial data by taking the population-weighted average.

Table A.4: Spatial Coverage of EPA Monitor Stations

Pollutant	Number of Mesh With Available Data	Number of Mesh With Available Data After Filter	Percent of Population Covered	Percent of Population Covered After Filter
CO	268	268	64.43	64.43
NO2	342	342	65.14	65.14
O3	703	703	86.62	86.62
PM10	462	462	70.58	70.58
PM2.5	384	134	60.48	6.80
SO2	403	403	69.45	69.45

Notes: The data are from the Daily Summary Data of the Pre-Generated Data Files of the United States Environmental Protection Agency.

A.3 Other Data

A.3.1 National Accounts

US Economy Data for the US economy are from the FRED database provided by the Federal Reserve Bank (Fed) of St. Louis. For monthly data, I use industrial production (INDPRO), CPI (CPIAUCSL), CPI of fuel price (CUSR0000SEHE), FFR (FEDFUNDS), and exchange rate of US dollar (TWEXBPA, RTWEXBGS)[25]. For quarterly data, I use GDP (GDPC1), gross fixed capital formation (USAGFCFQDSNAQ), private domestic investment (GPDIC1), and private fixed investment (FPIC1).

US Clean Investment The dataset for US aggregated clean energy investments is publicly available on the Clean Investment Monitor quarterly since 2018. The website is founded by the Rhodium Group and the MIT Center for Energy and Environmental Policy Research (CEEPR) to track clean energy investment and transition using the novel dataset. It provides clean investment by segment, including retail, manufacturing, and others. It also provides some aggregated statistics at the state level, such as retail investment.

Other For other countries, I obtain quarterly national indicators from the International Financial Statistics (IFS) of the International Monetary Fund (IMF). Indicators I use include GDP (NGDP_R_SA_XDC), CPI (PCPI_IX), consumption (NC_R_SA_XDC), private consumption (NCP_R_SA_XDC), government consumption (NCGG_R_SA_XDC), investment (NI_R_SA_XDC), export (NX_R_SA_XDC), import (NM_R_SA_XDC), current accounts (BG_BP6_USD), currency exchange rate to US dollar (ENDA_XDC_USD_RATE), employment (LE_PE_NUM), labor force population (LLF_PE_NUM), and unemployment (LU_PE_NUM). I also obtain annual population (LP_PE_NUM) and convert it to quarterly series through linear interpolation.[26]

I also obtain annual national indicators from the World Development Indicator (WDI) of the World Bank (WB). Indicators I use include real GDP per capita in local currency unit (NY.GDP.PCAP.KN), consumption (NE.CON.TOTL.ZS), investment (NE.GDI.TOTL.ZS), government spending (NE.CON.GOVT.ZS), import (NE.IMP.GNFS.ZS), export (NE.EXP.GNFS.ZS), current account (BN.CAB.XOKA.GD.ZS), population (SP.POP.TOTL), PPP conversion ratio (PA.NUS.PPPC.RF), nominal GDP in US dollar (NY.GDP.MKTP.CD), and GDP growth (NY.GDP.MKTP.KD).[27] Additionally, I add each country's annual average nighttime light (NTL) from the Light pollution map.

[25] I use TWEXBPA for the period before 2006, and RTWEXBGS for the period since 2006. I convert the RTWEXBGS series since 2006 to the TWEXBPA series using the ratio of TWEXBPA to RTWEXBGS in January 2006.

[26] Denote annual values as x, with x_{t-1} as last year's value, x_t as this year's value, and x_{t+1} as next year's value. For Q1, I use $\frac{3}{8}x_{t-1} + \frac{5}{8}x_t$. For Q2, I use $\frac{1}{8}x_{t-1} + \frac{7}{8}x_t$. For Q3, I use $\frac{7}{8}x_t + \frac{1}{8}x_{t+1}$. For Q4, I use $\frac{5}{8}x_t + \frac{3}{8}x_{t+1}$.

[27] For each country, when the annual data are not available, I use the quarterly data from IFS and convert them to annual values, by taking the sum (GDP and its components) or average (population, rates including exchange rate). When the data are also unavailable in IFS, I use the data from CEIC. If the data are only available at the quarterly frequency in CEIC, I convert them to annual values using the same method.

A.3.2 Firm Data

For each firm listed in the US, the Analyst-forecast-based Implied Cost of Capital (ICCA) is based on the values calculated by Lee et al. (2021) at the monthly frequency. Financial operation information is from Compstat (accessible through WRDS) at an annual frequency, where I use current assets, current liabilities, EBITDA, and revenue. Firm ESG records are from Refinitiv (accessible through WRDS) at annual frequency, where I use the ESG score (including its three components), emission of CO2 equivalent (total, scope 1, scope 2), environmental expenditure, renewable energy use, hazardous waste, environmental R&D, percentage of green products, renewable energy supply ratio, NOx emission, and SOx emission. As the key in Compstat data is gvkey, and the key in the Refinitiv ESG data is the Stock Exchange Daily Official List (sedol), and each gvkey can correspond to multiple sedol, I use the first occurrence of sedol (ascending order) within each gvkey as the representative when joining firm operation information with ESG records.

A.3.3 Financial Data

The equity data for the firms listed in the US are from Bloomberg Terminal. I use the daily adjusted closed price as the daily price of stock quotes since 2009. The stock quotes (indices) that I use include S&P 500, S&P 500 Energy, S&P 500 Financials, S&P Kensho Clean Energy, S&P Kensho Clean Power, S&P Kensho Cleantech, NASDAQ, NASDAQ Renewable Energy Equipment, NASDAQ Oil Gas and Coal, NASDAQ Investment Services, NASDAQ Financials, and NASDAQ Clean Edge Green Energy.

A.3.4 Power Plant

Power plant data are from the Global Energy Monitor (GEM). The dataset contains the operation statistics for each power plant, including each phase of each plant. It covers power plants around the world. Indicators include the operation status, technology used, commissioned capacity, year of commission, longitude, latitude, and the country and sub-nation divisions of each plant's location. I focus on the plants commissioned since 2009.

A.3.5 Carbon Emission

The Carbon emission geospatial data is the publicly accessible Open-Data Inventory for Anthropogenic Carbon dioxide (ODIAC) provided by the National Institute for Environmental Studies (NIES) of Japan. The dataset is available on a monthly frequency, with an available period starting in January 2000. The spatial resolution is as high as 1km, enabling accurate regional identification of carbon emission dynamics. In this study, I aggregate the geospatial map of carbon emission to national and state levels in the same way that I aggregate the geospatial maps of air pollution.

A.3.6 Weather

The temperature geospatial data are the publicly accessible Climatic Research Unit (CRU) gridded time series, Temperature and precipitation gridded data for global and regional domains derived from in-situ and satellite observations from the Climate Data

Store (CDS) of the Climate Change Service (CCS) implemented by the ECMWF, Copernicus, the Earth Observation component of the European Union's space programme. The data period starts in January 1901 and ends in December 2019 at a monthly frequency. The spatial resolution is as high as 0.5 degrees (about 50 km at the equator), enabling accurate regional weather identification. The key indicators in the data include average temperature, maximum temperature, minimum temperature, wind speed, and precipitation. In this study, I aggregate the geospatial map of the average temperature to national and state levels in the same way that I aggregate the geospatial maps of air pollution.

A.3.7 Population Density

The population density geospatial data are the publicly accessible Gridded Population of the World, Version 4 (GPWv4): Population Count, Revision 11. They record the population in each mesh from 2000 to 2020 with a five-year interval. Each mesh is a 30 arc-second (about 1 km at the equator) grid cell, enabling the accurate regional identification of population dynamics. In this study, I match the geospatial map of population density with each cell of the geospatial map of pollution by cropping the rectangle of the cell from the map of population density. In this way, I obtain population-weighted aggregated pollution (mesh average). Since the geospatial pollution series starts from 2003, I use the population data in 2000. I also aggregate the geospatial map of population density to overlay the geospatial map of weather (temperature) and obtain the population-weighted geospatial map of weather.[28]

A.3.8 Nighttime Light

The nighttime light (NTL) geospatial data is publicly accessible at Earth Observation Group (EOG), Payne Institute for Public Policy at the Colorado School of Mines. The group adjusts the original source from NASA by removing ephemeral light and cloud covers. The default version used in the paper uses the remote-sensing-based Visible Inferred Imaging Radiometer Suite (VIIRS) instrument, which has a high resolution of up to 15 arc-seconds (about 500 m at the equator), enabling accurate regional identification. The specification used in the paper is the vcmslcfg, which corrects for stray lights instead of removing them, leaving more spaces with available data. The dataset is available monthly since January 2014. In this study, I aggregate the geospatial map of NTL to the national level in the same way I aggregate the geospatial maps of air pollution.

For the period before 2014, another instrument, the Defense Meteorological Satellite Program (DMSP), is less accurate but sufficient for the study. It is also publicly available from EOG, which revises the original source from NASA. The available period of the annual and monthly datasets starts in 1992 and has a high resolution of up to 30 arc-seconds (about 1 km at the equator). However, it is upward censored and is therefore less accurate in places with high light density. When aggregating data for the same region in a year-month from different satellites, I take the average of the log NTL before taking the exponent and converting the data back to level values, as in line with previous literature (PS2016).

[28] When I overlay population density to the weather in each year-month, I use the year with population density information closest to the year of the year-month.

To exclude potential outliers in the monthly data, I exclude non-positive NTL values. For each region, I also remove the data points that are less than 60 percent of the previous month or more than five-thirds of the previous month. I do this step again after removing non-positive values.

Appendix B More Results on Responses

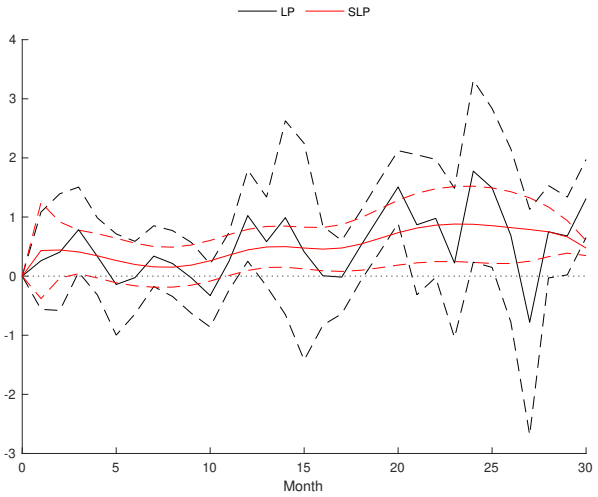

Figure B.1: Pollution Response to MPs, With Minimum Delay Assumption (GDP and Pollution)

Notes: The LP specification imposes the minimum delaying assumption with m starting from 1. MPs is aggregated to the monthly frequencies consistent with the dependent variable. The number of lags of the dependent variable (Q) and the shock (M) are selected by the AIC criteria for up to 4 periods. The dashed ribbons are the 90 percent confidence intervals generated based on the Newey-West standard errors.

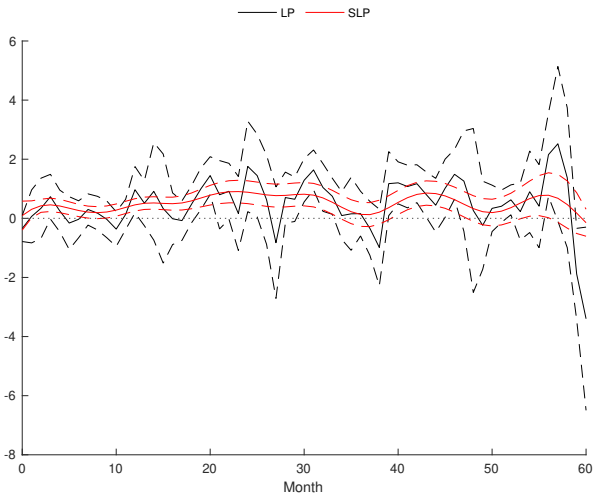

Figure B.2: Pollution Response to MPs, Baseline (Longer Horizon)

Notes: MPs is aggregated to the monthly frequencies consistent with the dependent variable. The number of lags of the dependent variable (Q) and the shock (M) are selected by the AIC criteria for up to 4 periods. The dashed ribbons are the 90 percent confidence intervals generated based on the Newey-West standard errors.

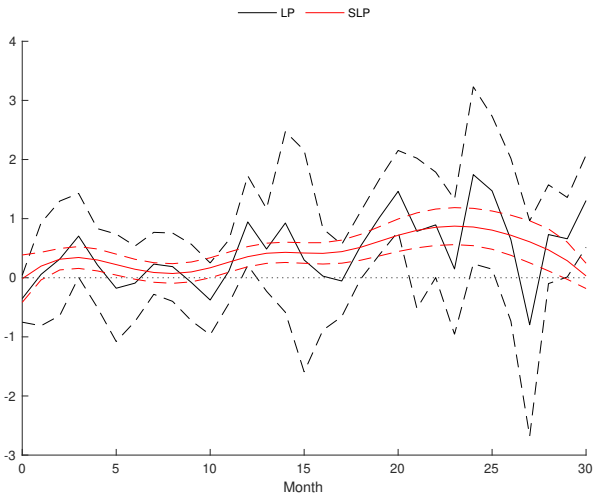

Figure B.3: Pollution Response to MPs, Without Lagged MPs

Notes: MPs is aggregated to the monthly frequencies consistent with the dependent variable. The dashed ribbons are the 90 percent confidence intervals generated based on the Newey-West standard errors.

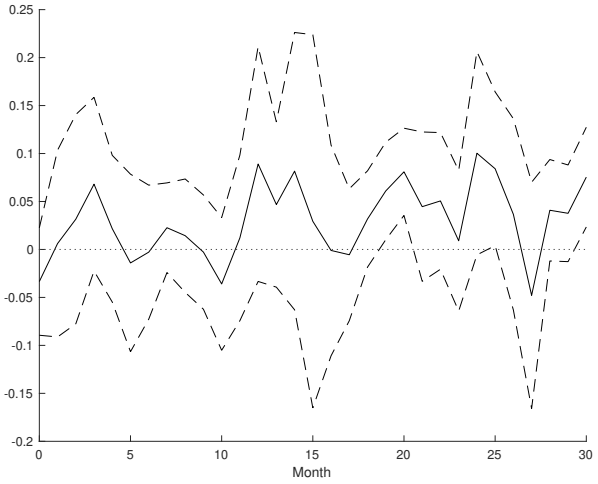

Figure B.4: Pollution Response to FFR (IV: MPs)

Notes: MPs is aggregated to the monthly frequencies consistent with the dependent variable. In the first stage, the number of lags of the endogenous variable is selected by the AIC criteria for up to 4 periods. In the second stage, the number of lags of the dependent variable (Q) and the endogenous variable (M) are selected by the AIC criteria for up to 4 periods. The dashed ribbons are the 90 percent confidence intervals generated by bootstrapping with 1,000 draws.

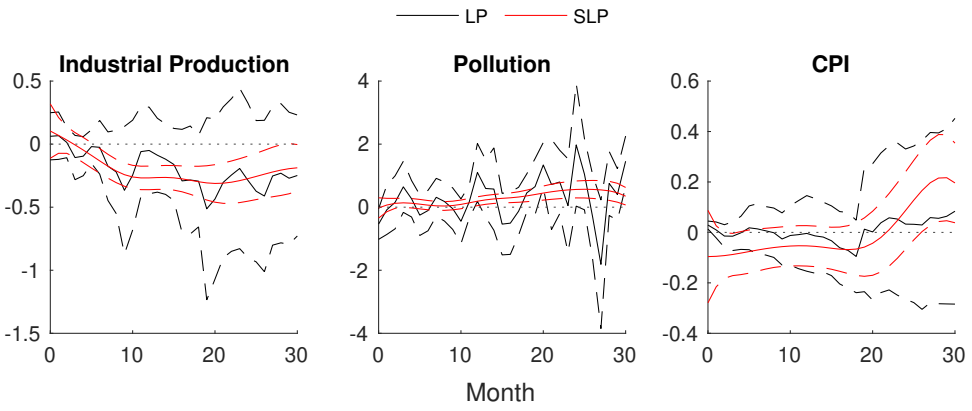

Figure B.5: Pollution Response to MPs, Using Industrial Production for Output

Notes: MPs is aggregated to the monthly frequencies consistent with the dependent variable. The number of lags of the dependent variable (Q) and the shock (M) are selected by the AIC criteria for up to 4 periods. The dashed ribbons are the 90 percent confidence intervals generated based on the Newey-West standard errors.

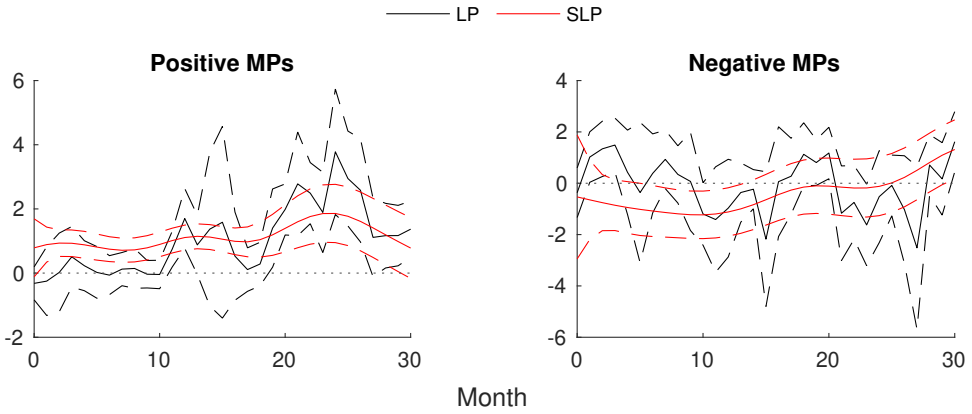

Figure B.6: Pollution Response to MPs, Asymmetric Responses

Notes: MPs is aggregated to the monthly frequencies consistent with the dependent variable. The number of lags of the dependent variable (Q) and the shock (M) are selected by the AIC criteria for up to 4 periods. The dashed ribbons are the 90 percent confidence intervals generated based on the Newey-West standard errors.

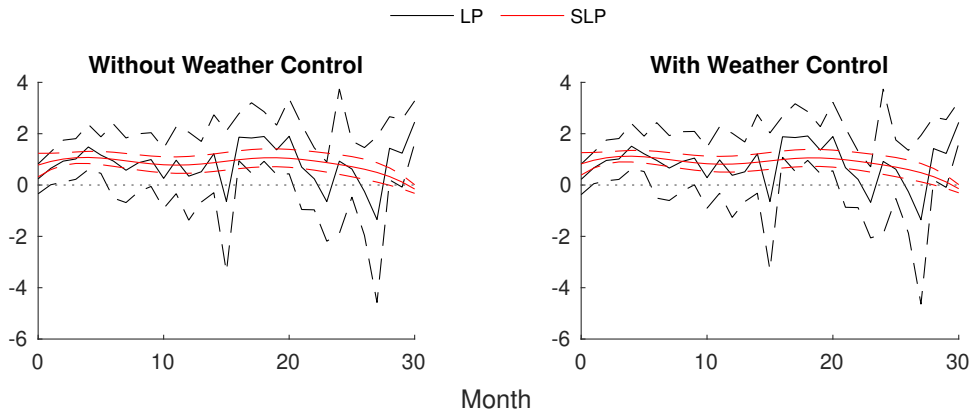

Figure B.7: Pollution Response to MPs, With Weather Controls

Notes: The regression panels are subsampled to the same period for each specification. MPs is aggregated to the monthly frequencies consistent with the dependent variable. The number of lags of the dependent variable (Q) and the shock (M) are selected by the AIC criteria for up to 4 periods. The dashed ribbons are the 90 percent confidence intervals generated based on the Newey-West standard errors.

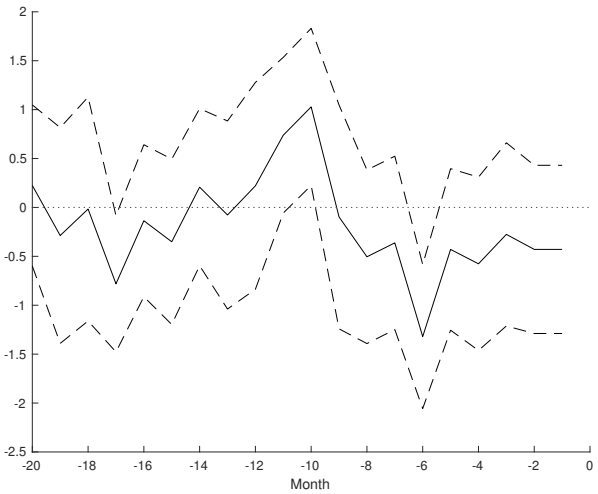

Figure B.8: Pollution Response to MPs, Pre-Trend

Notes: MPs is aggregated to the monthly frequencies consistent with the dependent variable. The dashed ribbons are the 90 percent confidence intervals generated based on the Newey-West standard errors.

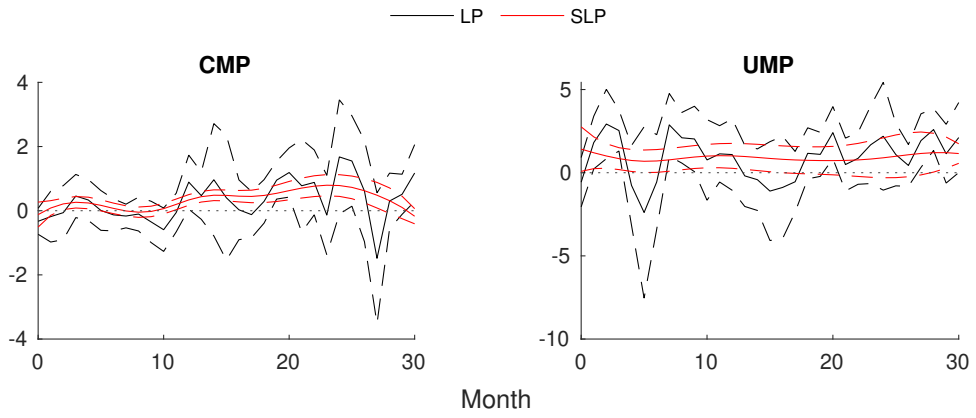

Figure B.9: Pollution Response to MPs, QE versus non-QE periods

Notes: The non-QE (CMP) period is from October 29th, 2014 to March 15th, 2020 and from March 9th, 2022 to late 2023. Correspondingly, the QE (UMP) period is from early 2009 to October 29th, 2014 and from March 15th, 2020 to March 9th, 2022. MPs is aggregated to the monthly frequencies consistent with the dependent variable. The number of lags of the dependent variable (Q) and the shock (M) are selected by the AIC criteria for up to 4 periods. The dashed ribbons are the 90 percent confidence intervals generated based on the Newey-West standard errors.

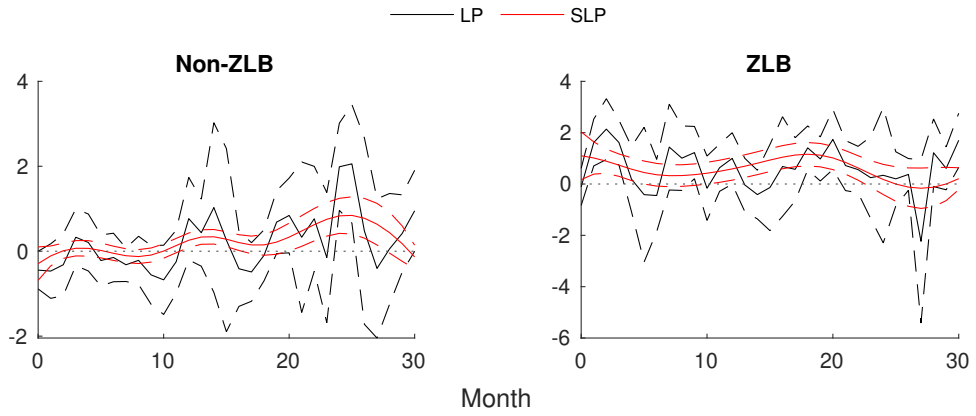

Figure B.10: Pollution Response to MPs, ZLB binding versus non-binding periods

Notes: The non-ZLB period is from December 16th, 2015 to March 16th, 2020 and from March 17th, 2022 to late 2023. Correspondingly, the ZLB period is from early 2009 to December 16th, 2015 and from March 16th, 2020 to March 17th, 2022. MPs is aggregated to the monthly frequencies consistent with the dependent variable. The number of lags of the dependent variable (Q) and the shock (M) are selected by the AIC criteria for up to 4 periods. The dashed ribbons are the 90 percent confidence intervals generated based on the Newey-West standard errors.

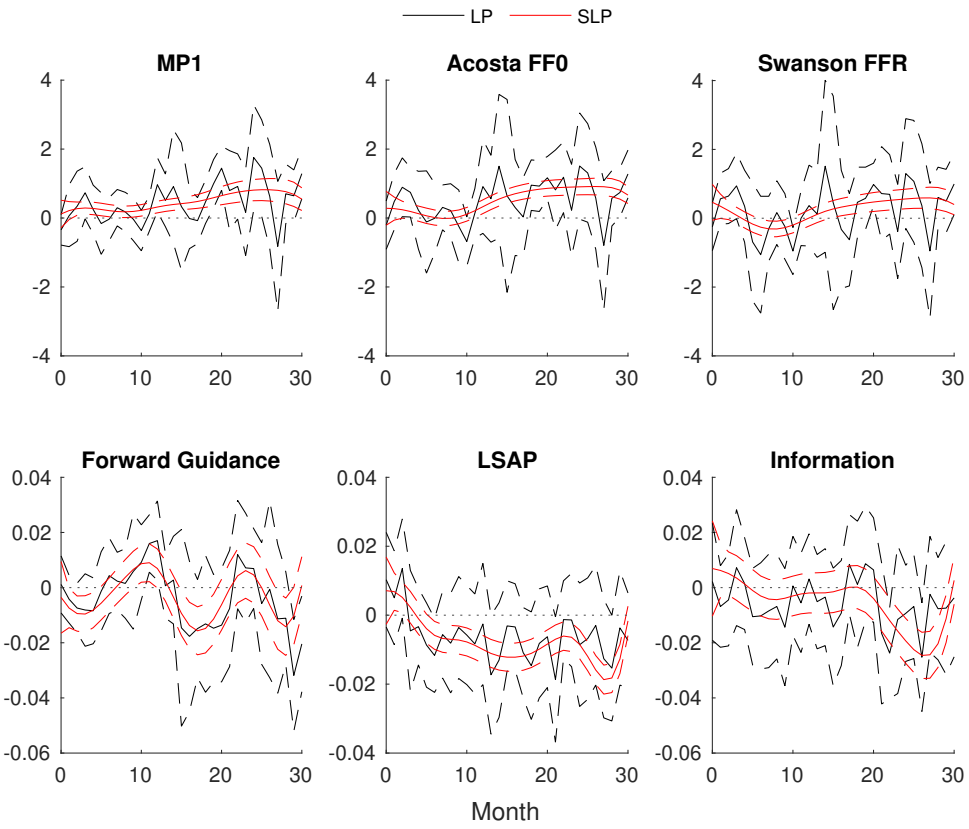

Figure B.11: Pollution Response to MPs, Other MPs

Notes: MPs is aggregated to the monthly frequencies consistent with the dependent variable. The number of lags of the dependent variable (Q) and the shock (M) are selected by the AIC criteria for up to 4 periods. The dashed ribbons are the 90 percent confidence intervals generated based on the Newey-West standard errors.

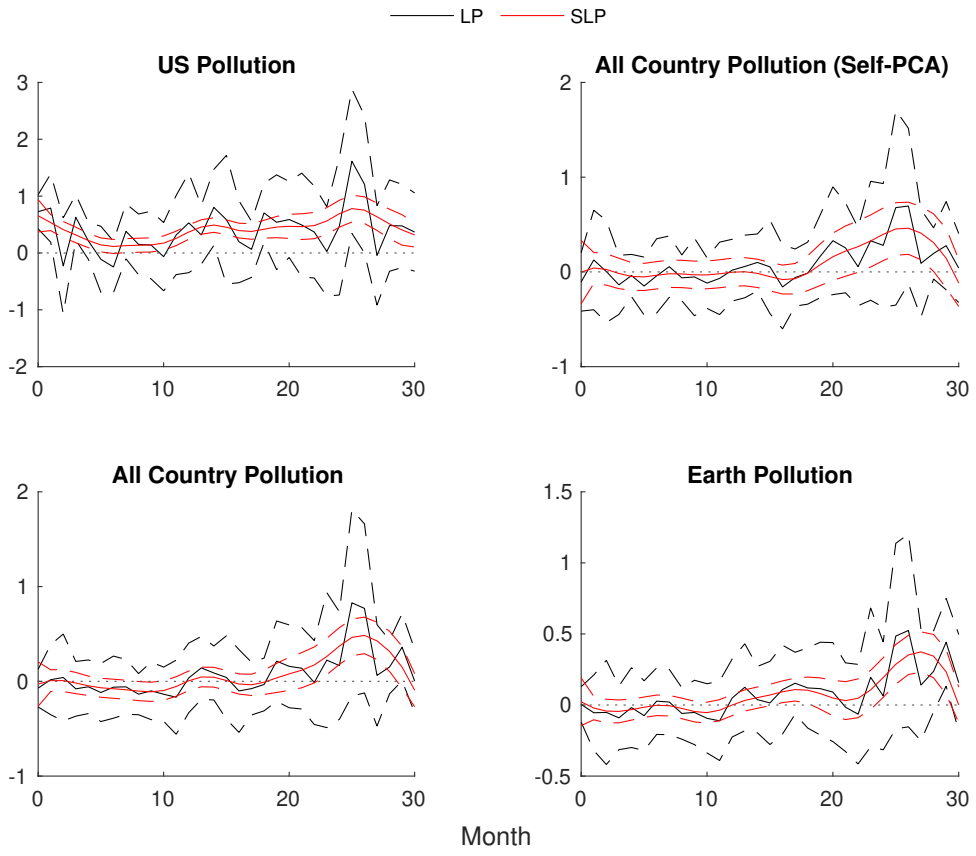

Figure B.12: Pollution Response to MPs, Other PCA Specifications

Notes: MPs is aggregated to the monthly frequencies consistent with the dependent variable. The number of lags of the dependent variable (Q) and the shock (M) are selected by the AIC criteria for up to 4 periods. The dashed ribbons are the 90 percent confidence intervals generated based on the Newey-West standard errors.

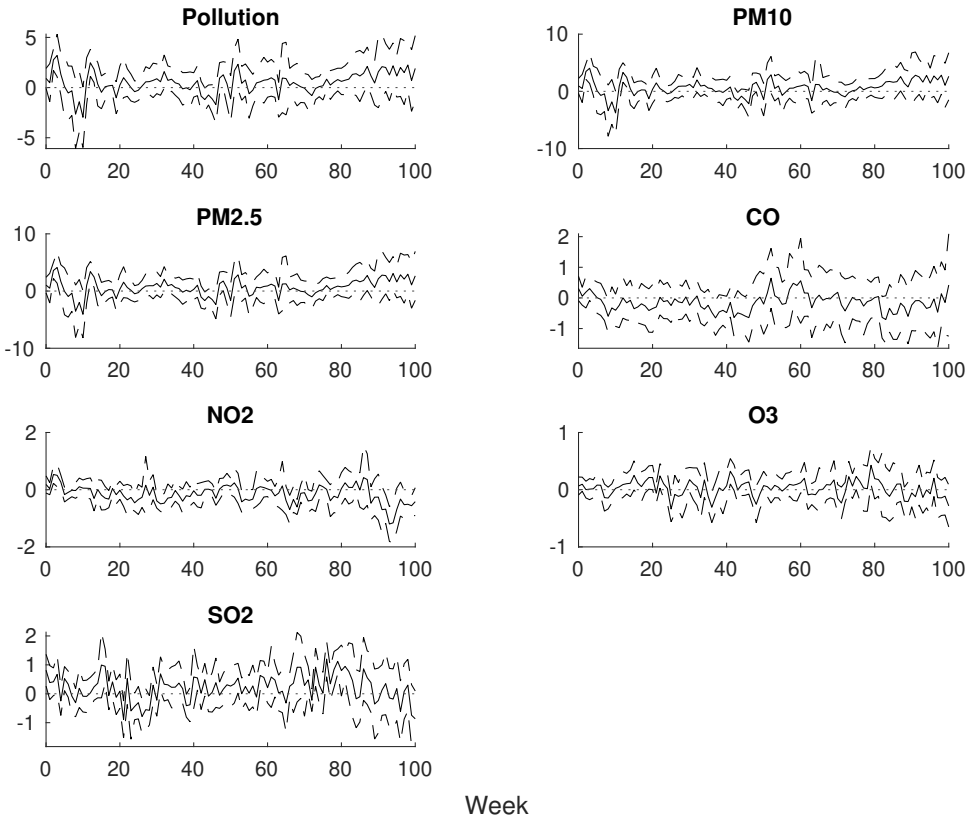

Figure B.13: Pollution Response to MPs, Weekly Series

Notes: MPs is aggregated to the weekly frequencies consistent with the dependent variable. The number of lags of the dependent variable (Q) and the shock (M) are selected by the AIC criteria for up to 20 periods. The dashed ribbons are the 90 percent confidence intervals generated based on the Newey-West standard errors.

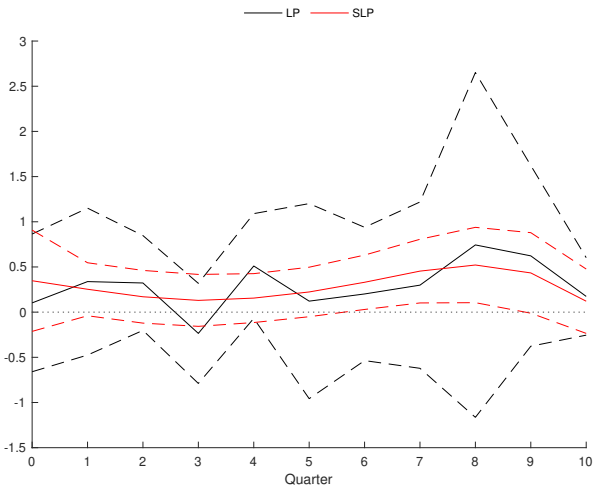

Figure B.14: Pollution Response to MPs, Aggregated to Quarterly

Notes: MPs is aggregated to the quarterly frequencies consistent with the dependent variable. The number of lags of the dependent variable (Q) and the shock (M) are selected by the AIC criteria for up to 4 periods. The dashed ribbons are the 90 percent confidence intervals generated based on the Newey-West standard errors.

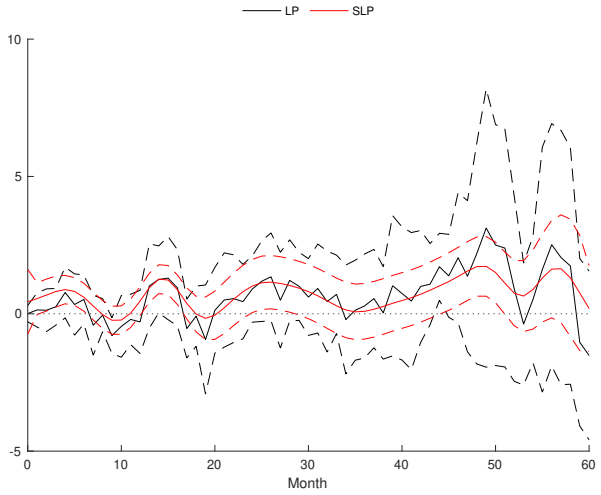

Figure B.15: Pollution Response to MPs, Monitor Station-Based Pollution Data

Notes: MPs is aggregated to the monthly frequencies consistent with the dependent variable. The number of lags of the dependent variable (Q) and the shock (M) are selected by the AIC criteria for up to 4 periods. The dashed ribbons are the 90 percent confidence intervals generated based on the Newey-West standard errors.

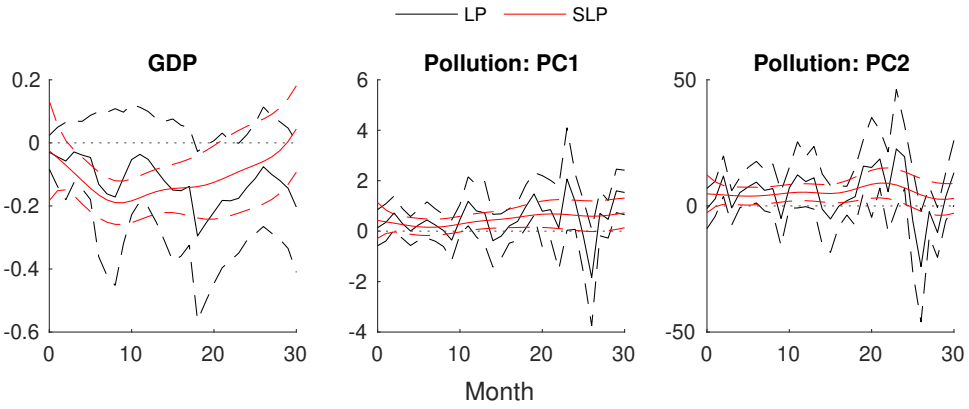

Figure B.16: Pollution Response to MPs (GDP and Pollution), Add PC2

Notes: The LP specification imposes the minimum delaying assumption with m starting from 1. MPs is aggregated to the monthly frequencies consistent with the dependent variable. The number of lags of the dependent variable (Q) and the shock (M) are selected by the AIC criteria for up to 4 periods. The dashed ribbons are the 90 percent confidence intervals generated based on the Newey-West standard errors.

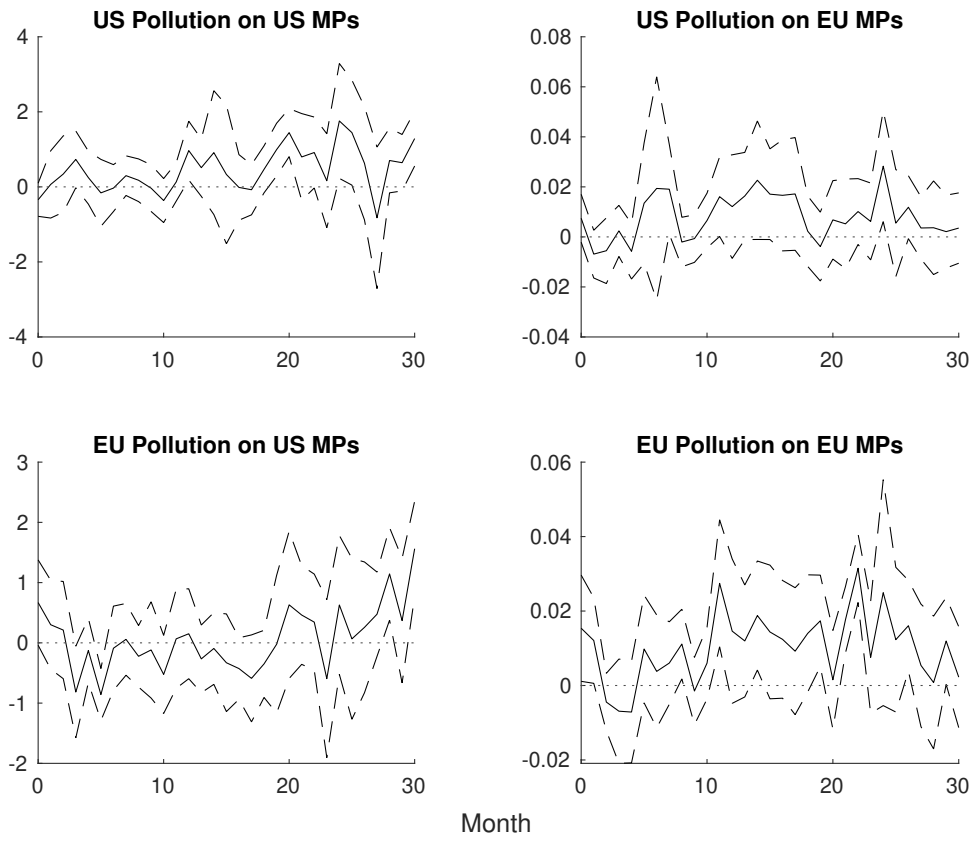

Figure B.17: Pollution Response to MPs, US and EU

Notes: MPs is aggregated to the monthly frequencies consistent with the dependent variable. The number of lags of the dependent variable (Q) and the shock (M) are selected by the AIC criteria for up to 4 periods. The dashed ribbons are the 90 percent confidence intervals generated based on the Newey-West standard errors.

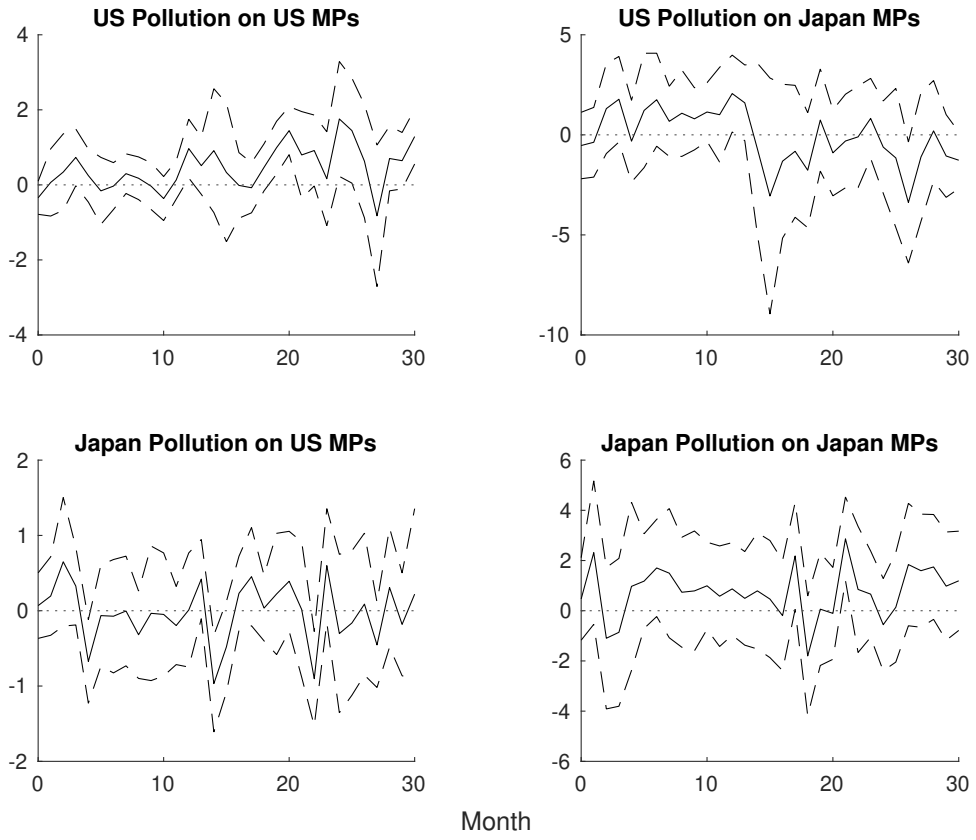

Figure B.18: Pollution Response to MPs, US and Japan

Notes: MPs is aggregated to the monthly frequencies consistent with the dependent variable. The number of lags of the dependent variable (Q) and the shock (M) are selected by the AIC criteria for up to 4 periods. The dashed ribbons are the 90 percent confidence intervals generated based on the Newey-West standard errors.

Appendix C More Results on Channel

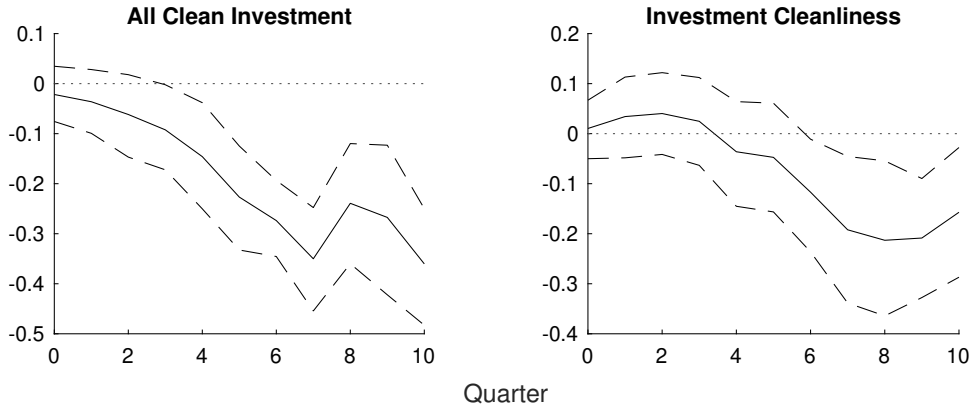

Figure C.1: Pollution per Unit of GDP Response to Clean Investment (IV: MPs)

Notes: MPs is aggregated to the quarterly frequencies consistent with the dependent variable. In the first stage, the number of lags of the endogenous variable is selected by the AIC criteria for up to 4 periods. In the second stage, the number of lags of the dependent variable (Q) and the endogenous variable (M) are selected by the AIC criteria for up to 4 periods. The dashed ribbons are the 90 percent confidence intervals generated by bootstrapping with 1,000 draws.

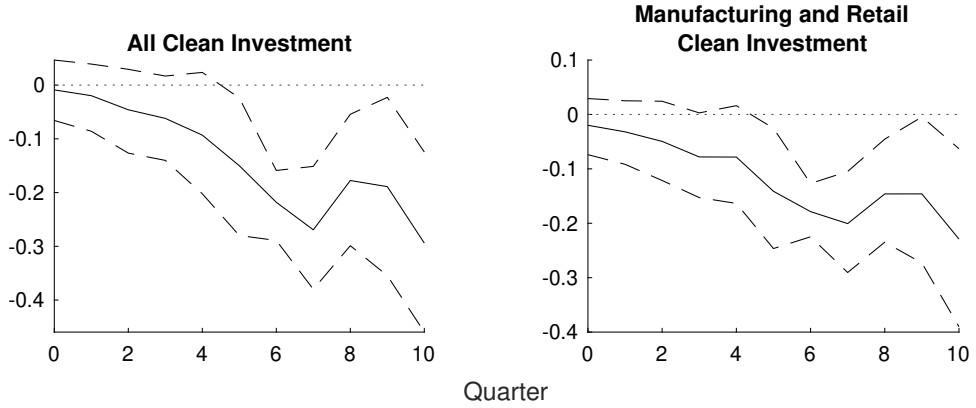

Figure C.2: Pollution Response to Clean Investment (IV: MPs), with Manufacturing and Retail Clean Investment

Notes: MPs is aggregated to the quarterly frequencies consistent with the dependent variable. In the first stage, the number of lags of the endogenous variable is selected by the AIC criteria for up to 4 periods. In the second stage, the number of lags of the dependent variable (Q) and the endogenous variable (M) are selected by the AIC criteria for up to 4 periods. The dashed ribbons are the 90 percent confidence intervals generated by bootstrapping with 1,000 draws.

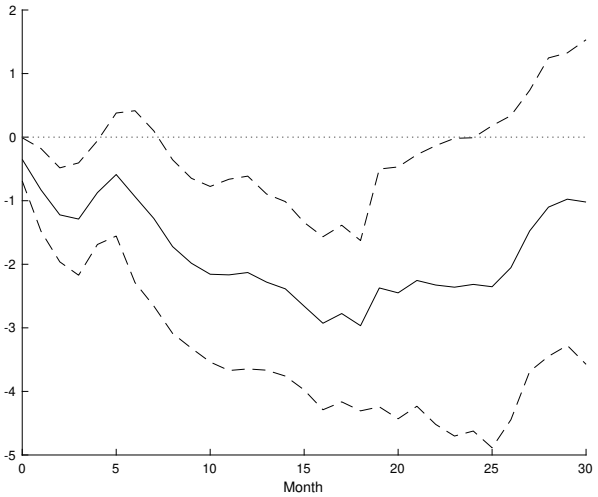

Figure C.3: Fuel Price Response to MPs

Notes: MPs is aggregated to the monthly frequencies consistent with the dependent variable. The number of lags of the dependent variable (Q) and the shock (M) are selected by the AIC criteria for up to 4 periods. The dashed ribbons are the 90 percent confidence intervals generated based on the Newey-West standard errors.

Table C.1: Firm Pollution Responses to MPs and Cleanliness: Dummies of Head and Tail in Distribution

	Renewable Energy Ratio		Emission Score		Resource Use Score	
$\mathbb{1}$(Rank $\geq$ P80)	0.0043		0.0327		0.0057	
	(0.0577)		(0.0260)		(0.0238)	
$\mathbb{1}$(Rank $\geq$ P80) $\times$ MPs	1.5862**		0.4857*		0.5601*	
	(0.6901)		(0.2689)		(0.2789)	
$\mathbb{1}$(Rank $\leq$ P20)		0.0581		-0.0369		-0.0760
		(0.0466)		(0.0460)		(0.0675)
$\mathbb{1}$(Rank $\leq$ P20) $\times$ MPs		-0.9768*		-2.5229**		-3.3422**
		(0.4698)		(0.9511)		(1.1611)
Firm FE	Yes	Yes	Yes	Yes	Yes	Yes
Year FE	Yes	Yes	Yes	Yes	Yes	Yes
N	1,132	1,132	4,716	4,716	4,716	4,716
Adjusted R^2	0.9771	0.9771	0.9802	0.9800	0.9802	0.9801

Notes: Significance levels are based on Firm standard-errors. For specifications with Year FE, they are based on Firm and Year standard-errors. Significance Codes: ***: 0.01, **: 0.05, *: 0.1, +: 0.2.

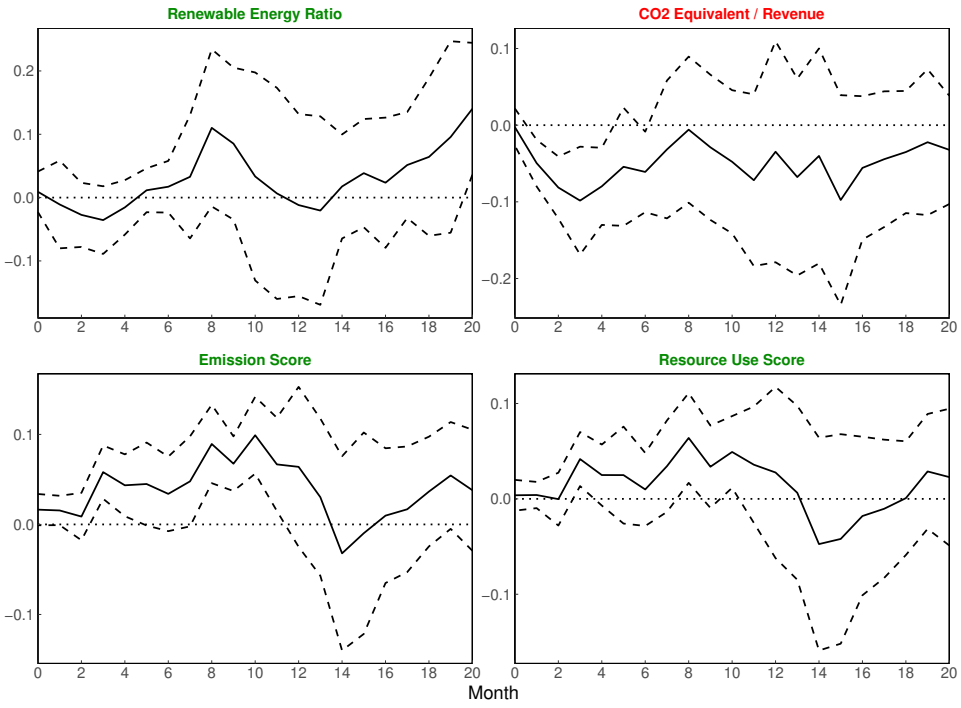

Figure C.4: ICCA Response to Interaction of US MPs and Clean Energy, Firm level

Notes: The dashed ribbons are the 90 percent confidence intervals generated based on standard errors clustered to firm and year.

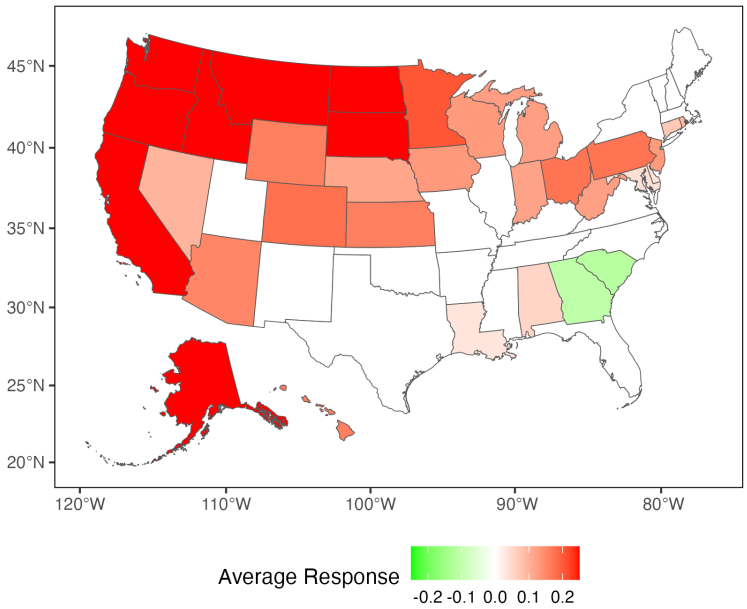

Figure C.5: Average Pollution Response to MPs by State

Notes: MPs is aggregated to the monthly frequencies consistent with the dependent variable. The number of lags of the dependent variable (Q) and the shock (M) are selected by the AIC criteria for up to 4 periods. When taking the average across the time horizon from the month the MPs is realized to 20 months later, insignificant values at a 90 percent confidence level are treated as zero. If the region has both significantly positive and significantly negative responses, the average response by the region is interpreted as zero. Extreme values with absolute values greater than 0.25 are winsorized on the map.

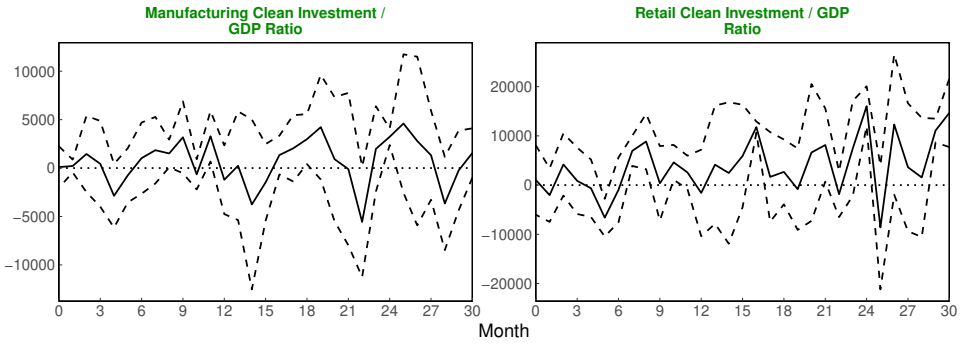

Figure C.6: Pollution Response to Interaction of US MPs and Clean Investment Share of GDP, State level

Notes: The dashed ribbons are the 90 percent confidence intervals generated based on standard errors clustered to region and year.

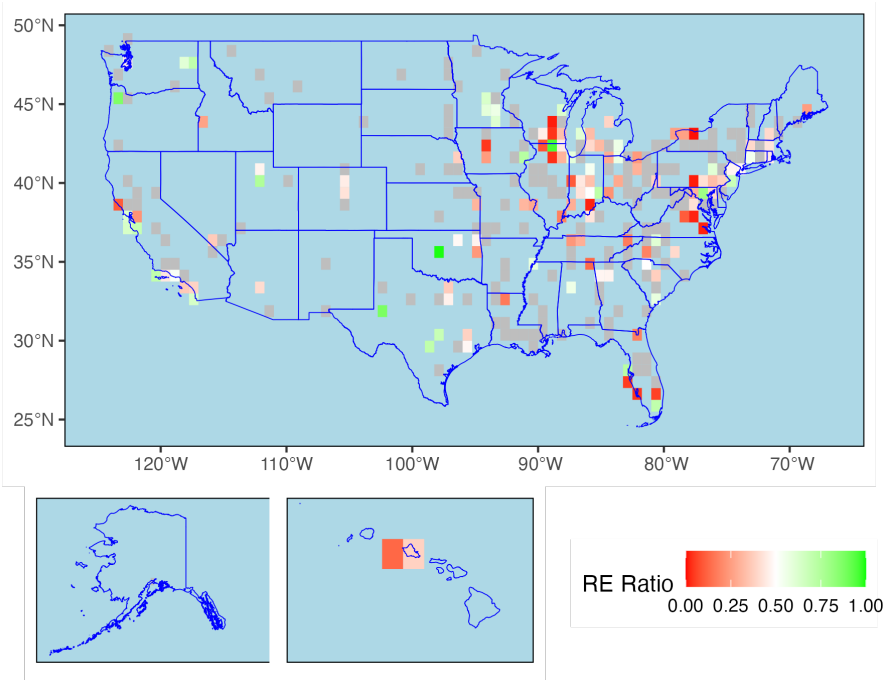

Figure C.7: Average Renewable Energy Usage Ratio by Mesh in 2022

Notes: Regions with firms but without available data are in gray.

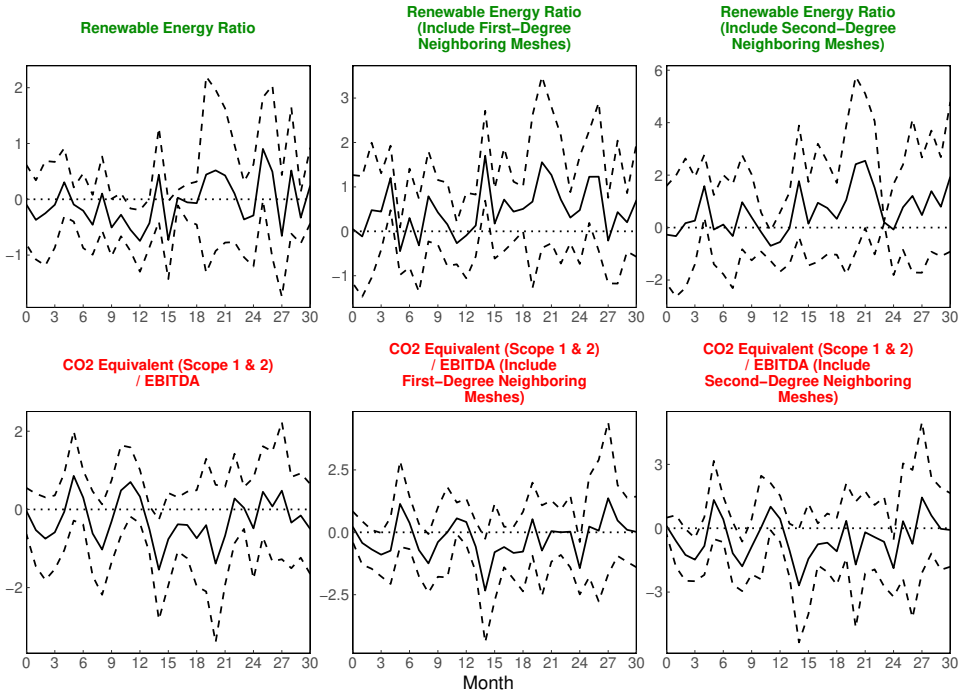

Figure C.8: Pollution Response to Interaction of US MPs and Firm Indicators, Mesh level

Notes: The dashed ribbons are the 90 percent confidence intervals generated based on standard errors clustered to region and year.

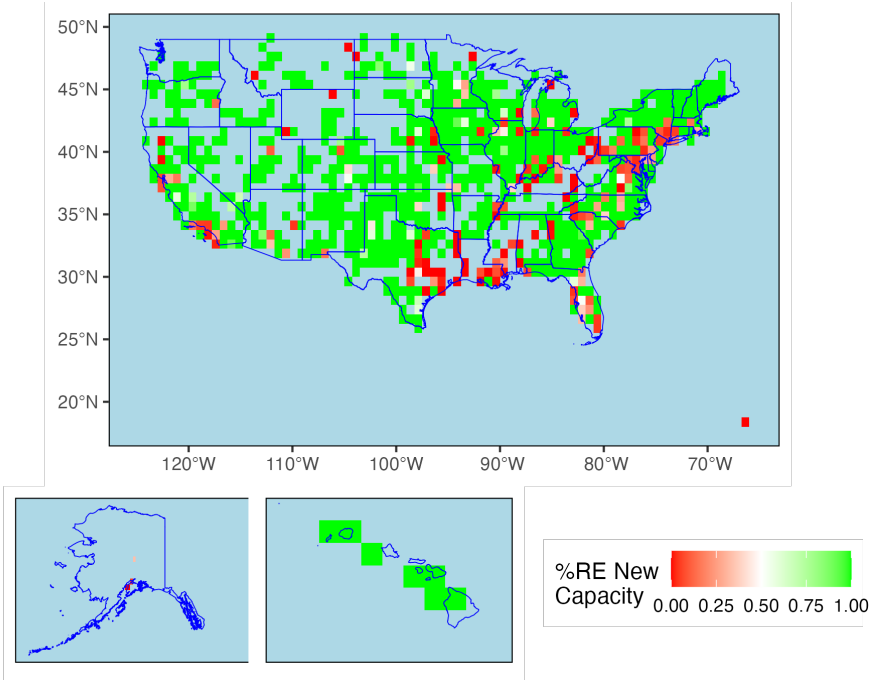

Figure C.9: Average Clean Energy New Commission Share by Mesh

Notes: The plants include all power plants commissioned since 2009 and are still operating in 2024.

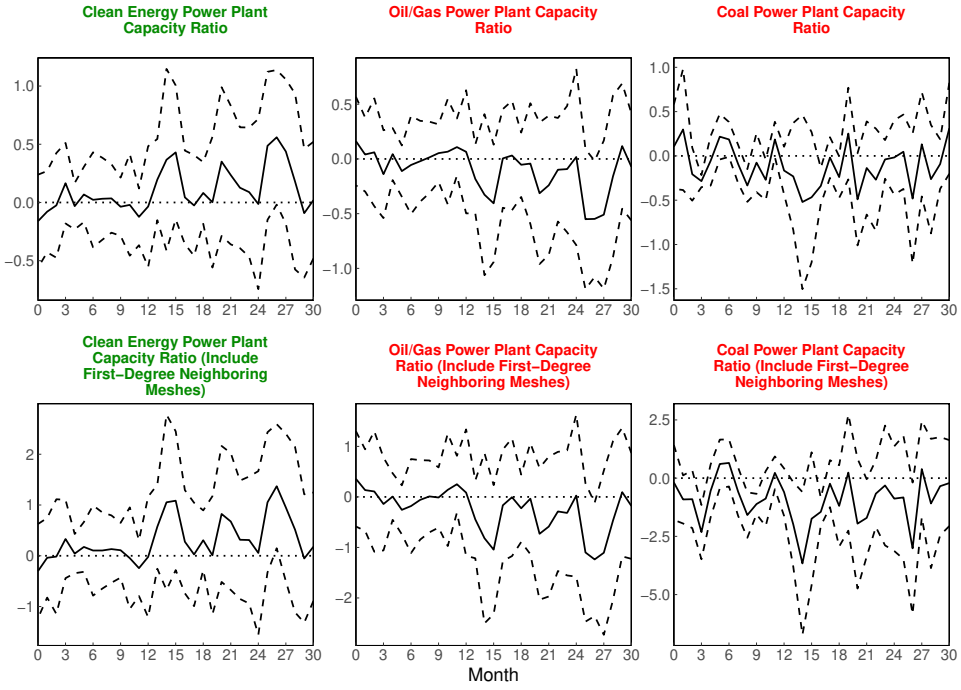

Figure C.10: Pollution Response to Interaction of US MPs and Clean Energy New Commission Share, Mesh level

Notes: The dashed ribbons are the 90 percent confidence intervals generated based on standard errors clustered to region and year.

Appendix D Model Details

D.1 Derivation

D.1.1 First Order Conditions

From the household utility maximization problem, set the Lagrangian:

$$\begin{aligned}\mathcal{L} = &\frac{\tilde{C}_t^{1-\sigma}}{1-\sigma} + \frac{\gamma}{1-b}\left(\frac{M_t}{P_t}\right)^{1-b} - \chi\frac{L_t^{1+\eta}}{1+\eta} \\ &\lambda_t\left[\frac{M_t}{P_t} + \frac{B_t}{P_t} + C_t + \frac{K_t}{1-g} + \frac{\Phi}{2(1-g)^2}\left(\frac{K_t}{K_{t-1}} - 1\right)^2 K_{t-1} + \phi_1 U_t^{\phi_2}(1-\Gamma)A_t K_{t-1}^{\alpha} L_t^{1-\alpha}\right. \\ &\left. -\frac{M_{t-1}}{P_t} - \frac{B_{t-1}R_{t-1}}{P_t} - w_t L_t - \left(r_t + \frac{1-\delta}{1-g}\right)K_{t-1} - \Pi_t\right]\end{aligned} \tag{D.1}$$

Here, the capital adjustment cost is:

$$\begin{aligned}&\frac{\Phi}{2}\left(\frac{I_t}{K_{t-1}} - \frac{\delta}{1-g}\right)^2 K_{t-1} = \frac{\Phi}{2}\left(\frac{K_t - (1-\delta)K_{t-1}}{(1-g)K_{t-1}} - \frac{\delta}{1-g}\right)^2 K_{t-1} \\ &= \frac{\Phi}{2(1-g)^2}\left(\frac{K_t}{K_{t-1}} - 1\right)^2 K_{t-1}\end{aligned} \tag{D.2}$$

Derive the FOC w.r.t. C_t, L_t, $\left(\frac{M}{P}\right)_t$, B_t, and K_t.[29]

$$\tilde{C}_t^{-\sigma}[w_t - (1-\alpha)\phi_1 U_t^{\phi_2}(1-\Gamma)A_t K_{t-1}^{\alpha} L_t^{-\alpha}] = \chi L_t^{\eta} \tag{D.3}$$

$$\frac{\gamma}{\tilde{C}_t^{-\sigma}}\left(\frac{M_t}{P_t}\right)^{b} = \frac{R_t - 1}{R_t} \tag{D.4}$$

$$\tilde{C}_t^{-\sigma} = \beta\tilde{C}_{t+1}^{-\sigma} R_t \frac{P_t}{P_{t+1}} \tag{D.5}$$

$$\begin{aligned}&\tilde{C}_t^{-\sigma}\left[\frac{1}{1-g} + \frac{\Phi}{(1-g)^2}\left(\frac{K_t}{K_{t-1}} - 1\right)\right] \\ &= \beta\tilde{C}_{t+1}^{-\sigma}\left[\underbrace{\left(r_{t+1} + \frac{1-\delta}{1-g}\right) + \frac{\Phi}{2(1-g)^2}\left(\frac{K_{t+1}}{K_t} - 1\right)\left(\frac{K_{t+1}}{K_t} + 1\right)}_{\text{A}} - \underbrace{\alpha\phi_1 U_{t+1}^{\phi_2}(1-\Gamma)A_{t+1}K_t^{\alpha-1}L_{t+1}^{1-\alpha}}_{\text{B}}\right]\end{aligned} \tag{D.6}$$

[29] The direct FOC w.r.t. $\tilde{C}_t$ is $\tilde{C}_t^{-\sigma} = -\lambda_t\frac{dC_t}{d\tilde{C}_t}$. Therefore, the FOC w.r.t. C_t is linearly convertible to the FOC w.r.t. $\tilde{C}_t$ with a factor of $\frac{dC_t}{d\tilde{C}_t}$. This property simplifies the household FOC conditions, as other FOC conditions are based on $\tilde{C}_t$ instead of C_t.

The relationship between R and r is:

$$R_t\left[\frac{1}{1-g}+\frac{\Phi}{(1-g)^2}\left(\frac{K_t}{K_{t-1}}-1\right)\right]$$
$$=\frac{P_{t+1}}{P_t}\left[\left(r_{t+1}+\frac{1-\delta}{1-g}\right)+\frac{\Phi}{2(1-g)^2}\left(\frac{K_{t+1}}{K_t}-1\right)\left(\frac{K_{t+1}}{K_t}+1\right)-\alpha\phi_1 U_{t+1}^{\phi_2}(1-\Gamma)A_{t+1}K_t^{\alpha-1}L_{t+1}^{1-\alpha}\right] \tag{D.7}$$

From the firm profit maximization problem, derive the FOC w.r.t. w_t, r_t, and U_t.

$$w_t=(1-\alpha)MCP_t\frac{Y_t}{L_t} \tag{D.8}$$

$$r_t=\alpha MCP_t\frac{Y_t}{K_{t-1}} \tag{D.9}$$

$$\phi_1\phi_2 U_t^{\phi_2-1}=\tau\varphi_t \Rightarrow U_t=\left(\frac{\tau\varphi_t}{\phi_1\phi_2}\right)^{\frac{1}{\phi_2-1}} \tag{D.10}$$

The New Keyesian Price Curve (NKPC) is:

$$\hat{\pi}_t=\beta\hat{\pi}_{t+1}+\kappa\widehat{MCP}_t,\ \kappa=\frac{(1-\omega)(1-\beta\omega)}{\omega} \tag{D.11}$$

D.1.2 Steady State

To my knowledge so far, the steady state has no analytical solution. I use function iteration method with r starting from $\left(\frac{1}{\beta}-(1-\delta)\right)\frac{1}{1-g}$ and φ starting from φ^f.[30]

From the TFP dynamics:

$$A=1 \tag{D.12}$$

At the steady state, price does not change:

$$\pi_t:=\frac{P_t}{P_{t-1}}\Rightarrow\pi=1 \tag{D.13}$$

From the household FOC w.r.t. B_t:

$$R=\frac{1}{\beta} \tag{D.14}$$

From the firm FOC w.r.t. U_t:

$$U=\left(\frac{\tau\varphi}{\phi_1\phi_2}\right)^{\frac{1}{\phi_2-1}} \tag{D.15}$$

[30] From the relationship between R and r, $R(\frac{1}{1-g})=\frac{1}{\beta(1-g)}=r+\frac{1-\delta}{1-g}-\alpha\phi_1U^{\phi_2}\frac{Y}{K}$. Ignoring the cost of abatement effort, $r=\left(\frac{1}{\beta}-(1-\delta)\right)\frac{1}{1-g}$. As $\frac{1}{\beta(1-g)}=r+\frac{1-\delta}{1-g}-\frac{\phi_1U^{\phi_2}}{MCP}r=r+\frac{1-\delta}{1-g}-\frac{\phi_1\left(\frac{\tau\varphi}{\phi_1\phi_2}\right)^{\frac{\phi_2}{\phi_2-1}}}{MCP}r$, the actual r should be greater than the starting value.

From the competitive market equilibrium:

$$\begin{aligned}
&(1-\Gamma)K^{\alpha}L^{1-\alpha} = rK + wL + \tau(1-U)Y + \phi_1 U^{\phi_2} Y \\
&\Rightarrow \underbrace{\{(1-\Gamma)(1-\tau(1-U)\varphi - \phi_1 U^{\phi_2})\}}_{\text{Friction}} K^{\alpha}L^{1-\alpha} - wL - rK = 0 \\
&\Rightarrow \{\cdots\}\left(\frac{K}{L}\right)^{\alpha} L = r\left(\frac{K}{L}\right)L + w
\end{aligned} \tag{D.16}$$

From the firm FOC w.r.t. w_t and r_t:

$$\left.\begin{aligned} w &= (1-\alpha)MCP\frac{Y}{L} \\ r &= \alpha MCP\frac{Y}{K} \end{aligned}\right\} \Rightarrow w = \frac{1-\alpha}{\alpha} r \frac{K}{L}$$

$$\begin{aligned}
&\Rightarrow \{\cdots\}\left(\frac{K}{L}\right)^{\alpha} L = r\left(\frac{K}{L}\right)L + \frac{1-\alpha}{\alpha} r\left(\frac{K}{L}\right)L \\
&\Rightarrow \left(\frac{K}{L}\right)^{\alpha-1} = \frac{r}{\alpha\{\cdots\}} \Rightarrow k_l := \frac{K}{L} = \left(\frac{\alpha\{\cdots\}}{r}\right)^{\frac{1}{1-\alpha}},\ k_l^{\text{nofric}} = \left(\frac{\alpha}{r}\right)^{\frac{1}{1-\alpha}} \\
&w = \frac{1-\alpha}{\alpha} r\left(\frac{\alpha\{\cdots\}}{r}\right)^{\frac{1}{1-\alpha}} = (1-\alpha)\left(\frac{\alpha}{r}\right)^{\frac{\alpha}{1-\alpha}} \{\cdots\}^{\frac{1}{1-\alpha}}
\end{aligned} \tag{D.17}$$

From traditional capital dynamics:

$$\begin{aligned}
&I = \frac{\delta}{1-g}K \overset{\text{def}}{=} s_I Y \Rightarrow K = \frac{(1-g)s_I}{\delta}Y \Rightarrow L = \frac{\frac{(1-g)s_I}{\delta}Y}{k_l} = \frac{(1-g)s_I}{\delta}\left(\frac{\alpha\{\cdots\}}{r}\right)^{-\frac{1}{1-\alpha}} Y \\
&\Rightarrow Y = (1-\Gamma)K^{\alpha}L^{1-\alpha} = (1-\Gamma)\frac{(1-g)s_I}{\delta}\left(\frac{\alpha\{\cdots\}}{r}\right)^{-1} Y \\
&\Rightarrow s_I = \frac{\alpha\delta\{\cdots\}}{r(1-g)(1-\Gamma)}
\end{aligned} \tag{D.18}$$

From the goods market clearing condition:

$$\begin{aligned}
Y &= C + I + \phi_1 U^{\phi_2} Y \\
&\Rightarrow C = (1 - s_I - \phi_1 U^{\phi_2})Y
\end{aligned} \tag{D.19}$$

By the definition of $\tilde{C}$:

$$\tilde{C} = \left[aC^{1-\phi} + (1-a)(Z^{-1})^{1-\phi}\right]^{\frac{1}{1-\phi}} \tag{D.20}$$

From the household FOC w.r.t. L_t:

$$\left.\begin{aligned} Z = (1-U)\varphi Y &= \frac{(1-U)\varphi C}{1 - s_I - \phi_1 U^{\phi_2}} \\ L = \frac{(1-g)s_I}{\delta}\left(\frac{\alpha\{\cdots\}}{r}\right)^{-\frac{1}{1-\alpha}} Y &= \frac{(1-g)s_I}{\delta}\left(\frac{\alpha\{\cdots\}}{r}\right)^{-\frac{1}{1-\alpha}} \frac{C}{1 - s_I - \phi_1 U^{\phi_2}} \end{aligned}\right\}$$

$$\begin{aligned}
&\Rightarrow \left[aC^{1-\phi} + (1-a)\left(\frac{1 - s_I - \phi_1 U^{\phi_2}}{(1-U)\varphi C}\right)^{1-\phi}\right]^{\frac{-\sigma}{1-\phi}} [w - (1-\alpha)\phi_1 U^{\phi_2}(1-\Gamma)k_l^{\alpha}] \\
&= \chi\left[\frac{(1-g)s_I}{\delta}\left(\frac{\alpha\{\cdots\}}{r}\right)^{-\frac{1}{1-\alpha}} \frac{C}{1 - s_I - \phi_1 U^{\phi_2}}\right]^{\eta}
\end{aligned} \tag{D.21}$$

Solve the C.

Obtain other steady state values subsequently.

$$\begin{aligned} L &= \frac{(1-g)s_I}{\delta}\left(\frac{\alpha\{\cdots\}}{r}\right)^{-\frac{1}{1-\alpha}}\frac{C}{1-s_I-\phi_1 U^{\phi_2}} \\ Y &= \frac{C}{1-s_I-\phi_1 U^{\phi_2}} \\ Z &= (1-U)\varphi Y \\ \tilde{C} &= \left[aC^{1-\phi}+(1-a)(Z^{-1})^{1-\phi}\right]^{\frac{1}{1-\phi}} \\ I &= s_I Y \end{aligned} \tag{D.22}$$

$$N = \frac{T+gI}{\delta_N} = \frac{\tau}{\delta_N}(1-U)\varphi Y + \frac{gI}{\delta_N} = \frac{\tau}{\delta_N}\left(1-\left(\frac{\tau\varphi^f\left(\frac{\mu}{\mu+N}\right)^h}{\phi_1\phi_2}\right)^{\frac{1}{\phi_2-1}}\right)\varphi^f\left(\frac{\mu}{\mu+N}\right)^h Y + \frac{gI}{\delta_N} \tag{D.23}$$

Solve the N.

$$\varphi = \varphi^f\left(\frac{\mu}{\mu+N}\right)^h \tag{D.24}$$

Compare the implied φ with the starting value, iterate until convergence.

From the relationship between R and r:

$$r = \frac{1}{1-g}\left(\frac{1}{\beta}-(1-\delta)\right)+\alpha\phi_1 U^{\phi_2}(1-\Gamma)k_l^{\alpha-1} \tag{D.25}$$

Compare the implied r with the starting value, iterate until convergence.

D.1.3 Log Linearlization

From the household FOC w.r.t. B_t, K_t, and C_t:

$$\hat{R}_t - \hat{\pi}_{t+1} = \sigma(\widehat{\tilde{C}}_{t+1} - \widehat{\tilde{C}}_t) \tag{D.26}$$

$$\begin{aligned} &\hat{R}_t - \hat{\pi}_{t+1} + \frac{\Phi}{1-g}(\hat{K}_t - \hat{K}_{t-1}) \\ &= \frac{\left[\underbrace{r(\widehat{MCP}_{t+1}+\hat{Y}_{t+1}-\hat{K}_t)+\frac{\Phi}{(1-g)^2}(\hat{K}_{t+1}-\hat{K}_t)}_{\text{A}} - \underbrace{\alpha\phi_1 U^{\phi_2}\frac{Y}{K}(\phi_2\hat{U}_{t+1}+\hat{Y}_{t+1}-\hat{K}_t)}_{\text{B}}\right]}{r+\frac{1-\delta}{1-g}-\alpha\phi_1 U^{\phi_2}\frac{Y}{K}} \end{aligned} \tag{D.27}$$

$$\begin{aligned} &\eta\hat{L}_t + \sigma\widehat{\tilde{C}}_t \\ &= \frac{w\left(\widehat{MCP}_t + \frac{\alpha}{1-\alpha}(\hat{K}_{t-1}-\hat{Y}_t)\right) - ((1-\alpha)\phi_1 U^{\phi_2}(1-\Gamma)k_l^{\alpha})(\phi_2\hat{U}_t + A_t + \alpha\hat{K}_{t-1} - \alpha\hat{L}_t)}{w-(1-\alpha)\phi_1 U^{\phi_2}(1-\Gamma)k_l^{\alpha}} \end{aligned} \tag{D.28}$$

From the firm production function:

$$\hat{Y}_t = \hat{A}_t + \alpha \hat{K}_{t-1} + (1-\alpha)\hat{L}_t \tag{D.29}$$

From traditional capital dynamics:

$$\hat{K}_t = (1-\delta)\hat{K}_{t-1} + \delta \hat{I}_t \tag{D.30}$$

From the goods market clearing condition:

$$\hat{Y}_t = \frac{(1 - s_I - \phi_1 U^{\phi_2})\hat{C}_t + s_I \hat{I}_t}{1 - \phi_1 U^{\phi_2}} \tag{D.31}$$

NKPC:

$$\hat{\pi}_t = \beta \hat{\pi}_{t+1} + \kappa \widehat{MCP}_t \tag{D.32}$$

From the household FOC w.r.t. $(\frac{M}{P})_t$:

$$b(\hat{M}_t - \hat{P}_t) = \sigma \widehat{\tilde{C}}_t - \frac{\beta}{1-\beta}\hat{R}_t \tag{D.33}$$

Monetary policy:

$$\hat{R}_t = \rho_R \hat{R}_{t-1} + (1-\rho_R)(\psi_\pi \hat{\pi}_t + \psi_Y \hat{Y}_t) + \varepsilon_{R,t} \tag{D.34}$$

TFP:

$$\hat{A}_t = \rho_A \hat{A}_{t-1} + (1-\rho_A)\varepsilon_{A,t} \tag{D.35}$$

From the firm FOC w.r.t. U_t:

$$(\phi_2 - 1)\hat{U}_t = \hat{\varphi}_t \tag{D.36}$$

From the pollution factor as a function of environmental capital, with sticky technology:

$$\hat{\varphi}_t = \omega_\varphi \left(-h \frac{N}{\mu + N} \hat{N}_t \right) + (1-\omega_\varphi)\hat{\varphi}_{t-1} \tag{D.37}$$

From the environmental capital dynamics:

$$\hat{N}_t = \frac{(1-\delta_N)N\hat{N}_{t-1} + T\hat{T}_t + gI\hat{I}_t}{(1-\delta_N)N + T + gI} \tag{D.38}$$

From the pollution determination:

$$\hat{Z}_t = \hat{\varphi}_t + \hat{Y}_t - \frac{U}{1-U}\hat{U}_t \tag{D.39}$$

From the pollution tax as a function of pollution, with linearly proportional relationship:

$$\hat{T}_t = \hat{Z}_t \tag{D.40}$$

By the definition of $\tilde{C}$:

$$\widehat{\tilde{C}}_t = \frac{aC^{1-\phi}\hat{C}_t + (1-a)(Z^{-1})^{1-\phi}(-\hat{Z}_t)}{aC^{1-\phi} + (1-a)(Z^{-1})^{1-\phi}} \tag{D.41}$$

Since the model-generated elasticity of environmental capital to MPs, ε_{NI} relative to that of traditional capital, ε_{KI}, does not match the empirical results, I adjust the response dynamics of the two types of capital with a difference operator Δ_ε.

$$\begin{aligned}\hat{K}_t &= (1-\delta)\hat{K}_{t-1} + (\delta - \Delta_\varepsilon)\hat{I}_t \\ \hat{N}_t &= \frac{(1-\delta_N)N\hat{N}_{t-1} + T\hat{T}_t + gI\hat{I}_t}{(1-\delta_N)N + T + gI} + \frac{K}{N}\Delta_\varepsilon \hat{I}_t\end{aligned} \tag{D.42}$$

The magnitude of the difference operator depends on the relative elasticity, $\frac{\varepsilon_{NI}}{\varepsilon_{KI}}$.

$$\left.\begin{aligned}\varepsilon_{NI} = \frac{gI}{(1-\delta_N)N + T + gI} + \frac{K}{N}\Delta_\varepsilon \\ \varepsilon_{KI} = \delta - \Delta_\varepsilon\end{aligned}\right\}$$
$$\begin{aligned}\Rightarrow \frac{\varepsilon_{NI}}{\varepsilon_{KI}} &= \frac{\frac{gI}{(1-\delta_N)N+T+gI} + \frac{K}{N}\Delta_\varepsilon}{\delta - \Delta_\varepsilon} \\ \Rightarrow \Delta_\varepsilon &= \frac{\delta\left(\frac{\varepsilon_{NI}}{\varepsilon_{KI}}\right) - \frac{gI}{(1-\delta_N)N+T+gI}}{\frac{K}{N} + \frac{\varepsilon_{NI}}{\varepsilon_{KI}}}\end{aligned} \tag{D.43}$$

From above, when the relative elasticity is 1, $\Delta_\varepsilon < 1$ because the government partly funds the clean investment. The model assumes that only firms maximize marginal discounted cash flow and match the relative elasticity with the relative duration. $\frac{\varepsilon_{NI}}{\varepsilon_{KI}}$ is only for firms' private investment and ignores government behavior. Therefore, I have to multiply a factor, ξ, when obtaining the difference operator. As the difference operator should be zero when $\frac{\varepsilon_{NI}}{\varepsilon_{KI}} = 1$, I have:

$$\begin{aligned}\xi &= \frac{gI}{\delta[(1-\delta_N)N + T + gI]} \\ \Rightarrow \Delta_\varepsilon &= \frac{\delta\xi\left(\frac{\varepsilon_{NI}}{\varepsilon_{KI}}\right) - \frac{gI}{(1-\delta_N)N+T+gI}}{\frac{K}{N} + \xi\frac{\varepsilon_{NI}}{\varepsilon_{KI}}}\end{aligned} \tag{D.44}$$

The difference operator is partially tuned down because of government involvement in clean investment.

D.1.4 Relative Elasticity

This part derives the relative elasticity of environmental versus traditional capital after a MPs.

$$\begin{aligned}\Pi_t &= P_tY_t - w_tL_t - r_tK_t - T_t - \mathcal{CA}_t \\ &= \left[P_t - \tau(1-U_t)\varphi_t - \phi_1 U_t^{\phi_2}\right]Y_t - w_tL_t - r_tK_t \\ &= \left[P_t - \tau\left(1 - \left(\frac{\tau}{\phi_1\phi_2}\right)^{\frac{1}{\phi_2-1}}\varphi_t^{\frac{1}{\phi_2-1}}\right)\varphi_t - \phi_1\left(\frac{\tau}{\phi_1\phi_2}\right)^{\frac{\phi_2}{\phi_2-1}}\varphi_t^{\frac{\phi_2}{\phi_2-1}}\right]Y_t - w_tL_t - r_tK_t\end{aligned} \tag{D.45}$$

From the relationship between $\tilde{\varphi}$ and N:

$$\begin{aligned}\frac{d\tilde{\varphi}_t}{dN_t} &= \varphi^f h \left(\frac{\mu}{\mu + N_t}\right)^{h-1} \mu \frac{-1}{(\mu + N_t)^2} = \frac{-\varphi^f h \mu^h}{(\mu + N_t)^{h+1}} \\ \Rightarrow \frac{d\tilde{\varphi}_{t+n}}{dN_{t+n}} &= \frac{-\varphi^f h \mu^h}{(\mu + N_{t+n})^{h+1}}\end{aligned} \tag{D.46}$$

$$\begin{aligned}\varphi_t &= \omega_\varphi \tilde{\varphi}_t + (1-\omega_\varphi)\omega_\varphi \tilde{\varphi}_{t-1} + (1-\omega_\varphi)^2 \omega_\varphi \tilde{\varphi}_{t-2} + \cdots + (1-\omega_\varphi)^n \omega_\varphi \tilde{\varphi}_{t-n} + (1-\omega_\varphi)^{n+1} \varphi_{t-n-1} \\ \Rightarrow \varphi_{t+n} &= \omega_\varphi \tilde{\varphi}_{t+n} + (1-\omega_\varphi)\omega_\varphi \tilde{\varphi}_{t+n-1} + \cdots + (1-\omega_\varphi)^n \omega_\varphi \tilde{\varphi}_t + (1-\omega_\varphi)^{n+1} \varphi_{t-1} \\ &= \omega_\varphi \sum_{i=0}^{n} (1-\omega_\varphi)^{n-i} \tilde{\varphi}_{t+i} + (1-\omega_\varphi)^{n+1} \varphi_{t-1} \\ \Rightarrow \frac{d\varphi_{t+n}}{dN_t} &= \omega_\varphi \sum_{i=0}^{n} (1-\omega_\varphi)^{n-i} \frac{d\tilde{\varphi}_{t+i}}{dN_t} \\ &= \omega_\varphi \sum_{i=0}^{n} (1-\omega_\varphi)^{n-i} \frac{d\tilde{\varphi}_{t+i}}{dN_{t+i}} \frac{dN_{t+i}}{dN_t}\end{aligned} \tag{D.47}$$

A simplification here is:

$$\frac{dN_{t+1}}{dN_t} = 1 - \delta_N \tag{D.48}$$

While the complete form should be:

$$
\begin{aligned}
\frac{dN_{t+1}}{dN_t} &= 1-\delta_N+\frac{d\tau(1-U_{t+1})\varphi_{t+1}Y_{t+1}}{dN_t}\\
&= 1-\delta_N+\tau Y_{t+1}\frac{d(1-U_{t+1})\varphi_{t+1}}{dN_t}\\
&= 1-\delta_N+\tau Y_{t+1}\left((1-U_{t+1})\frac{d\varphi_{t+1}}{dN_t}+\varphi_{t+1}\frac{d(1-U_{t+1})}{dN_t}\right)\\
&= 1-\delta_N+\tau Y_{t+1}\omega_\varphi\left(1-\left(\frac{\tau}{\phi_1\phi_2}\right)^{\frac{1}{\phi_2-1}}\varphi_t^{\frac{1}{\phi_2-1}}-\varphi_{t+1}\left(\frac{\tau}{\phi_1\phi_2}\right)^{\frac{1}{\phi_2-1}}\frac{1}{\phi_2-1}\right)\\
&\times\left(\frac{d\tilde{\varphi}_{t+1}}{dN_t}+(1-\omega_\varphi)\frac{d\tilde{\varphi}_t}{dN_t}\right)\\
&= 1-\delta_N+\tau Y_{t+1}\omega_\varphi\left(1-\left(\frac{\tau}{\phi_1\phi_2}\right)^{\frac{1}{\phi_2-1}}\varphi_t^{\frac{1}{\phi_2-1}}-\varphi_{t+1}\left(\frac{\tau}{\phi_1\phi_2}\right)^{\frac{1}{\phi_2-1}}\frac{1}{\phi_2-1}\right)\varphi^f h\mu^h\\
&\times\left(\frac{-1}{(\mu+N_{t+1})^{h+1}}\frac{dN_{t+1}}{dN_t}+(1-\omega_\varphi)\frac{-1}{(\mu+N_{t+1})^{h+1}}\right)\\
\Rightarrow\frac{dN_{t+1}}{dN_t} &= \frac{1-\delta_N+\tau Y_{t+1}\omega_\varphi[\cdots]\varphi^f h\mu^h(1-\omega_\varphi)\frac{-1}{(\mu+N_t)^{h+1}}}{1-\tau Y_{t+1}\omega_\varphi[\cdots]\varphi^f h\mu^h\frac{-1}{(\mu+N_{t+1})^{h+1}}},\\
\cdots &= \left((1-\omega_\varphi)\varphi_t+\omega_\varphi\varphi^f\left(\frac{\mu}{\mu+N_{t+1}}\right)^h\right)^{\frac{1}{\phi_2-1}}+\left((1-\omega_\varphi)\varphi_t+\omega_\varphi\varphi^f\left(\frac{\mu}{\mu+N_{t+1}}\right)^h\right)\frac{1}{\phi_2-1}\\
&= 1-\delta_N^*
\end{aligned}
\tag{D.49}
$$

The result above implies the actual $\delta_N^* > \delta_N$. Therefore, the duration will be slightly overestimated using the simplification. However, my numerical simulation of up to 1,200 months' horizon under baseline calibration implies the impact is trivial.

$$
\begin{aligned}
\frac{d\varphi_{t+n}}{dN_t} &= \omega_\varphi\sum_{i=0}^{n}(1-\omega_\varphi)^{n-i}\frac{d\tilde{\varphi}_{t+i}}{dN_{t+i}}\frac{dN_{t+i}}{dN_t}\\
&= \omega_\varphi\sum_{i=0}^{n}(1-\omega_\varphi)^{n-i}\frac{-\varphi^f h\mu^h}{(\mu+N_{t+i})^{h+1}}\left(\frac{dN_{t+1}}{dN_t}\right)^i\\
&= \omega_\varphi\varphi^f h\mu^h\frac{-(1-\omega_\varphi)^n}{(\mu+N_t)^{h+1}}\sum_{i=0}^{n}\left(\frac{1-\delta_N}{1-\omega_\varphi}\right)^i\\
&= -\frac{\omega_\varphi\varphi^f h\mu^h((1-\delta_N)^{n+1}-(1-\omega_\varphi)^{n+1})}{(\mu+N_t)^{h+1}(\omega_\varphi-\delta_N)} < 0
\end{aligned}
\tag{D.50}
$$

as $\omega_\varphi > \delta_N$

Look back at the firm's profit:

$$\Pi_t = \left[P_t - \tau \left(1 - \left(\frac{\tau}{\phi_1 \phi_2} \right)^{\frac{1}{\phi_2 - 1}} \varphi_t^{\frac{1}{\phi_2 - 1}} \right) \varphi_t - \phi_1 \left(\frac{\tau}{\phi_1 \phi_2} \right)^{\frac{\phi_2}{\phi_2 - 1}} \varphi_t^{\frac{\phi_2}{\phi_2 - 1}} \right] Y_t - w_t L_t - r_t K_t \tag{D.51}$$

Then, derive the MPI of two capital types:

$$\begin{aligned} MPI_t^K &= \sum_{n=1}^{\infty} \frac{1}{(1+r_t)^n} \frac{d\Pi_{t+n}}{dK_{t+n-1}} \frac{dK_{t+n-1}}{dK_{t-1}} \\ &= \sum_{n=1}^{\infty} \frac{1}{(1+r_t)^n} ([...]_{t+n} \frac{\alpha Y_{t+n}}{K_{t+n-1}} - r_t)(1-\delta)^n \end{aligned} \tag{D.52}$$

$$\begin{aligned} MPI_t^N &= \sum_{n=1}^{\infty} \frac{1}{(1+r_t)^n} \frac{d\Pi_{t+n}}{d\varphi_{t+n}} \frac{d\varphi_{t+n}}{dN_t} \\ &= \sum_{n=1}^{\infty} \frac{1}{(1+r_t)^n} \frac{d\varphi_{t+n}}{dN_t} \frac{d}{d\varphi_{t+n}} \left[\tau \left(\frac{\tau}{\phi_1 \phi_2} \right)^{\frac{1}{\phi_2 - 1}} \varphi_{t+n}^{\frac{1}{\phi_2 - 1} + 1} - \tau \varphi_{t+n} - \phi_1 \left(\frac{\tau}{\phi_1 \phi_2} \right)^{\frac{\phi_2}{\phi_2 - 1}} \varphi_{t+n}^{\frac{\phi_2}{\phi_2 - 1}} \right] \\ &= \sum_{n=1}^{\infty} \frac{1}{(1+r_t)^n} \frac{d\varphi_{t+n}}{dN_t} \left[\frac{\tau}{\phi_2 - 1} \left(\frac{\tau}{\phi_1 \phi_2} \right)^{\frac{1}{\phi_2 - 1}} \varphi_{t+n}^{\frac{1}{\phi_2 - 1}} + \tau \left(\frac{\tau}{\phi_1 \phi_2} \right)^{\frac{1}{\phi_2 - 1}} \varphi_{t+n}^{\frac{1}{\phi_2 - 1}} - \tau \right. \\ &\left. - \frac{\phi_1 \phi_2}{\phi_2 - 1} \left(\frac{\tau}{\phi_1 \phi_2} \right)^{\frac{\phi_2}{\phi_2 - 1}} \varphi_{t+n}^{\frac{1}{\phi_2 - 1}} \right] \\ &= \sum_{n=1}^{\infty} \frac{1}{(1+r_t)^n} \frac{d\varphi_{t+n}}{dN_t} \left[\frac{\phi_2 \tau}{\phi_2 - 1} \left(\frac{\tau}{\phi_1 \phi_2} \right)^{\frac{1}{\phi_2 - 1}} \varphi_{t+n}^{\frac{1}{\phi_2 - 1}} - \tau - \frac{\tau}{\phi_2 - 1} \left(\frac{\tau}{\phi_1 \phi_2} \right)^{\frac{1}{\phi_2 - 1}} \varphi_{t+n}^{\frac{1}{\phi_2 - 1}} \right] \\ &= \sum_{n=1}^{\infty} \frac{1}{(1+r_t)^n} \frac{d\varphi_{t+n}}{dN_t} \underbrace{\left(\left(\frac{\tau}{\phi_1 \phi_2} \right)^{\frac{1}{\phi_2 - 1}} \varphi_{t+n}^{\frac{1}{\phi_2 - 1}} - 1 \right)}_{<0} \tau \\ &= \sum_{n=1}^{\infty} \frac{\tau}{(1+r_t)^n} \left(1 - \left(\frac{\tau}{\phi_1 \phi_2} \right)^{\frac{1}{\phi_2 - 1}} \varphi_{t+n}^{\frac{1}{\phi_2 - 1}} \right) \frac{\omega_\varphi \varphi^f h \mu^h}{(\mu + N_t)^{h+1} (\omega_\varphi - \delta_N)} ((1-\delta_N)^{n+1} - (1-\omega_\varphi)^{n+1}) \end{aligned} \tag{D.53}$$

Calculate the durations:[31]

$$\begin{aligned} Dur_t^K &= \frac{\sum_{n=0}^{\infty} n \left(\frac{1-\delta}{1+r_t} \right)^n}{\sum_{n=0}^{\infty} \left(\frac{1-\delta}{1+r_t} \right)^n} \\ &= \frac{\frac{1-\delta}{1+r_t}}{1 - \frac{1-\delta}{1+r_t}} \\ &= \frac{1-\delta}{r_t + \delta} \end{aligned} \tag{D.54}$$

[31] Here I use the property: $\sum_{k=0}^{n} k a^k = \frac{a}{1-a} \left(\frac{1-a^{n+1}}{1-a} - (n+1) a^n \right) \; \forall 0 < a < 1$.

$$
\begin{aligned}
Dur_t^N &= \frac{\sum_{n=0}^{\infty} n\left(\left(\frac{1-\delta_N}{1+r_t}\right)^{n+1} - \left(\frac{1-\omega_\varphi}{1+r_t}\right)^{n+1}\right)}{\sum_{n=0}^{\infty}\left(\left(\frac{1-\delta_N}{1+r_t}\right)^{n+1} - \left(\frac{1-\omega_\varphi}{1+r_t}\right)^{n+1}\right)} \\
&= \frac{\sum_{n=0}^{\infty}(n+1)\left(\left(\frac{1-\delta_N}{1+r_t}\right)^{n+1} - \left(\frac{1-\omega_\varphi}{1+r_t}\right)^{n+1}\right)}{\sum_{n=0}^{\infty}\left(\left(\frac{1-\delta_N}{1+r_t}\right)^{n+1} - \left(\frac{1-\omega_\varphi}{1+r_t}\right)^{n+1}\right)} - 1 \\
&= \frac{\frac{1-\delta_N}{1+r_t}\left(\frac{r_t+\omega_\varphi}{1+r_t}\right)^2 - \frac{1-\omega_\varphi}{1+r_t}\left(\frac{r_t+\delta_N}{1+r_t}\right)^2}{\left(\frac{\omega_\varphi-\delta_N}{1+r_t}\right)\left(\frac{r_t+\delta_N}{1+r_t}\right)\left(\frac{r_t+\omega_\varphi}{1+r_t}\right)} - 1 \\
&= \frac{(1-\delta_N)(r_t+\omega_\varphi)^2 - (1-\omega_\varphi)(r_t+\delta_N)^2}{(\omega_\varphi-\delta_N)(r_t+\delta_N)(r_t+\omega_\varphi)} - 1 \\
&= \frac{1}{\omega_\varphi-\delta_N}\left(\frac{(1-\delta_N)(r_t+\omega_\varphi)}{r_t+\delta_N} - \frac{(1-\omega_\varphi)(r_t+\delta_N)}{r_t+\omega_\varphi}\right) - 1
\end{aligned}
\tag{D.55}
$$

Then, the relative sensitivity is:

$$
\left(\frac{\varepsilon_{NI}}{\varepsilon_{KI}}\right)_t = \frac{Dur_t^N}{Dur_t^K} \tag{D.56}
$$

D.1.5 Duration and Technology Adaption

For the duration of environmental capital:

$$
Dur_t^N = \frac{1}{\omega_\varphi-\delta_N}\left(\frac{(1-\delta_N)(r_t+\omega_\varphi)}{r_t+\delta_N} - \frac{(1-\omega_\varphi)(r_t+\delta_N)}{r_t+\omega_\varphi}\right) - 1 \tag{D.57}
$$

Take derivative w.r.t. ω_φ:

$$\begin{aligned}
\frac{\partial Dur_t^N}{\partial \omega_\varphi} &= -\frac{1}{(\omega_\varphi - \delta_N)^2}\left(\frac{(1-\delta_N)(r_t+\omega_\varphi)}{r_t+\delta_N} - \frac{(1-\omega_\varphi)(r_t+\delta_N)}{r_t+\omega_\varphi}\right) \\
&+ \frac{1}{\omega_\varphi - \delta_N}\left(\frac{1-\delta_N}{r_t+\delta_N} - (r_t+\delta_N)\frac{-(r_t+\omega_\varphi)-(1-\omega_\varphi)}{(r_t+\omega_\varphi)^2}\right) \\
&= \frac{1}{\omega_\varphi - \delta_N}\left(-\frac{(1-\delta_N)(r_t+\omega_\varphi)}{(r_t+\delta_N)(\omega_\varphi-\delta_N)} + \frac{(1-\omega_\varphi)(r_t+\delta_N)}{(r_t+\omega_\varphi)(\omega_\varphi-\delta_N)} + \frac{1-\delta_N}{r_t+\delta_N} + \frac{(r_t+\delta_N)(1+r_t)}{(r_t+\omega_\varphi)^2}\right) \\
&= \frac{1}{\omega_\varphi - \delta_N}\left(\frac{(1-\omega_\varphi)(r_t+\delta_N)^2 - (1-\delta_N)(r_t+\omega_\varphi)^2}{(r_t+\delta_N)(r_t+\omega_\varphi)(\omega_\varphi-\delta_N)} + \frac{(r_t+\delta_N)(1+r_t)}{(r_t+\omega_\varphi)^2} + \frac{1-\delta_N}{r_t+\delta_N}\right) \\
&= \frac{1}{\omega_\varphi - \delta_N}\left(\frac{(1-\omega_\varphi)(r_t+\delta_N)^2(r_t+\omega_\varphi) - (1-\delta_N)(r_t+\omega_\varphi)^3 + (r_t+\delta_N)^2(1+r_t)(\omega_\varphi-\delta_N)}{(r_t+\delta_N)(r_t+\omega_\varphi)^2(\omega_\varphi-\delta_N)}\right. \\
&\left.+\frac{1-\delta_N}{r_t+\delta_N}\right) \\
&= \frac{1}{(r_t+\delta_N)(r_t+\omega_\varphi)^2(\omega_\varphi-\delta_N)^2}\big((1-\omega_\varphi)(r_t+\delta_N)^2(r_t+\omega_\varphi) - (1-\delta_N)(r_t+\omega_\varphi)^3 \\
&+(r_t+\delta_N)^2(1+r_t)(\omega_\varphi-\delta_N) + (1-\delta_N)(r_t+\omega_\varphi)^2(\omega_\varphi-\delta_N)\big) \\
&= \frac{(1-\omega_\varphi)(r_t+\delta_N)^2(r_t+\omega_\varphi) + (1+r_t)(r_t+\delta_N)^2(\omega_\varphi-\delta_N) - (1-\delta_N)(r_t+\delta_N)(r_t+\omega_\varphi)^2}{(r_t+\delta_N)(r_t+\omega_\varphi)^2(\omega_\varphi-\delta_N)^2} \\
&= \frac{(1-\omega_\varphi)(r_t+\delta_N)(r_t+\omega_\varphi) + (1+r_t)(r_t+\delta_N)(\omega_\varphi-\delta_N) - (1-\delta_N)(r_t+\omega_\varphi)^2}{(r_t+\omega_\varphi)^2(\omega_\varphi-\delta_N)^2} < 0
\end{aligned} \tag{D.58}$$

Look at the numerator, which determines the sign of the first-order derivative:

$$\begin{aligned}
&(1-\omega_\varphi)(r_t+\delta_N)(r_t+\omega_\varphi) + (1+r_t)(r_t+\delta_N)(\omega_\varphi-\delta_N) - (1-\delta_N)(r_t+\omega_\varphi)^2 \\
&= (r_t+\delta_N)r_t + (r_t+\delta_N)(1-r_t)\omega_\varphi + (r_t+\delta_N)(-\omega_\varphi^2) + (1+r_t)(r_t+\delta_N)\omega_\varphi \\
&- (r_t+\delta_N)(1+r_t)\delta_N - (1-\delta_N)r_t^2 - (1-\delta_N)\omega_\varphi^2 - (1-\delta_N)2r_t\omega_\varphi \\
&= -(1+r_t)\omega_\varphi^2 + 2\delta_N(1+r_t)\omega_\varphi - \delta_N^2(1+r_t)
\end{aligned} \tag{D.59}$$

Let $f(x) = -(1+r_t)x^2 + 2\delta_N(1+r_t)x - \delta_N^2(1+r_t), x \in (0,1)$. Take derivative of $f(x)$ w.r.t x, obtain: $f'(x) = -2(1+r_t)x + 2\delta_N(1+r_t)$. Therefore, $x^* = \delta_N$, and $f(x^*) = f(\delta_N) = 0$. Then, $f(x) \leq 0\ \forall x \in (0,1)$.

Since $\frac{\partial Dur_t^N}{\partial \omega_\varphi} \leq 0$ as $\omega_\varphi \in (0,1)$, when ω_φ decreases, Dur_t^N increases.

Then, look at the difference between Dur^N and Dur^K:

$$Dur_t^N - Dur_t^K = \frac{1}{\omega_\varphi - \delta_N}\left(\frac{(1-\delta_N)(r_t+\omega_\varphi)}{r_t+\delta_N} - \frac{(1-\omega_\varphi)(r_t+\delta_N)}{r_t+\omega_\varphi}\right) - \frac{1+r_t}{r_t+\delta} \tag{D.60}$$

When $\omega_\varphi = 1$:

$$Dur_t^N - Dur_t^K = (1+r_t)(\frac{1}{r_t+\delta_N} - \frac{1}{r_t+\delta}) \tag{D.61}$$

Therefore, if $\delta_N < \delta$, $Dur_t^N - Dur_t^K > 0 \ \forall \omega_\varphi \in (\delta_N, 1)$. If $\delta_N > \delta$, the break point will be $x^* = x^*(r_t, \delta_N) = \frac{-b-\sqrt{b^2-4ac}}{2a}$ s.t. $a = (1-\delta_N)(r_t+\delta) - (1+r_t)(r_t+\delta_N)$, $b = 2(1-\delta_N)(r_t+\delta)r_t + (r_t+\delta_N)^2(r_t+\delta) - (1+r_t)(r_t+\delta_N)(r_t-\delta_N)$, $c = (1-\delta_N)(r_t+\delta)r_t^2 - (r_t+\delta_N)^2(r_t+\delta) + (1+r_t)(r_t+\delta_N)\delta_N r_t$, and $Dur_t^N - Dur_t^K > 0 \ \forall \omega_\varphi \in (\delta_N, x^*)$.[32]

D.1.6 Pollution and Clean Investment Share

From the log linearlized equations, obtain:

$$\hat{Z}_t = \left(1 - \frac{U}{1-U}\frac{1}{\phi_2 - 1}\right)\hat{\varphi}_t + \hat{Y}_t \tag{D.62}$$

After several months, the output gradually recovers, and the impact of pollution mainly comes from the changed pollution technology. Therefore:

$$\left.\frac{\partial \hat{Z}_t}{\partial \hat{\varphi}_t}\right|_{\hat{Y}_t=0} = 1 - \frac{U}{1-U}\frac{1}{\phi_2 - 1} \tag{D.63}$$

For simplicity, I do not incorporate the gradual technological adoption here. The dynamics of the case with such gradual adoption are qualitatively identical.

From the log linearlized equation of $\hat{\varphi}_t$ w.r.t. $\hat{N}_t$ and that of $\hat{N}_t$ w.r.t. $\hat{N}_{t-1}$, $\hat{T}_t$, and $\hat{I}_t$:

$$\hat{N}_t = \frac{(1-\delta_N)N\hat{N}_{t-1} + T\hat{T}_t + gI\hat{I}_t}{(1-\delta_N)N + T + gI} + \frac{K}{N}\frac{\delta\xi\left(\frac{\varepsilon_{NI}}{\varepsilon_{KI}}\right) - \frac{gI}{(1-\delta_N)N+T+gI}}{\frac{K}{N} + \xi\frac{\varepsilon_{NI}}{\varepsilon_{KI}}}\hat{I}_t \tag{D.64}$$

combine with that of $\hat{T}_t$ w.r.t. $\hat{Z}_t$ and that of $\hat{Z}_t$ w.r.t $\hat{\varphi}_t$ and $\hat{Y}_t$:

$$\hat{T}_t = \hat{Z}_t = \left(1 - \frac{U}{1-U}\frac{1}{\phi_2 - 1}\right)\hat{\varphi}_t + \hat{Y}_t \tag{D.65}$$

Therefore:

$$\begin{aligned}&\left(1 + h\frac{T}{(1-\delta_N)N + T + gI}\left(1 - \frac{U}{1-U}\frac{1}{\phi_2 - 1}\right)\frac{N}{\mu + N}\right)\hat{N}_t \\ &= \frac{(1-\delta_N)N}{(1-\delta_N)N + T + gI}\hat{N}_{t-1} + \left[\frac{gI}{(1-\delta_N)N + T + gI} + \frac{\left(\frac{\varepsilon_{NI}}{\varepsilon_{KI}}\right) - 1}{\frac{N}{\delta K}\left(\frac{\varepsilon_{NI}}{\varepsilon_{KI}}\right) + \frac{(1-\delta_N)N+T+gI}{gI}}\right]\hat{I}_t\end{aligned} \tag{D.66}$$

[32] Using the parameter estimates by the gradient algorithm, $x^* = 0.1804$. Using the Bayesian optimum, $x^* = 0.2716$.

Obtain:

$$\left.\frac{\partial \hat{Z}_t}{\partial \hat{I}_t}\right|_{\hat{Y}_t=0} = \left(1-\frac{U}{1-U}\frac{1}{\phi_2-1}\right)\left(-h\frac{N}{\mu+N}\right)\frac{\frac{gI}{(1-\delta_N)N+T+gI}+\frac{\left(\frac{\varepsilon_{NI}}{\varepsilon_{KI}}\right)-1}{\frac{N}{\delta K}\left(\frac{\varepsilon_{NI}}{\varepsilon_{KI}}\right)+\frac{(1-\delta_N)N+T+gI}{gI}}}{1+h\frac{T}{(1-\delta_N)N+T+gI}\left(1-\frac{U}{1-U}\frac{1}{\phi_2-1}\right)\frac{N}{\mu+N}}$$

$$\overset{\text{s.s.}}{=} \left(1-\frac{U}{1-U}\frac{1}{\phi_2-1}\right)\left(-h\frac{N}{\mu+N}\right)\frac{\frac{gI}{N}+\frac{\left(\frac{\varepsilon_{NI}}{\varepsilon_{KI}}\right)-1}{\frac{N}{I}\left(\frac{\left(\frac{\varepsilon_{NI}}{\varepsilon_{KI}}\right)}{1-g}+\frac{1}{g}\right)}}{1+h\frac{T}{N}\left(\frac{\varphi}{\varphi^f}\right)^{\frac{1}{h}}\left(1-\frac{U}{1-U}\frac{1}{\phi_2-1}\right)}$$

$$= -h\frac{N}{\mu+N}\frac{\frac{gI}{N}+\frac{\left(\frac{\varepsilon_{NI}}{\varepsilon_{KI}}\right)-1}{\frac{N}{I}\left(\frac{\left(\frac{\varepsilon_{NI}}{\varepsilon_{KI}}\right)}{1-g}+\frac{1}{g}\right)}}{\frac{1}{1-\frac{U}{1-U}\frac{1}{\phi_2-1}}+h\frac{T}{N}\left(\frac{\varphi}{\varphi^f}\right)^{\frac{1}{h}}} \tag{D.67}$$

When g increases, φ decreases, $U=(\frac{\tau\varphi}{\phi_1\phi_2})^{\frac{1}{\phi_2-1}}$ decreases, $\frac{U}{1-U}$ decreases, $(1-\frac{U}{1-U}\frac{1}{\phi_2-1})$ increases. As Z decreases after g increases, $T=\tau Z$ decreases. As N increases when g increases, $\frac{T}{N}$ decreases when g increases. At s.s., $\delta_N=\frac{T+gI}{N}$. Therefore, when g increases, $\frac{gI}{N}$ increases. The first fraction increases as N increases. For the second fraction, the denominator decreases as all components that vary with g decrease. For the numerator, it increases when $\frac{\varepsilon_{NI}}{\varepsilon_{KI}}$ is unity as only the first term is non-zero, and it increases with g. When $\frac{\varepsilon_{NI}}{\varepsilon_{KI}}>1$, the second term cannot dominate with g when $\frac{\varepsilon_{NI}}{\varepsilon_{KI}}$ is not far away from 1.[33] Therefore, $\left|\frac{d}{dg}\left[\left.\frac{\partial \hat{Z}_t}{\partial \hat{I}_t}\right|_{\hat{Y}_t=0}\right]\right|>0$, and pollution increases more after a positive MPs if the clean investment share increases.

[33] Look at the term $\frac{gI}{N}+\frac{\left(\frac{\varepsilon_{NI}}{\varepsilon_{KI}}\right)-1}{\frac{N}{I}\left(\frac{\left(\frac{\varepsilon_{NI}}{\varepsilon_{KI}}\right)}{1-g}+\frac{1}{g}\right)}$. Numerically, for the initially calibrated parameters, when g increases by 0.0001 (step), the term increases by 0.0049 times step. For the parameters estimated by the gradient algorithm, the increase is 0.0008 times step. For the parameters of the Bayesian optimum, the increase is 0.0032 times step.

D.2 Estimation

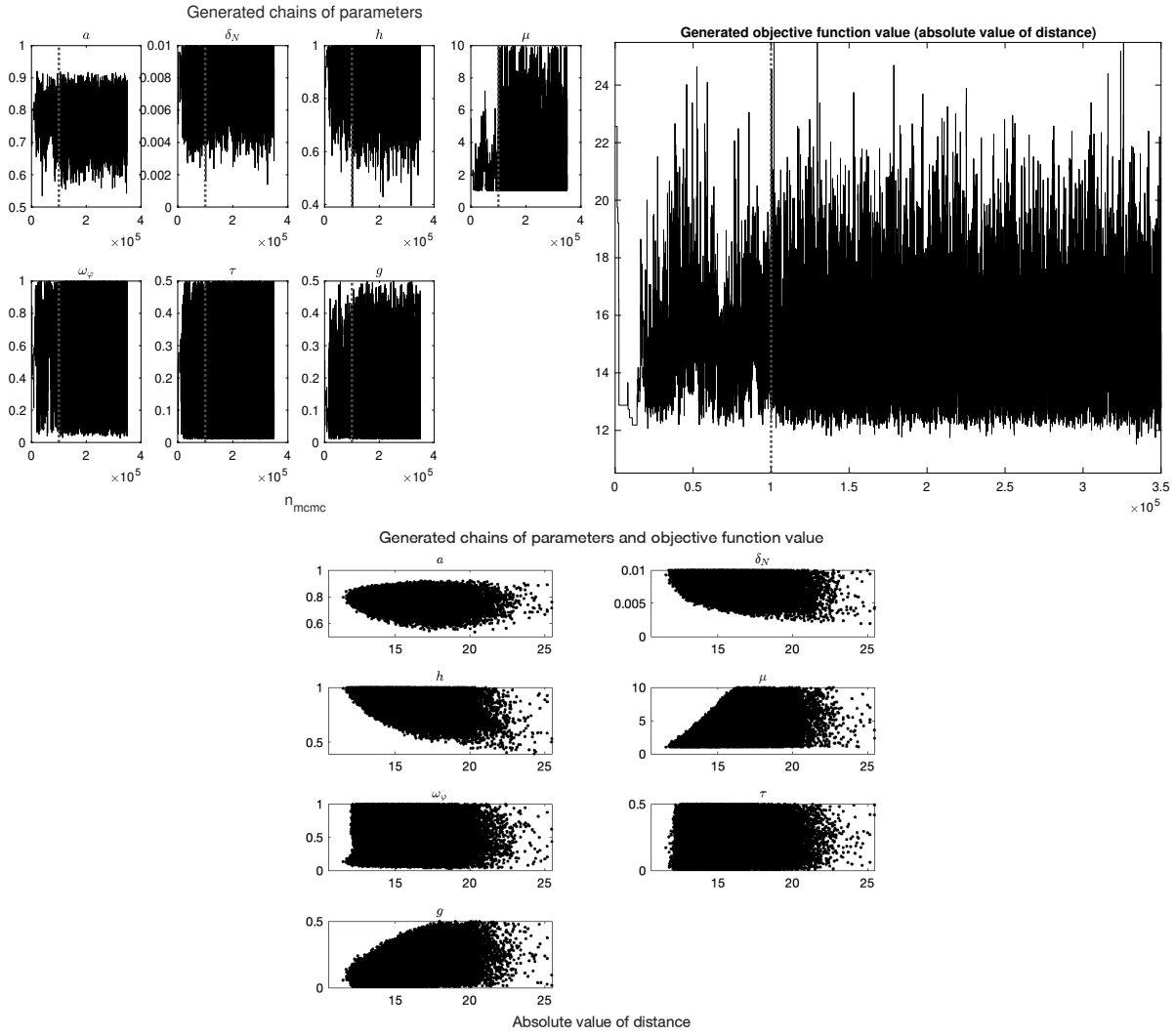

Figure D.1: Bayesian Estimation of the Model: Statistics

Notes: (a) I apply the Metropolis-Hastings algorithm with Random Walk draws. The first 100,000 draws use the identity matrix to draw shifts from a multivariable normal distribution. After the 100,000 draws, I calculate the covariance matrix of the generated chains of parameters and use it as the covariance matrix of the random draw for the next 250,000 draws.
(b) As in Uribe and Schmitt-Grohe (2017), I assign each estimated parameter a uniform prior with an upper bound and a lower bound using reasonable values, and I skip a draw if any of the resulting parameter is out of the boundary, or if there is no stable steady state based on the generated parameters.

Table D.1: Bayesian Estimation Statistics

Variable	Distribution	Prior				Posterior				
		Mean	Min	Max	SD	Min	5th Percentile	Median	95th Percentile	Max
Parameters										
a	Uniform	0.75	0.5	1	0.08333	0.5423	0.7368	0.7747	0.8092	0.9189
δ_N	Uniform	0.0055	0.001	0.01	0.0015	0.0014	0.0075	0.0085	0.0093	0.0100
h	Uniform	0.55	0.1	1	0.15	0.3903	0.8586	0.9245	0.9667	1.0000
μ	Uniform	5.5	1	10	1.5	1.0001	1.5797	2.3921	3.7892	9.9975
ω_φ	Uniform	0.505	0.01	1	0.165	0.0263	0.3391	0.5618	0.7816	1.0000
τ	Uniform	0.255	0.01	0.5	0.08167	0.0100	0.1012	0.2049	0.3319	0.4999
g	Uniform	0.255	0.01	0.5	0.08167	0.0100	0.0788	0.1351	0.2041	0.4997
Derived Variables										
$\frac{\varepsilon_{I^N,MP}}{\varepsilon_{I^K,MP}}$						1.9082	1.9377	2.0377	2.2753	3.3900

Notes: (a) I apply the Metropolis-Hastings algorithm with Random Walk draws. The first 100,000 draws use the identity matrix to draw shifts from a multivariable normal distribution. After the 100,000 draws, I calculate the covariance matrix of the generated chains of parameters and use it as the covariance matrix of the random draw for the next 250,000 draws.
(b) The posterior statistics shown are for the last 250,000 draws.

D.3 Comparative Statics

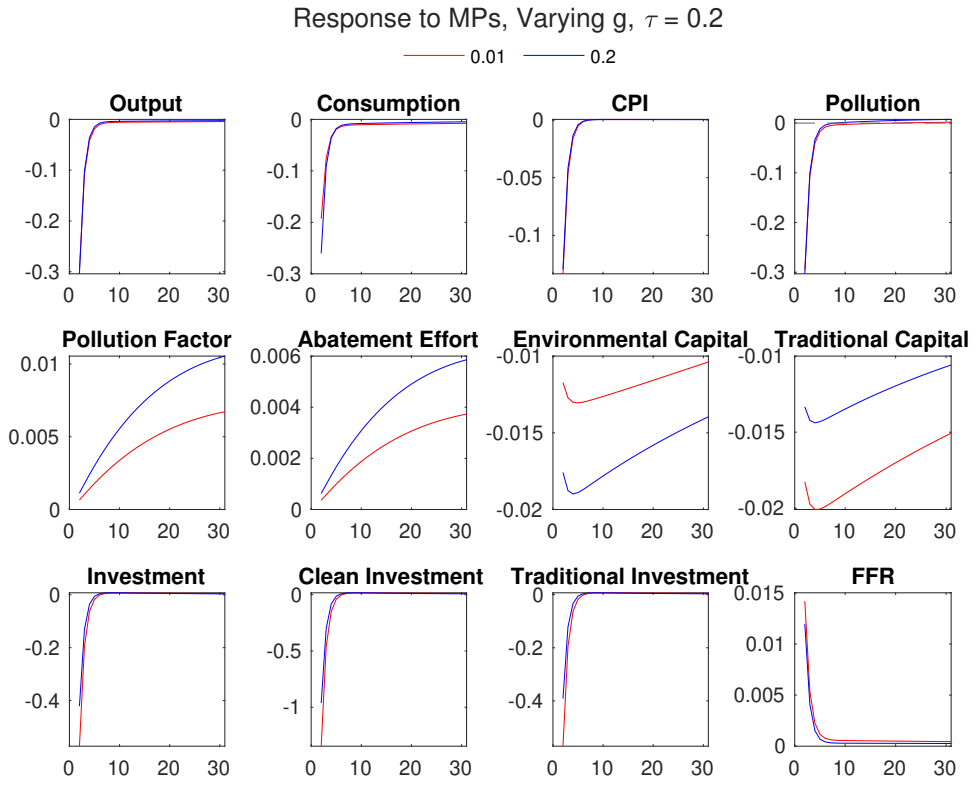

Figure D.2: IRF, by Environmental Capital Share

Notes: For the parameters to be estimated, the steady-state values are the initial values in the estimations.

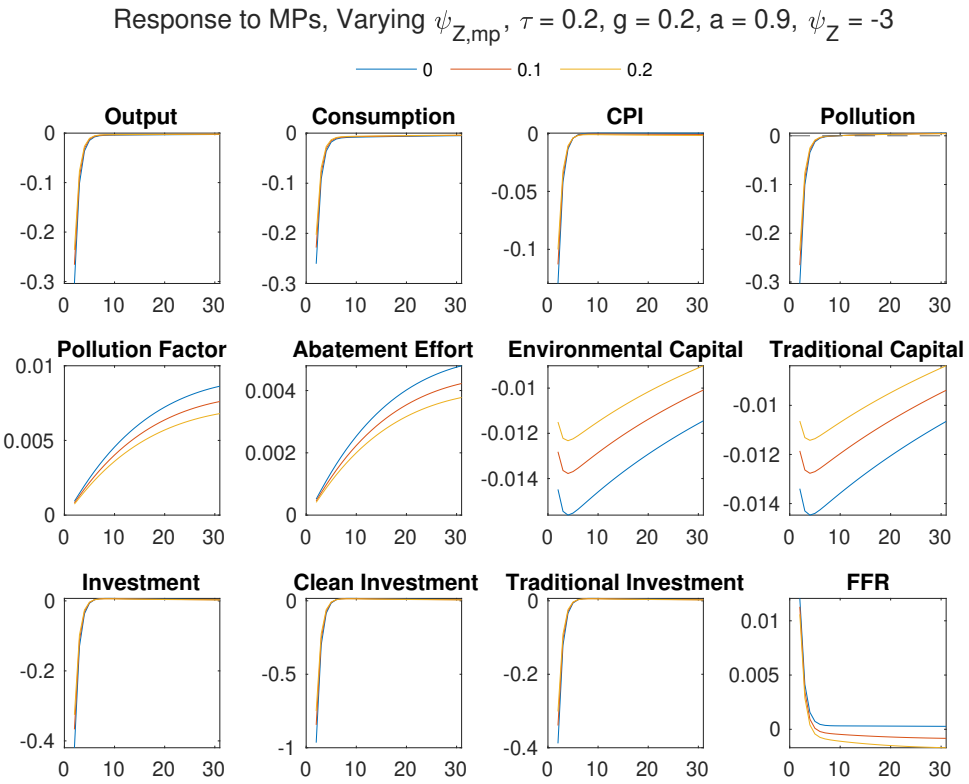

Figure D.3: IRF, by MP Response Coefficient to Pollution

Notes: For the parameters to be estimated, the steady-state values are the initial values in the estimations.

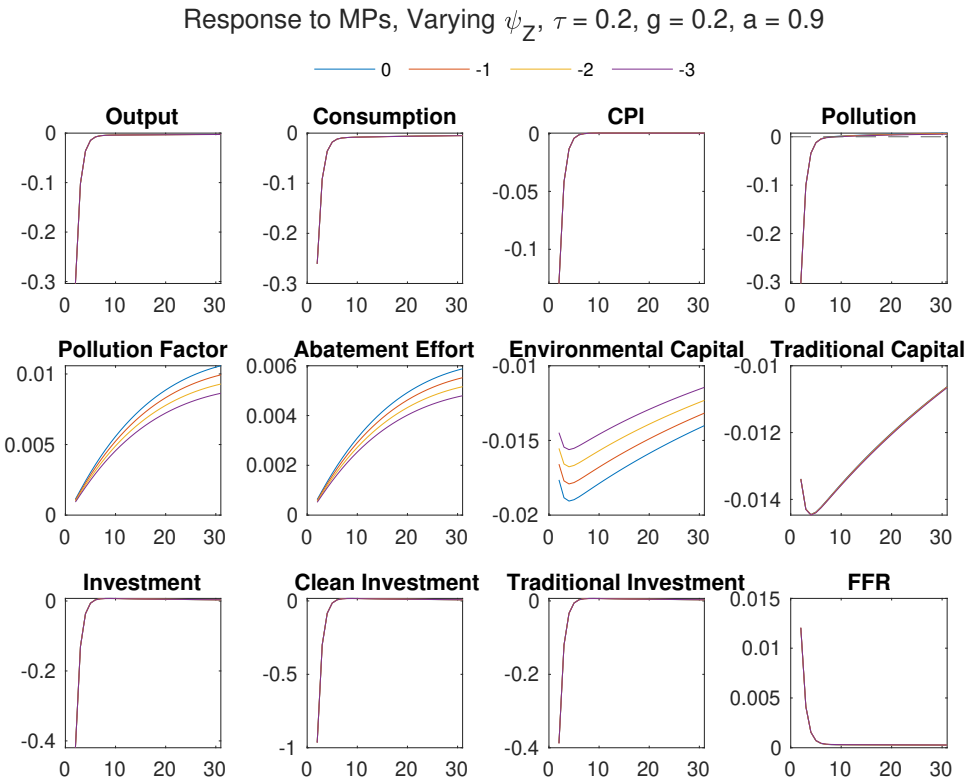

Figure D.4: IRF, by Pollution Tax Response Coefficient to Pollution

Notes: For the parameters to be estimated, the steady-state values are the initial values in the estimations.

Appendix E More Results on Extension

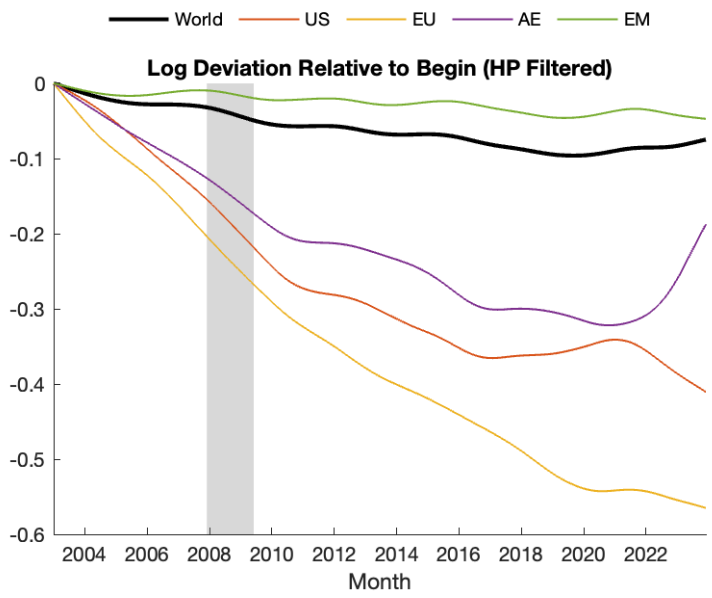

Figure E.1: Global Pollution Dyamics

Notes: The lambda parameter of the HP filter is 14,400. The gray rectangle represents the period from December 2007 to June 2009, corresponding to the Global Financial Crisis (GFC).

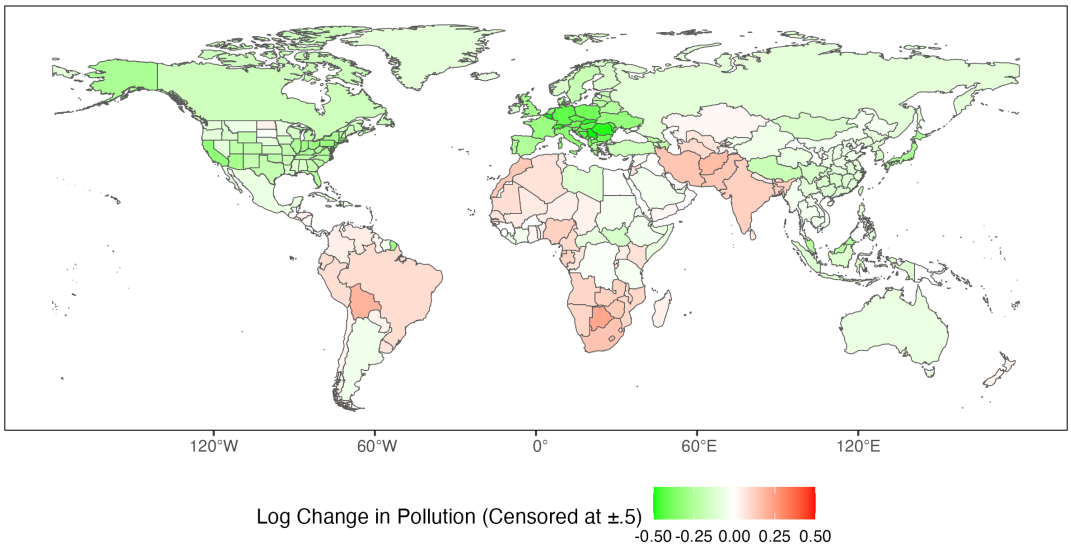

Figure E.2: Pollution Change from 2009 to 2023 by Country and Region

Notes: Log change in pollution is the change in PC1. Extreme values with absolute values greater than 0.5 are winsorized on the map.

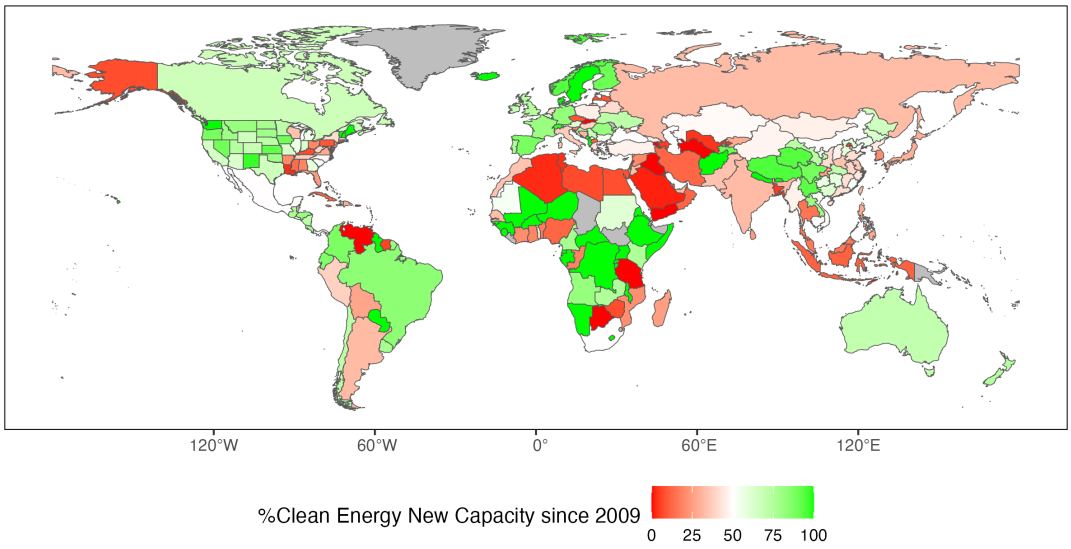

Figure E.3: Ratio of Clean Energy in Newly Commissioned Power Plant Capacity from 2009 to 2023 by Country and Region

Notes: The ratio is calculated based on the cumulative new commission from 2009 to 2023 by technology.

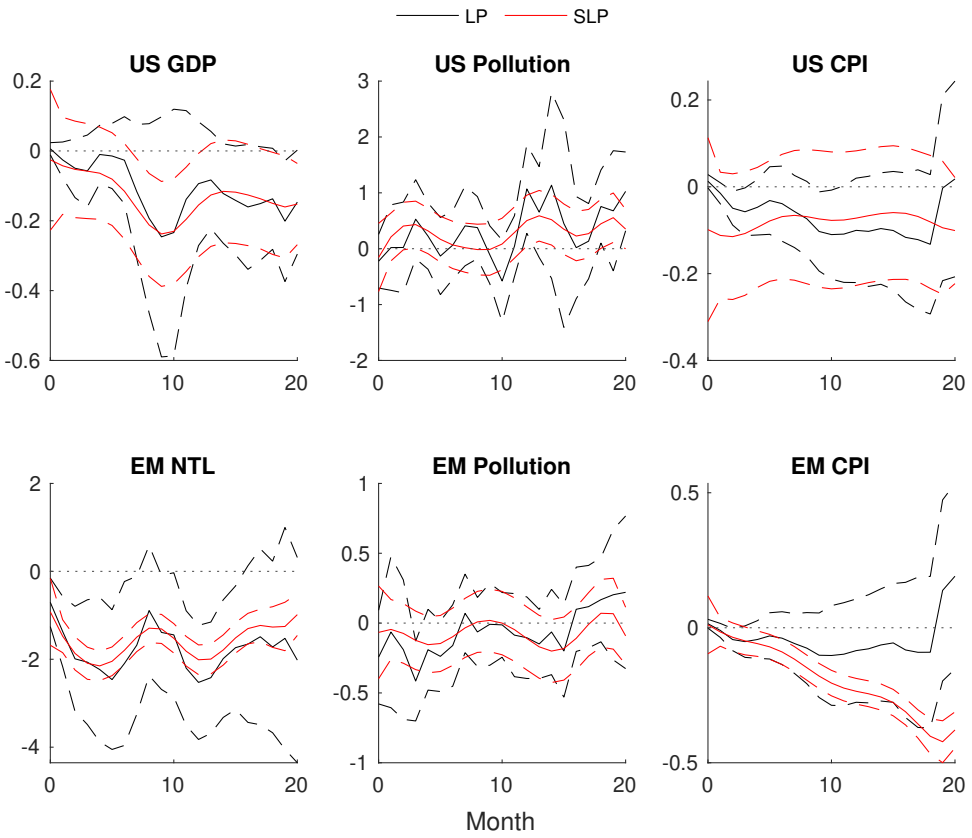

Figure E.4: Pollution Response to MPs, Baseline (US and EM)

Notes: MPs is aggregated to the monthly frequencies consistent with the dependent variable. The number of lags of the dependent variable (Q) and the shock (M) are selected by the AIC criteria for up to 4 periods. The dashed ribbons are the 90 percent confidence intervals generated based on the Newey-West standard errors.

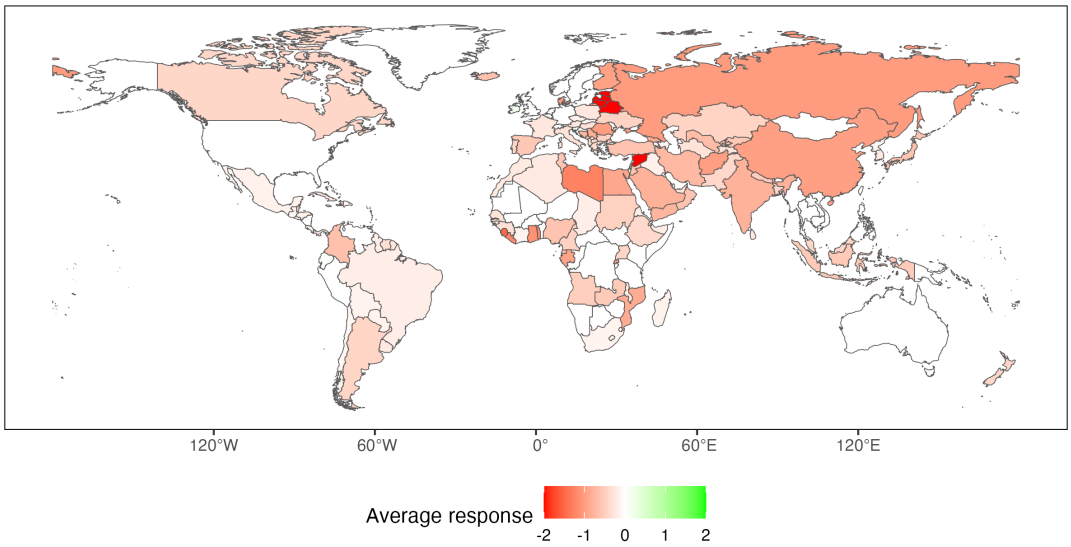

Figure E.5: Average NTL Response to MPs by Country and Region

Notes: MPs is aggregated to the monthly frequencies consistent with the dependent variable. The number of lags of the dependent variable (Q) and the shock (M) are selected by the AIC criteria for up to 4 periods. When taking the average across the time horizon from the month the MPs is realized to 20 months later, insignificant values at a 90 percent confidence level are treated as zero. If the region has both significantly positive and significantly negative responses, the average response by the region is interpreted as zero. Extreme values with absolute values greater than 2 are winsorized on the map.

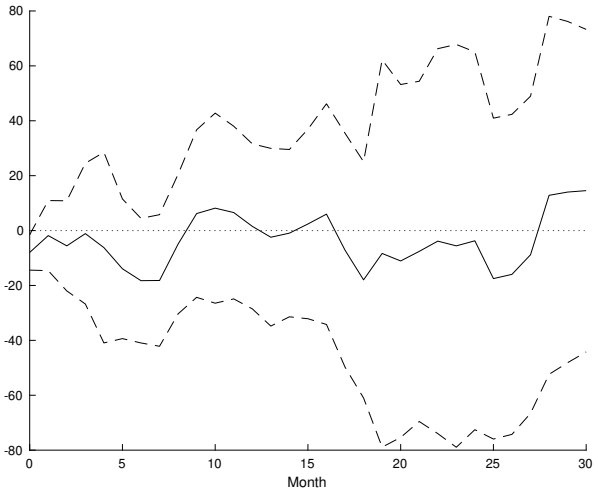

Figure E.6: Exchange Rate Response to MPs

Notes: MPs is aggregated to the monthly frequencies consistent with the dependent variable. The number of lags of the dependent variable (Q) and the shock (M) are selected by the AIC criteria for up to 4 periods. The dashed ribbons are the 90 percent confidence intervals generated based on the Newey-West standard errors.